

2015

# Integrating Tunable Anion Exchange with Reverse Osmosis for Enhanced Recovery During Inland Brackish Water Desalination

Ryan Casey Smith  
*Lehigh University*

Follow this and additional works at: <http://preserve.lehigh.edu/etd>



Part of the [Environmental Engineering Commons](#)

---

## Recommended Citation

Smith, Ryan Casey, "Integrating Tunable Anion Exchange with Reverse Osmosis for Enhanced Recovery During Inland Brackish Water Desalination" (2015). *Theses and Dissertations*. 2812.  
<http://preserve.lehigh.edu/etd/2812>

This Dissertation is brought to you for free and open access by Lehigh Preserve. It has been accepted for inclusion in Theses and Dissertations by an authorized administrator of Lehigh Preserve. For more information, please contact [preserve@lehigh.edu](mailto:preserve@lehigh.edu).

**INTEGRATING TUNABLE ANION EXCHANGE WITH REVERSE  
OSMOSIS FOR ENHANCED RECOVERY DURING INLAND  
BRACKISH WATER DESALINATION**

by

Ryan C. Smith

A Dissertation

Presented to the Graduate and Research Committee

of Lehigh University

in Candidacy for the Degree of

Doctor of Philosophy

in

Environmental Engineering

Lehigh University

May 2015

Copyright

Ryan C. Smith

2015

## Approval of the Doctoral Committee

Approved and recommended for acceptance as a dissertation in partial fulfillment of the requirements for the degree of Doctor of Philosophy in Environmental Engineering on this date of \_\_\_\_\_.

---

Derick G. Brown, Ph.D.  
Committee Chairperson  
*Department of Civil and Environmental  
Engineering*  
Lehigh University

---

Arup K. SenGupta, Ph.D.  
Dissertation Supervisor and Advisor  
*Department of Civil and Environmental  
Engineering*  
Lehigh University

---

Kristen Jellison, Ph.D.  
Committee Member  
*Department of Civil and Environmental  
Engineering*  
Lehigh University

---

James E. Roberts, Ph.D.  
External Committee Member  
*Department of Chemistry*  
Lehigh University

---

Mark A. Snyder, Ph.D.  
External Committee Member  
*Department of Chemical Engineering*  
Lehigh University

Date Accepted: \_\_\_\_\_

## **Acknowledgements**

It is difficult to succinctly express gratitude to all those who helped me throughout this process because there are too many to name. I want to thank my friends from Rowan and Lehigh for keeping me sane, and my parents for their continuous support throughout my time in grad school.

I am incredibly grateful for the input and never-ending patience from my dissertation and research supervisor Dr. SenGupta, and for my committee members Drs. Jellison, Brown, Roberts, and Snyder for their comments and suggestions along the way.

# Table of Contents

<b>List of Tables</b>	<b>viii</b>
<b>List of Figures</b>	<b>ix</b>
<b>Abstract</b>	<b>1</b>
<b>1. Introduction</b>	<b>2</b>
1.1 Brackish water desalination in the United States	2
1.1.1 Concentrate management strategies	3
1.1.2 Scaling prevention measures	4
1.2 Ion exchange as a pretreatment method	5
1.3 Research Objectives	6
<b>2. Conceptualized Hybrid Ion Exchange-Reverse Osmosis Process</b>	<b>7</b>
2.1 Hybrid Ion Exchange-Reverse Osmosis (HIX-RO) Process overview	7
2.2 Previous research on ion exchange assisted desalination	10
2.3 Control of sulfate removal by mixing of ion exchange resins	11
2.4 Reduction in CaSO <sub>4</sub> Scaling	15
<b>3. Experimental Methodology</b>	<b>17</b>
3.1 Water analysis	17
3.1.1 pH and conductivity	17
3.1.2 Chloride	17
3.1.3 Sulfate	17
3.1.4 Ion Chromatography	18
3.1.5 Atomic Absorption Spectroscopy	18
3.2 Classification of ion exchange resin	18
3.2.1 Resin capacity measurement	20
3.2.2 Batch sulfate/chloride isotherms	20
3.2.3 Column sulfate/chloride isotherms	21
3.2.4 Scanning electron microscopy	21
3.3 HIX-RO Runs	21
3.3.1 Run 1: Mixed bed polystyrene and polyacrylic with Feedwater “A”	25
3.3.2 Run 2: Pure strong base polyacrylic with Feedwater “A”	25

3.3.3	Run 3: Pure weak base polyacrylic with Feedwater “B”	25
3.3.4	Run 4: Pure strong base polystyrene with Feedwater “C”	25
3.3.5	Run 5: Mixed bed polystyrene and polyacrylic with phosphate selective resin with Feedwater “D”	26
3.3.6	Run 6: Pure polystyrene with triethylamine functional groups with Feedwater “E”	27
3.4	Ion Exchange	27
3.5	Reverse Osmosis	27
3.6	Measuring CaSO <sub>4</sub> Precipitation Kinetics	28
3.7	In-Column CaSO <sub>4</sub> Precipitation	28
<b>4.</b>	<b>Control of ion exchange selectivity through mixing</b>	<b>31</b>
4.1	Background on ion exchange chemistry	31
4.2	Determination of resin separation factor using a batch system	33
4.3	Determination of resin separation factor using a column system	35
4.4	Determination of resin separation factor from the selectivity coefficient	35
4.5	Theoretical prediction of resin separation factor for two mixed resins	37
4.6	Classification of resin properties affecting sulfate selectivity	39
4.7	Experimental measurement of individual resin separation factor	42
4.8	Experimental measurement of mixed resin separation factors	43
4.9	Individual resin selectivity compared to bulk resin selectivity	45
<b>5.</b>	<b>Modeling a Hybrid Ion Exchange-Reverse Osmosis System</b>	<b>52</b>
5.1	Background	52
5.2	Modeling a Reverse Osmosis System	52
5.3	Modeling an ion exchange column	53
5.4	Importance of resin selectivity on process efficiency	56
<b>6.</b>	<b>Lab-scale study of a Hybrid Ion Exchange-Reverse Osmosis System</b>	<b>60</b>
6.1	Results from HIX-RO Runs	60
6.1.1	Run 1: Mixed bed polystyrene and polyacrylic resins with Feedwater “A”	61
6.1.2	Run 2: Pure strong base polyacrylic with feedwater “A”	65
6.1.3	Run 3: Pure weak base polyacrylic with feedwater “B”	68

6.1.4	Run 4: Pure strong base polystyrene with feedwater “C”	70
6.1.5	Run 5: Mixed bed polystyrene and polyacrylic with phosphate selective resin with feedwater “D”	72
6.1.6	Run 6: Pure polystyrene with triethylamine functional groups with feedwater “E”	77
6.2	Summary of all HIX-RO Runs	78
6.3	Characterization of potential for in-column precipitation of CaSO <sub>4</sub>	79
6.3.1	Measurement of CaSO <sub>4</sub> Precipitation Kinetics	80
6.3.2	Small scale in-column precipitation study	81
6.3.3	Explanation for lack of in-column precipitation	86
<b>7.</b>	<b>Key Contributions and Future Work</b>	<b>88</b>
7.1	Key Findings	88
7.2	Future Work	90
7.2.1	Field-scale testing	90
7.2.2	Phosphate removal	90
7.2.3	Improved ion exchange modeling	91
	<b>References</b>	<b>92</b>
<b>8.</b>	<b>Appendix I – Cost Analysis</b>	<b>103</b>
8.1	Assumptions	103
8.2	Resin Costs	104
8.3	Dosing Costs	104
8.4	Revenue from increased recovery	104
8.5	Pumping Requirements	104
<b>9.</b>	<b>Appendix II – Isotherm Data</b>	<b>108</b>
	<b>Vita</b>	<b>110</b>



## **List of Tables**

<b>Table 1.1</b> Commonly dosed chemicals/antiscalants	5
<b>Table 2.1</b> Composition of San Joaquin Valley agricultural drainage water	12
<b>Table 3.1</b> Properties of anion exchange resins used	19
<b>Table 3.2</b> Feedwater composition for all HIX-RO Runs	23
<b>Table 3.3</b> Summary of all HIX-RO Runs	24
<b>Table 3.4</b> Soubility of commonly found precipitates in desalination processes	27
<b>Table 3.5</b> Composition of synthetic feedwater and regenerant solution	29
<b>Table 4.1</b> Measured pure resin parameters	43
<b>Table A1.1</b> Assumptions made when calculating head loss	106
<b>Table A1.2</b> Calculation of pumping costs per day	107

## List of Figures

<b>Figure 2.1</b> Flow chart of HIX-RO Process	8
<b>Figure 2.2</b> Theoretical polystyrene selectivity curve at 80 meq/L and 400 meq/L	13
<b>Figure 2.3</b> Theoretical polyacrylate selectivity curve at 80 meq/L and 400 meq/L	14
<b>Figure 2.4</b> Theoretical 50/50 mixture of polystyrene and polyacrylic resins at 80 meq/L and 400 meq/L	15
<b>Figure 2.5</b> Variation in SI of CaSO <sub>4</sub> with recovery of desalination process	16
<b>Figure 4.1</b> Generalized isotherm curves for sulfate/chloride system	34
<b>Figure 4.2</b> Variation in theoretical $\alpha_{S/Cl}^*$ with changing mixing ratio	39
<b>Figure 4.3</b> Effect of changing basicity of functional group	41
<b>Figure 4.4</b> Batch testing results for strong base polystyrene, strong base polyacrylic resin and polystyrene with triethylamine functional group at 80 meq/L	42
<b>Figure 4.5</b> Batch isotherms for 50/50 mixture of polystyrene and polyacrylic resins at 80 meq/L and 400 meq/L	43
<b>Figure 4.6</b> Variation in $\alpha_{S/C}$ with changing fraction of polyacrylic resin at 80 meq/L	44
<b>Figure 4.7</b> Four possible configurations for a two column HIX-RO system	46
<b>Figure 4.8</b> Breakthrough curve for unfavorable and favorable isotherms	47
<b>Figure 4.9</b> Theoretical breakthrough curves for both scenarios	48
<b>Figure 4.10</b> Theoretical comparison between two columns in series with one mixed column	49
<b>Figure 4.11</b> Depression of $\alpha_{S/Cl}$ with increasing $x_S$	51
<b>Figure 5.1</b> Simplification of ion exchange column as a series of CSTRs	55
<b>Figure 5.2</b> Theoretical SO <sub>4</sub> <sup>2-</sup> concentration in RO feed with fixed $\alpha_{S/C} = 1.5$	57
<b>Figure 5.3</b> Theoretical SO <sub>4</sub> <sup>2-</sup> concentration in RO feed with $\alpha_{S/C} = 1.5$ and $\alpha_{S/C} = 0.5$	58
<b>Figure 6.1</b> Concentration of sulfate at feed to RO for Run 1	61
<b>Figure 6.2</b> Calculated SI values for CaSO <sub>4</sub> in RO Concentrate for Run 1	62
<b>Figure 6.3</b> Mass balance on sulfate entering/exiting system for Run 1	63
<b>Figure 6.4</b> Mass balance on chloride entering/exiting system for Run 1	64
<b>Figure 6.5</b> Concentration of sulfate at feed to RO for Runs 1 and 2	65
<b>Figure 6.6</b> Mass balance for polyacrylic HIX-RO Run	66

<b>Figure 6.7</b> Calculated SI Values for CaSO <sub>4</sub> in RO Concentrate for Runs 1 and 2	67
<b>Figure 6.8</b> Concentration of sulfate at feed to RO for Runs 1 and 3	68
<b>Figure 6.9</b> Mass balance on sulfate entering/exiting system for Run 3	69
<b>Figure 6.10</b> Calculated SI values for CaSO <sub>4</sub> in RO Concentrate for Runs 1 and 3	70
<b>Figure 6.11</b> Calculated SI values for CaSO <sub>4</sub> in RO Concentrate for Run 4	71
<b>Figure 6.12</b> Calculated SI values for CaSO <sub>4</sub> in RO Concentrate for Run 5	73
<b>Figure 6.13</b> Mass balance on sulfate for Run 5	74
<b>Figure 6.14</b> Concentration of phosphate in influent and IX effluent/RO feed	75
<b>Figure 6.15</b> Mass balance on phosphate for Run 5	76
<b>Figure 6.16</b> Calculated SI values for CaSO <sub>4</sub> in RO Concentrate for Run 6	77
<b>Figure 6.17</b> Concentration of phosphate at feed to RO for Run 6	78
<b>Figure 6.18</b> Time for visible precipitation of CaSO <sub>4</sub> with varying SI values	81
<b>Figure 6.19</b> Formation of CaSO <sub>4</sub> precipitate after 120 minutes	83
<b>Figure 6.20</b> CaSO <sub>4</sub> SI values immediately after exiting and after 24 hours	84
<b>Figure 6.21</b> Representative EDX spectrum of resin bead	85
<b>Figure A2.1</b> Pure A400 isotherm at 80 meq/L	108
<b>Figure A2.2</b> 25% A400/75% A850 column run at 80 meq/L	108
<b>Figure A2.3</b> 50% A400/50% A850 column run at 80 meq/L	109
<b>Figure A2.4</b> Pure A850 Isotherm at 80 meq/L	109

## **Abstract**

For inland desalination plants, managing and discarding produced brine leftover from the production of pure drinking water can be a significant operating cost. By increasing the recovery of the desalination process, brine volume and disposal costs will be reduced. Achieving high recovery is not immediately possible as when the recovery is increased, there is a higher potential for the precipitation of calcium sulfate which, for reverse osmosis (RO) processes, can foul and damage the RO membrane.

Ion exchange may be used as a pretreatment method to selectively remove and replace sulfate by chloride which does not pose any threat to fouling. The RO process can then be operated at higher recoveries without any threat of sulfate scaling due to its removal by the ion exchange column. After RO the leftover concentrate, highly concentrated chloride brine, can be used as a regenerant for the ion exchange column without requiring the purchase of additional chemical regenerant. By changing the type and/or mixing together characteristically different ion exchange resins, the selectivity of the ion exchange column can be precisely tuned to remove sulfate regardless of feedwater composition.

Results demonstrate that a properly designed Hybrid Ion Exchange-Reverse Osmosis (HIX-RO) system can effectively eliminate the potential for  $\text{CaSO}_4$  scaling sustainably without requiring external regenerant. The selectivity of the ion exchange resin has a significant role in controlling sulfate removal, and it is possible to precisely predict how resin selectivity changes depending on solution composition or mixing ratio with another resin.

# 1. Introduction

## 1.1 Brackish water desalination in the United States

Throughout the United States, 71% of the population receives its drinking water from surface water sources such as lakes and streams.<sup>1</sup> However in recent years, surface and groundwater resources have been declining.<sup>2,3</sup> Due to anthropogenic climate change, temperatures in arid regions such as the US Southwest have been increasing resulting in reductions in precipitation. In the future, water availability in this region will decline.<sup>4</sup> As a result, the desalination of previously untapped saline water sources is now being considered an option for supplying water to arid regions.<sup>5-8</sup> In these cases, standard methods of drinking water treatment are unable to reduce the total dissolved solids (TDS) content enough for human consumption and advanced desalination treatment methods are required.<sup>9</sup> As of 2006, the US produces approximately 5.6 million m<sup>3</sup>/day of drinking water by desalination.<sup>10</sup> Currently there are approximately 250 desalination plants operating within the US with most located in Florida, California, and Texas.<sup>11</sup> Of all the desalination facilities in the US, 65% use brackish water sources. Brackish water refers to water that has a TDS content of 500 mg/L to 10,000 mg/L.<sup>12</sup>

The most common method of desalination in the United States is reverse osmosis (RO).<sup>9</sup> A semi-permeable RO membrane is used to physically separate pure water from dissolved ions in solution. The solution that passes through the membrane is referred to as permeate while any remaining saline solution is referred to as concentrate. For brackish water desalination plants, the management of excess volumes of leftover concentrate constitutes a significant problem as there is no easy method of concentrate

disposal.<sup>13</sup> The costs associated with concentrate disposal can contribute to a significant portion, in some cases up to 50%, of the operating costs of the desalination plant.<sup>9</sup> Increasing the recovery of the RO process, even by a small amount, could result in a large reduction in the volume of concentrate produced. For example, increasing the recovery of an RO plant from 80% to 90% would result in a 50% decrease in the volume of concentrate produced. This reduction would not only help reduce the operating costs, but would also decrease the environmental impact due to the lower volume of discharged brine.

### **1.1.1 Concentrate management strategies**

There are several commonly practiced methods of concentrate disposal: discharge to surface water, sewer disposal, deep well injection, evaporation ponds, and land application.<sup>14</sup> Each method has its own drawbacks and the disposal choice for a municipality is largely dictated by geographical location and plant size.<sup>15</sup> Considering a large brackish water desalination plant, greater than 6 million gallons per day (MGD), sewer disposal, evaporation ponds, and land application are not viable options even under normal operating conditions.<sup>14</sup> Sewer disposal is only possible if the receiving wastewater treatment plant (WWTP) grants permission, evaporation ponds are prohibitively expensive due to the large land requirements, and the high salinity and volume of produced concentrate makes land disposal impossible. In arid regions such as the Southwest United States sites for surface water discharge are not immediately available leaving deep well injection as the only possible solution.

Concentrate produced by RO desalination is classified as an industrial waste as part of the industrial classification codes used by the United States Environmental

Protection Agency (USEPA), and therefore requires a Class I well for disposal<sup>14</sup> Regulations require stricter monitoring and other preventative measures to ensure that the discharged waste does not contaminate any local drinking water aquifers, but do not stipulate what quality of water can be injected into the well. Therefore if measures are taken to reduce the volume of water produced resulting in an increased salinity, currently practiced disposal methods will not need to be changed.

### **1.1.2 Scaling prevention measures**

During normal RO operation, the concentration of solution at the surface of the membrane is several times more concentrated than the bulk solution due to the phenomenon of concentration polarization. Precipitates such as  $\text{CaCO}_3$ , silica, or  $\text{CaSO}_4$  tend to precipitate on the surface of the membrane resulting in membrane scaling and fouling.<sup>16-26</sup> In order to prevent and inhibit their formation, antiscalant chemicals are dosed in the feedwater. Prevention of carbonate and silicate scaling can be controlled through feed water pretreatment by acid dosing or chemical precipitation.<sup>27</sup> For high sulfate feedwaters, chemical precipitation is not feasible for the prevention  $\text{CaSO}_4$  and acid dosing has little effect.<sup>20</sup> Instead, antiscalant addition is practiced which inhibits, but cannot prevent,  $\text{CaSO}_4$  scaling making it more difficult to control than other types. **Table 1.1** lists several commonly dosed chemicals and antiscalants and their dosing concentrations.

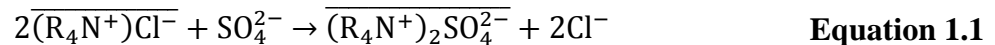
**Table 1.1 Commonly dosed chemicals/antiscalants**

Additive	Average Dosing <sup>28</sup> (mg/L)
Sulfuric Acid	50
Sodium Hexametaphosphate	6
Polyacrylic acid	3
Phosphonate	2

## 1.2 Ion exchange as a pretreatment method

Most methods for increasing the recovery of desalination processes focus on recovering water from the produced concentrate using forward osmosis to further concentrate the brine, or inducing precipitation of common scaling compounds as an intermediate treatment step.<sup>29-39</sup>

The removal of sulfate from the feed water would prevent the formation of CaSO<sub>4</sub> during RO. Ion exchange resins may serve as a simple and effective method for the selective removal of SO<sub>4</sub><sup>2-</sup> from background ions. as demonstrated in **Equation 1.1**.



In this case, sulfate is being selectively removed and replaced by chloride. Compared to sulfate salts, the solubility of chloride salts are orders of magnitude higher. Therefore, by passing the feed brackish water through a column of anion exchange resin preloaded in chloride form, sulfate will be selectively removed and replaced by the more soluble chloride, and the RO process can be operated at higher recoveries without any threat to CaSO<sub>4</sub> scaling.



Ion exchange resins have a fixed capacity and eventually, all chloride will be exhausted and the column will need to be regenerated. During typical ion exchange regeneration concentrated chloride brine would be passed through the column to displace sulfate in favor of chloride. In the place of a prepared regenerant solution the concentrate stream itself may serve as a substitute regenerant, since it is a concentrated chloride brine, resulting in a cyclic ion exchange-RO process that does not require any external regenerant.

### **1.3 Research Objectives**

The goals of this study were to classify and identify the key factors of ion exchange which ensure a sustained cyclical desalination process. Specifically:

1. Determine which resin properties control sulfate selectivity
2. Demonstrate resin mixing gives control over the sulfate/chloride separation factor
3. Perform HIX-RO process at higher than normal recoveries and prevent the formation of solid  $\text{CaSO}_4$
4. Demonstrate the HIX-RO process is sustainable and does not require additional chemical input
5. Show that an improperly designed ion exchange column will result in failure of the HIX-RO process resulting in the formation of  $\text{CaSO}_4$

## 2. Conceptualized Hybrid Ion Exchange-Reverse Osmosis

### Process

#### 2.1 Hybrid Ion Exchange-Reverse Osmosis (HIX-RO) Process overview

As described in **Chapter 1**, prevention of scaling from  $\text{CaSO}_4$  during brackish water desalination processes constitutes a significant challenge. The difficulty lies in the fact that there is no low cost method of preventing scaling but merely mitigation through antiscalant dosing. Only by physically removing  $\text{SO}_4^{2-}$  from solution can  $\text{CaSO}_4$  scaling be absolutely prevented.

Ion exchange resins selectively remove and replace certain ions from solution. Furthermore, they are unique in that the selectivity of ion exchange resins is dependent upon the ionic strength of the solution. Replacement of sulfate with chloride would eliminate the threat to scaling since the solubility of  $\text{CaCl}_2$  is orders of magnitude higher than that of  $\text{CaSO}_4$ . In the case of chloride/sulfate selectivity, at low ionic strength sulfate is more likely to be preferred by the resin making sulfate removal favorable. At higher ionic strengths, chloride is more likely to be preferred meaning that regeneration of the ion exchange resin may be accomplished using the concentrate stream from the RO process.

Chloride/sulfate selectivity is an inherent property of the ion exchange resin and may be controlled by selecting or mixing together different types of resin. In order to select the proper type of resin, both the ionic strength of the feedwater and the selectivity properties of the resin itself must be known. A flow chart of the process is shown in **Figure 2.1**.

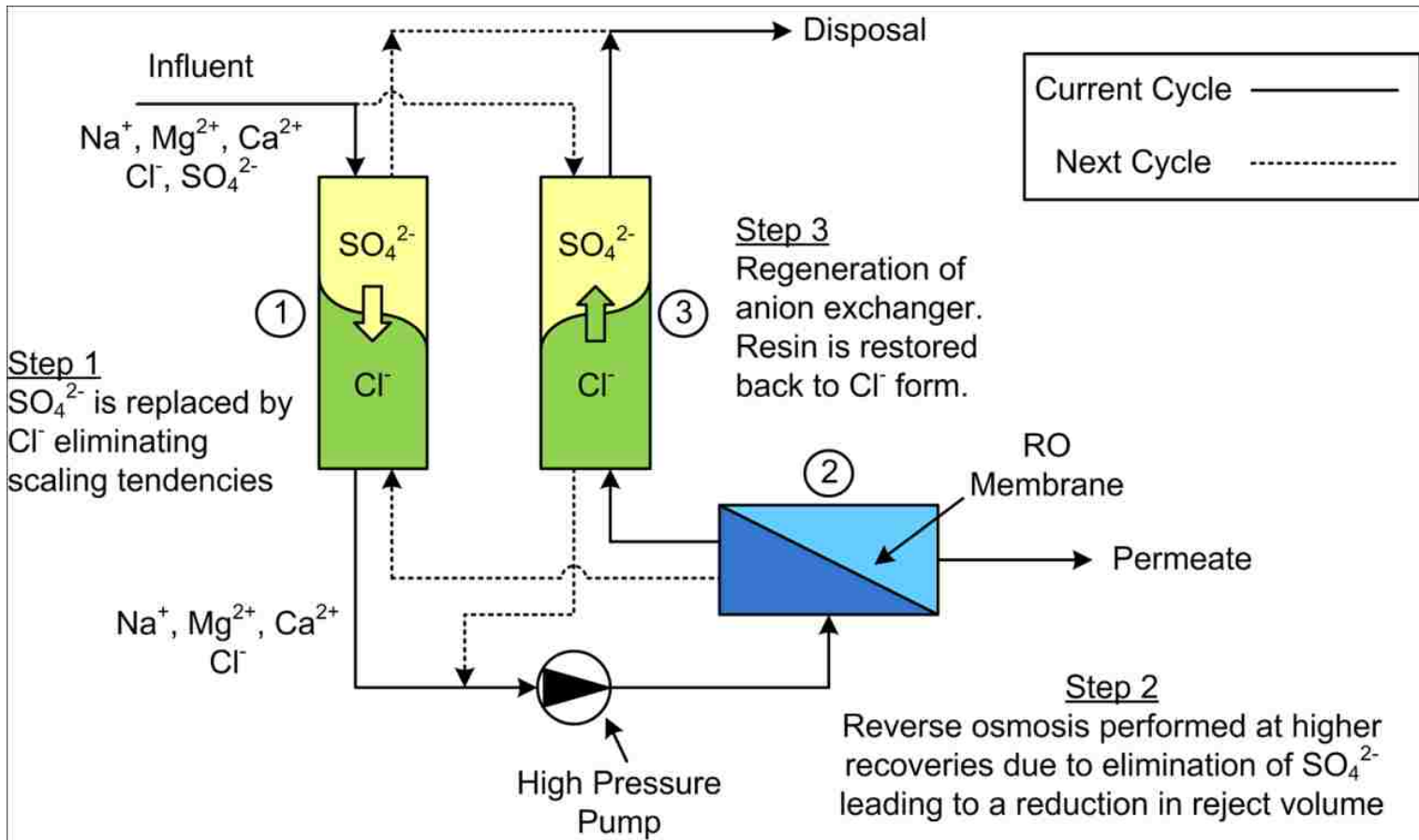
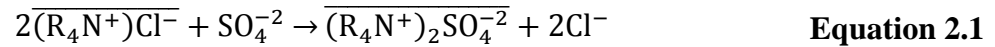


**Figure 2.1** Flow chart of HIX-RO Process

Individual steps of the process are as follows:

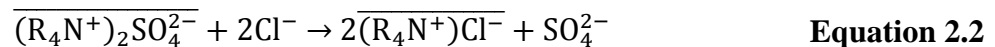
1. Influent feed solution is passed through a column of ion exchange resin in chloride form and sulfate is selectively removed by the following reaction:



In which the overbar denotes the resin phase and  $\text{R}_4\text{N}^+$  is the fixed functional group of the resin. For this step, the ion exchange column needs to be properly designed such that at the influent feedwater concentration, sulfate is preferred over chloride.

2. After passing through the ion exchange column, the effluent should have little to no sulfate and desalination by RO at higher recoveries is possible without any threat to  $\text{CaSO}_4$  scaling.

3. The concentrate stream from the RO process, highly concentrated chloride brine, is used as a regenerant for the exhausted ion exchange and no external chemical input is needed. Sulfate is replaced by chloride through the following reaction:



Again, the ion exchange column must be designed properly to ensure that the concentration of the RO concentrate is high enough that sulfate is preferred over chloride. A combination of a properly designed ion exchange column in combination with the high fraction of chloride in solution means that the regeneration process should be thermodynamically favorable.

Upon completion of desalination, a lower volume of reject stream is then discarded in the same manner as previously practiced at the RO treatment facility. No additional chemical input or change in concentrate management practices is necessary.

## **2.2 Previous research on ion exchange assisted desalination**

Cyclical ion exchange processes have been studied in the past. The earliest examples include a French Patent from 1938 and a US Patent from 1946 both describing the use of ion exchange as a pretreatment method for boiler feed and using the waste stream from the blowdown as a regenerant.<sup>40,41</sup> Initial studies during 1950 to 1960 researched using cation exchange to soften seawater by selectively replacing calcium by sodium before use in boilers and using the blowdown to regenerate the resin.<sup>42,43</sup> Dow Chemical had also published work on their own research on seawater softening systems based on cyclic cation exchange desalination systems.<sup>44</sup> In the 1970s, researchers began trying to apply the same cyclic cation exchange/desalination systems to brackish water desalination.<sup>45</sup> In fact, early plans for the Yuma Desalination Plant in Arizona included the use of cyclic ion exchange-RO processes.<sup>46</sup> Researchers continued to focus on cation exchange pretreatment for calcium removal up until 2008.<sup>47-53</sup> No studies found before 2008 used anion exchange as a pretreatment method.

An early study performed in our lab researched the replacement of chloride with sulfate to reduce the osmotic pressure of the feed solution allowing reduced energy requirements.<sup>54</sup> In 2012, researchers described the modeling and removal of divalent cations using ion exchange and a multi-stage reverse osmosis system.<sup>55</sup> To date, no research on the use of mixed anion exchange resin columns was found during literature

review. Furthermore, besides the previous study in our lab, no research on cyclic anion exchange desalination systems was found in the open literature.<sup>56</sup>

### **2.3 Control of sulfate removal by mixing of ion exchange resins**

The inherent success of the HIX-RO process relies on the fact that resin selectivity toward sulfate or chloride is not absolute and can vary with total ionic strength. The relative preference for an ion exchange resin for one ion over another ion is the separation factor,  $\alpha$ . The symbol  $\alpha$  is also used in chromatography to describe the relative separation between peaks. The separation factor  $\alpha$  and chromatography  $\alpha$  are related to each other in the sense that both describe the relative preference for one species over the other, but the methods of calculation are different. Here,  $\alpha$  is calculated by **Equation 2.3** where it takes into account the fraction of each species both on the resin,  $y$ , and in solution,  $x$ . Subscripts S and C indicate sulfate and chloride, respectively.<sup>57</sup>

$$\alpha_{S/C} = \frac{y_S x_C}{x_S y_C} \qquad \text{Equation 2.3}$$

Depending on the type of resin chosen the selectivity of the resin towards sulfate will change. There are two main parameters that can be chosen for a given anion exchange resin: (i) the composition of the matrix and (ii) the functional group of the resin. The resin matrix is an insoluble crosslinked polymer that makes up the composition of the bead. The most commonly found resins are those made of polystyrene or polyacrylate. Given the same functional group, polyacrylic resins will remove more sulfate than

polystyrene resin. Furthermore, for resins with amine functional groups sulfate preference follows the following sequence:<sup>58-60</sup>

primary > secondary > tertiary > quaternary

For example, the feedwater detailed in **Table 2.1** is an agricultural drainage water with high sulfate concentration from the San Joaquin Valley, CA<sup>27</sup>

**Table 2.1** Composition of San Joaquin Valley agricultural drainage water

<b>Component</b>	
TDS	5250 mg/L
Na <sup>+</sup>	1150 mg/L
Mg <sup>2+</sup>	60.7 mg/L
Ca <sup>2+</sup>	555 mg/L
Cl <sup>-</sup>	2010 mg/L
HCO <sub>3</sub> <sup>-</sup>	291 mg/L
SO <sub>4</sub> <sup>2-</sup>	1020 mg/L
pH	7.7
Conductivity	8.26 mS

At this feedwater concentration, 80 meq/L, **Figure 2.2** shows theoretically generated isotherms for a strong base polystyrene resin at influent (80 meq/L) and RO concentrate (400 meq/L) concentrations.

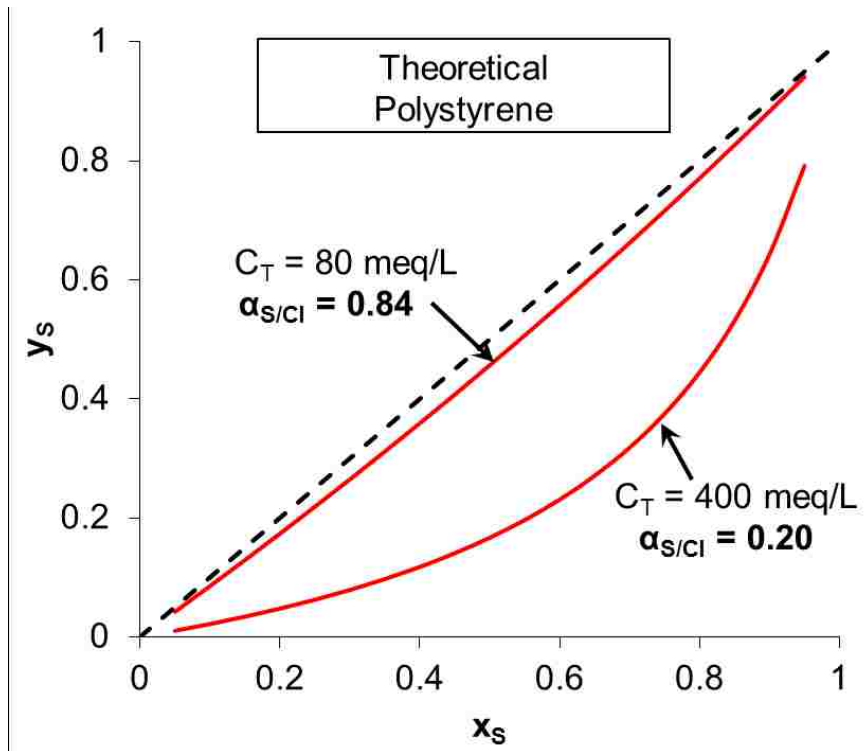


**Figure 2.2** Theoretical polystyrene selectivity curve at 80 meq/L and 400 meq/L

These curves were generated based on selectivity data from Clifford and Weber Jr.<sup>58</sup> Sulfate will be selectively removed for isotherm curves above the dashed line while chloride will be selectively removed for curves below the diagonal. The axis labels  $x_s$  and  $y_s$  represent the fraction of sulfate in solution and on the resin, respectively, and  $\alpha_{S/C}$  represents the selectivity coefficient of sulfate compared to chloride. When  $\alpha_{S/C}$  is greater than 1, sulfate is the preferred species and when  $\alpha_{S/C}$  is less than one chloride is preferred. The polystyrene resin alone would be unsuitable for the given feedwater due to the low sulfate selectivity at feedwater concentration. The same analysis can be performed for a polyacrylic resin shown in **Figure 2.3**.



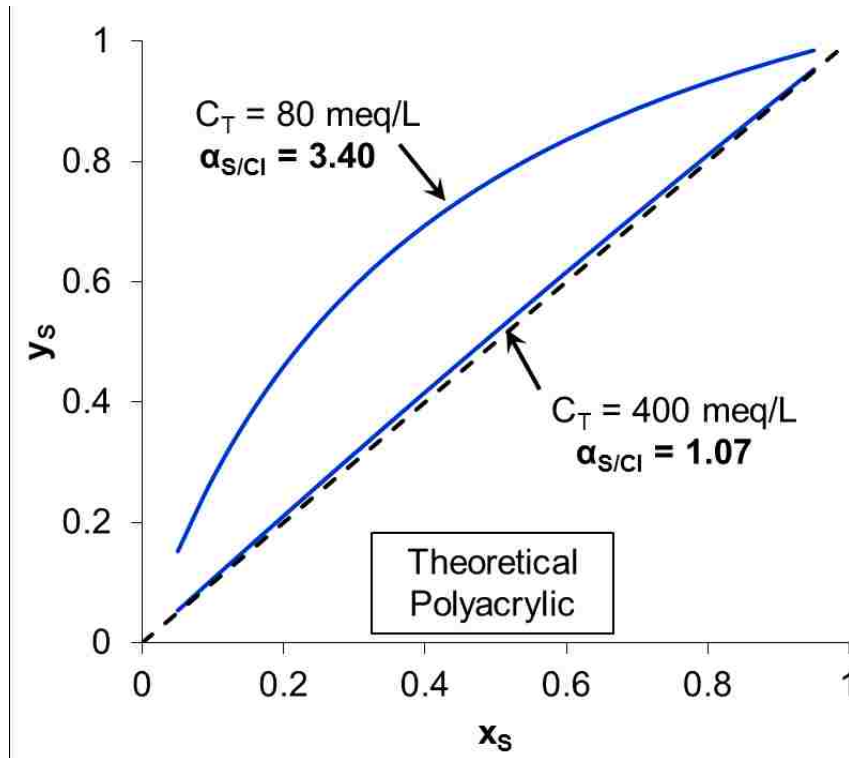


**Figure 2.3** Theoretical polyacrylate selectivity curve at 80 meq/L and 400 meq/L

Here, the opposite situation occurs: high sulfate selectivity at feedwater concentrations but low chloride selectivity at RO reject concentrations. In order for the HIX-RO process to be sustainable,  $\alpha_{S/C}$  must be greater than 1 at feedwater concentrations, and  $\alpha_{S/C}$  should be less than 1 at RO concentrate concentrations. Neither the polystyrene resin nor the polyacrylic resin alone possesses this quality.

However, if the two resins were mixed together, shown in **Figure 2.4**, the selectivity curves match up with desired criteria: high sulfate selectivity at 80 meq/L (feedwater concentration) and high chloride affinity at 400 meq/L (RO reject concentration).

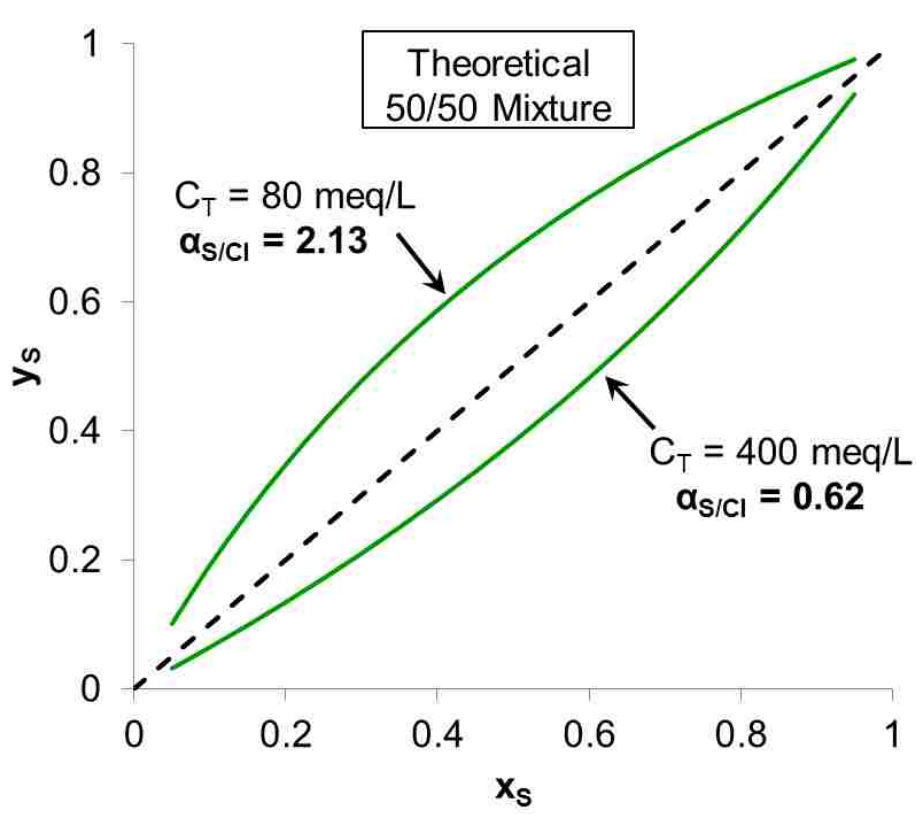


**Figure 2.4** Theoretical 50/50 mixture of polystyrene and polyacrylic resins at 80 meq/L and 400 meq/L

## 2.4 Reduction in CaSO<sub>4</sub> Scaling

The ultimate goal of HIX-RO is to reduce the influent sulfate concentration to prevent the formation of solid CaSO<sub>4</sub>. In order to determine if CaSO<sub>4</sub> precipitation is thermodynamically favorable, the supersaturation index (SI) can be calculated using **Equation 2.4** for a given a feedwater composition.<sup>20</sup>

$$SI = \frac{\{Ca^{2+}\}\{SO_4^{2-}\}}{K_{sp}} \quad \text{Equation 2.4}$$

In which curly brackets indicate species activity and  $K_{sp}$  is the solubility product for CaSO<sub>4</sub>. The SI for CaSO<sub>4</sub> is plotted against the recovery of the RO process in **Figure**

2.5 for both the feedwater and if 80% of sulfate was removed and replaced by chloride. Both curves were generated using the water modeling software Stream Analyzer by OLI Systems.<sup>61</sup>

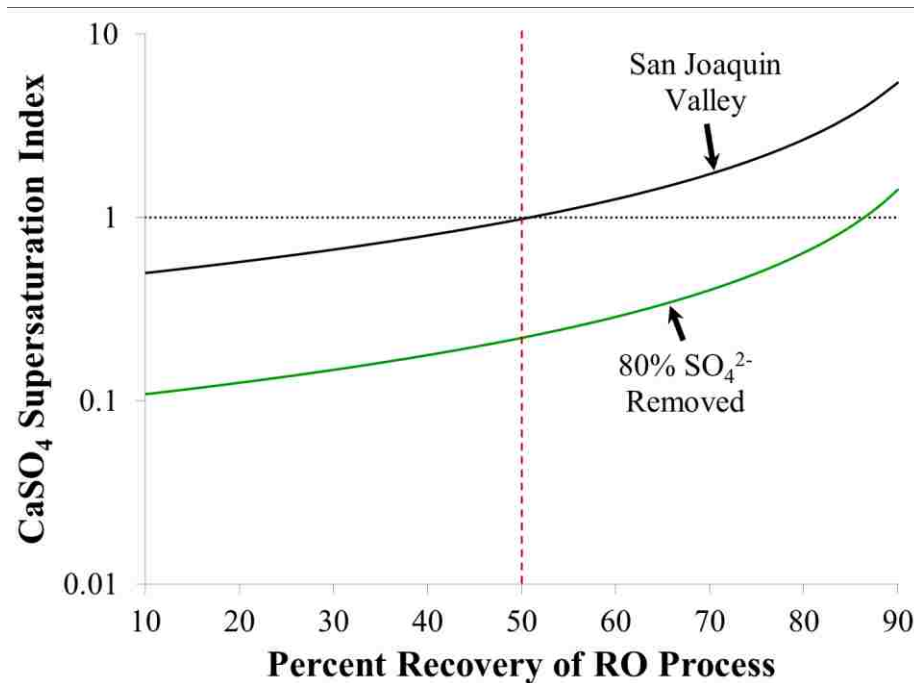


**Figure 2.5** Variation in SI of CaSO<sub>4</sub> with recovery of desalination process

Based on the theoretical isotherm curves generated in **Figure 2.4**, a 50/50 mixture of strong base polyacrylic and strong base polystyrene resins should be able to ensure high sulfate removal for the feedwater in **Table 2.1**. For a high sulfate removal, recovery of 80% is possible and the concentration of the RO reject brine is high enough to induce selectivity reversal resulting in efficient regeneration of the ion exchange column. No additional chemical input would be required other than the concentrate from the RO process.

## **3. Experimental Methodology**

### **3.1 Water analysis**

#### **3.1.1 pH and conductivity**

A handheld Oakton pH meter (Model #WD-35613-10) was used to measure pH. Conductivity was measured using a handheld Accumet conductivity meter (Model #AP75).

#### **3.1.2 Chloride**

Chloride was analyzed by the argentometric titration method. Samples were diluted to a volume of 100 mL and placed in a 250 mL Erlenmeyer flask and pH was adjusted to between 7 and 10 using 2% NaOH. One mL of 5%  $K_2CrO_4$  indicator was added. The sample was placed on a stir plate and titrated against standardized 0.0141 N  $AgNO_3$ . Chloride precipitates with  $Ag^+$  to form solid  $AgCl$ . Once all  $Cl^-$  has been precipitated,  $Ag^+$  will form the dark red precipitate  $Ag_2CrO_4$  and the solution will change color from yellow to pink.<sup>62</sup>

#### **3.1.3 Sulfate**

Analysis of sulfate was performed using a commercially available sulfate testing kit available from the Hach Company (SulfaVer 4 Method #8051). An aliquot of 10 mL is placed in a glass sample cell and one pillow of powdered  $BaCl_2$  is added. The cell is then swirled to dissolve  $BaCl_2$ , and any sulfate present will precipitate as  $BaSO_4$ . The sample is left to react for 5 minutes and then analyzed using Hach Spectrophotometer

(Model DR 7000) in which sample absorbance of the sample is directly correlated to mg/L as  $\text{SO}_4^{2-}$ .<sup>63</sup>

### **3.1.4 Ion Chromatography**

In addition to the methods described in **Sections 3.1.2** and **3.1.3**, ion chromatography was also used to determine the concentration of  $\text{Cl}^-$  and  $\text{SO}_4^{2-}$ . Analysis was performed using a Dionex ICS-1000 Ion Chromatograph with chromatography column AS10 and a conductivity detector. Based on the manufacturer recommendations, a 9.0 mM  $\text{Na}_2\text{CO}_3$  buffer was used as the eluent at a flow rate of 1.0 mL/min<sup>64</sup>

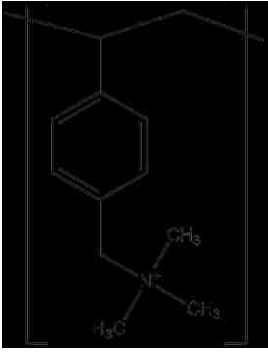
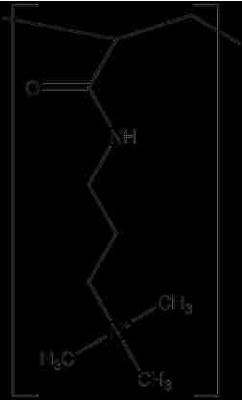
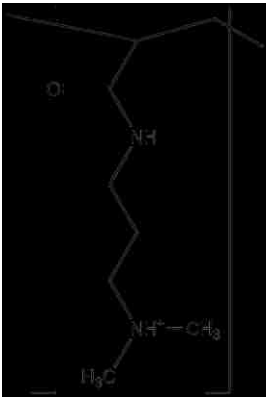
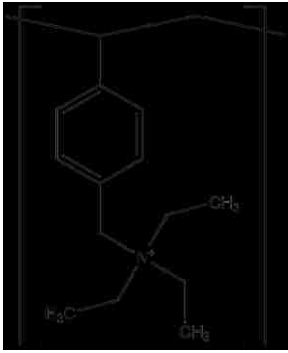
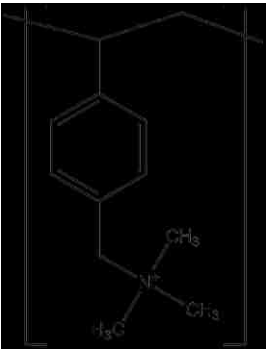
### **3.1.5 Atomic Absorption Spectroscopy**

Total aqueous concentrations of Na, Mg, and Ca were measured using a Perkin Elmer Flame Atomic Absorption Spectrometer (AAAnalyst 200). Five-point calibration curves were prepared from primary standards (Ricca Chemical). For all analyses, an acetylene/air flame was used.<sup>65</sup> Any samples exceeding the concentration of the highest standard were diluted accordingly.

## **3.2 Classification of ion exchange resin**

Five different anion exchange resins were used in this study and their properties are shown in **Table 3.1**.

**Table 3.1** Properties of anion exchange resins used

<b>Manufacturer</b>	Purolite, Inc.	Purolite, Inc.	Purolite Inc.	Rohm and Haas Co	Layne Christensen
<b>Trade Name</b>	A400	A850	A830	IRA-900	LayneRT
<b>Type</b>	Strong Base	Strong Base	Weak Base	Strong Base	Strong Base
<b>Matrix</b>	Polystyrene	Polyacrylic	Polyacrylic	Polystyrene	Polystyrene
<b>Functional Group</b>	Quaternary Trimethylamine	Quaternary Trimethylamine	Tertiary Trimethylamine	Quaternary Triethylamine	Quaternary Trimethylamine with impregnated iron oxide nanoparticles
<b>Structure</b>					

### **3.2.1 Resin capacity measurement**

Anion exchange resins were put in chloride form by packing a glass column with a known mass of air-dried resin and passing a dilute sodium chloride solution through the column until the influent and effluent solution had the same concentration of chloride. For the weak base polyacrylic resin, concentrated HCl was also added to the chloride solution and both pH and chloride measurements were taken. Columns were then washed with DI water. Next, a dilute sulfate solution was prepared and passed through the conditioned resin. Effluent was collected in a container until influent and effluent sulfate concentrations were equivalent. The total volume of collected effluent was measured, and resin capacity was calculated by measuring the total concentration of sulfate chloride. The total mass of chloride in the effluent solution was then assumed to be the total mass of chloride present on the column, and therefore the resin capacity.

### **3.2.2 Batch sulfate/chloride isotherms**

Resins were first conditioned by packing in a glass column and passing a dilute sodium chloride solution until the influent and effluent chloride concentrations were equal. The column was then washed with DI water. The resins were then removed from the glass column and placed on the lab bench to air dry at room temperature for at least 48 hours.

Next, varying masses of air dried ion exchange resin were placed in plastic bottles. A stock solution of sulfate at the desired isotherm concentration was prepared and equal volumes of solution were added to each bottle containing a known mass of resin. The bottles were then capped, sealed with Parafilm, and placed on a rotary shaker

for at least 24 hours. The solution was decanted from the resin and the composition was analyzed for chloride and sulfate.

### **3.2.3 Column sulfate/chloride isotherms**

A known mass of air dried ion exchange resin was packed in a glass column and a dilute sodium chloride solution was passed through the column at a constant flow rate using a ceramic peristaltic pump until the influent and effluent chloride concentrations were equal. The column was washed with DI water and a prepared solution containing both chloride and sulfate was passed. Effluent solution was collected in glass test tubes using an Eldex Universal Fractional Collector and the column was run until the effluent chloride and sulfate concentrations matched the influent concentration.

### **3.2.4 Scanning electron microscopy**

Cross sectional analysis of ion exchange resin was performed using a Philips XL-30 Environmental Scanning Electron Microscope. Samples were prepared by slicing individual ion exchange beads with razor blades that had been immersed in liquid nitrogen. The bead halves were mounted onto pegs using double sided carbon tape and sputter coated with iridium using an Electron Microscopy Sciences high vacuum sputter coater (Model EMS575X).<sup>66</sup>

## **3.3 HIX-RO Runs**

Six different runs of HIX-RO were performed using a different combination of feedwater and resin composition for each. For all cycles, 20L of influent solution was



prepared and passed down flow through 1 L of ion exchange resin. The effluent solution was collected and subjected to reverse osmosis. Finally, the concentrate stream from RO was passed upflow through the ion exchange column. This process of ion exchange, RO, and ion exchange regeneration constitutes one “cycle” and a group of cycles was considered to be a “run”. Before beginning a run, the resin was first conditioned by passing a dilute chloride solution until the influent and effluent chloride concentrations were equal and washed with DI water. In between cycles, the resin bed was not washed or disturbed in any way. Any remaining solution from a previous cycle remained inside the column at the start of the next cycle.

Several different synthetic influent solutions were prepared based on the composition given in **Table 2.1**. For each run, the feedwater was modified slightly to accommodate the new resin type, and the composition for each is detailed in **Table 3.2**.

In addition to different feedwaters, the type of resin mixture used in the ion exchange column was also varied. A list of the overall mixing ratios and feedwater composition used for all six HIX-RO runs is in **Table 3.3**.

**Table 3.2** Feedwater composition for all HIX-RO Runs

	Feedwater "A"	Feedwater "B"	Feedwater "C"	Feedwater "D"	Feedwater "E"
Na <sup>+</sup>	75 meq/L	75 meq/L	141 meq/L	75 meq/L	75 meq/L
Mg <sup>2+</sup>	5 meq/L	5 meq/L	9 meq/L	5 meq/L	5 meq/L
Cl <sup>-</sup>	60 meq/L	60 meq/L	112 meq/L	55 meq/L	55 meq/L
SO <sub>4</sub> <sup>2-</sup>	20 meq/L	20 meq/L	38.5 meq/L	20 meq/L	20 meq/L
Phosphate	-	-	-	0.5 - 1.0 mg/L as P	2 mg/L as P
Alkalinity	-	-	-	190 mg/L as CaCO <sub>3</sub>	190 mg/L as CaCO <sub>3</sub>
pH	7.0	5.0	7.0	8.0	8.0

**Table 3.3** Summary of all HIX-RO Runs

	Run 1	Run 2	Run 3	Run 4	Run 5 (Cycles 1-9)	Run 5 (Cycles 10-13)	Run 6
Feedwater (see Table 3.2)	A	A	B	C	D	D	E
Fraction polystyrene resin	0.5	-	-	1	0.45	0.5	-
Fraction polyacrylic resin	0.5	1	-	-	0.45	0.5	-
Fraction weak base polyacrylic resin	-	-	1	-	-	-	-
Fraction phosphate selective resin	-	-	-	-	0.1	-	-
Fraction triethylamine resin	-	-	-	-	-	-	1

### **3.3.1 Run 1: Mixed bed polystyrene and polyacrylic with Feedwater “A”**

For the first mixed polystyrene and polyacrylic run, 10 cycles of HIX-RO were performed. The feedwater solution was modified such that any equivalent concentration of bicarbonate was converted to chloride under the assumption that hydrochloric acid had been dosed to eliminate the threat to carbonate scaling. In addition, all calcium was converted to an equivalent amount of sodium to ensure that no scaling occurs during the cycles (Feedwater “A”). The pH was adjusted to 7.0 at the beginning of all cycles through addition of dilute hydrochloric acid or sodium hydroxide solutions.

### **3.3.2 Run 2: Pure strong base polyacrylic with Feedwater “A”**

Ten cycles of HIX-RO were performed using only strong base polyacrylic resin and the same feedwater as Run 1 (Feedwater “A”).

### **3.3.3 Run 3: Pure weak base polyacrylic with Feedwater “B”**

Twenty five cycles of HIX-RO was performed using only weak base polyacrylic resin. Influent solution was the same as the Run 1 except pH was artificially lowered to 5.0 using dilute hydrochloric acid (Feedwater “B”). Adjustment to pH was necessary because at high pH ( $\text{pH} > 8.0$ ), the polyamine functional groups can be converted back to their free base form eliminating any ion exchange properties.

### **3.3.4 Run 4: Pure strong base polystyrene with Feedwater “C”**

Ten cycles of HIX-RO was performed using only strong base polystyrene resin. Influent solution was a modified version of Feedwater “A” in which the individual ratio of ions

was kept the same but scaled up to make the total concentration 150 meq/L (Feedwater “C”).

### **3.3.5 Run 5: Mixed bed polystyrene and polyacrylic with phosphate selective resin with Feedwater “D”**

Nine cycles of HIX-RO were performed using an ion exchange bed containing 900 mL of a 50/50 mixture of strong base polyacrylic and strong base polystyrene resins and 100 mL of a phosphate selective resin. The feedwater composition for 9 cycles was similar to Feedwater “A” except both bicarbonate and phosphate were dosed (Feedwater “D”). This composition is closer to the actual feedwater (**Table 2.1**) but with added phosphate. The bicarbonate concentration was 190 mg/L as  $\text{CaCO}_3$  and phosphate was 0.5 mg/L. After completing cycle 9, 75 mL of the phosphate selective resin was removed (as much as could be removed) from the column to determine if there would be a difference in phosphate removal. In addition, the influent feedwater phosphate concentration was doubled to 1.0 mg/L. Another 4 cycles of HIX-RO was performed using the doubled phosphate feedwater and no phosphate selective resin; in total 13 cycles of HIX-RO were performed.

Phosphate was added because it is a commonly found ion in surface and waste water and, as shown in **Table 3.4** calcium phosphate is much more insoluble than calcium sulfate.<sup>67</sup>

**Table 3.4** Solubility of commonly found precipitates in desalination processes

Species	$pK_{sp}$
$Ca_3(PO_4)_2$ (s)	24.0
$CaHPO_4$ (s)	6.66
$CaSO_4$ (s)	4.59

### **3.3.6 Run 6: Pure polystyrene with triethylamine functional groups with Feedwater “E”**

Ten cycles of HIX-RO were performed using a strong base polystyrene resin with triethylamine functional groups. The feedwater was similar to Feedwater “D” except phosphate concentration was increased to 2.0 mg/L (Feedwater “E”).

## **3.4 Ion Exchange**

A custom made ion exchange column was used during all HIX-RO cycles. The main body of the column was constructed from clear PVC with screw-on PVC end caps. The inner diameter was 5 cm and the total length of the column was 68 cm. Glass wool was packed into the top and bottom to prevent any loss of ion exchange resin during use. Solution was fed using a variable speed peristaltic pump.

## **3.5 Reverse Osmosis**

Influent solution was stored in a polyethylene tank and fed using a stainless steel piston pump (Cat Pumps, Model 2SF35SEEL) powered by a 1.5 hp electric motor. A filter (GE SmartWater GXWH20F) was placed before the membrane to prevent damage from any particulate matter in the feedwater. Desalination was performed using a Dow

Filmtec SW30-2540 Spirally Wound Reverse Osmosis Membrane. All tubing was made of 316 stainless steel to avoid corrosion. A cooling coil was immersed in the feed solution and tap water was fed through to maintain temperature at 20 °C to 25 °C.

### **3.6 Measuring CaSO<sub>4</sub> Precipitation Kinetics**

The induction time for CaSO<sub>4</sub> precipitation was measured by setting up a time lapse experiment. Two stock solutions of 0.03M CaCl<sub>2</sub> and 0.03M Na<sub>2</sub>SO<sub>4</sub> were prepared using ACS grade chemicals. Equal volumes of stock solution were then mixed with varying ratios of DI water in 20 x 170 mm test tubes to form supersaturated solutions of CaSO<sub>4</sub>. The exact SI values were calculated using OLI Stream Analyzer.<sup>61</sup> The test tubes were covered in Parafilm and vigorously shaken until the solution was well mixed. The test tubes were then placed in a test tube rack in front of a black background. A digital video camera with time lapse function was programmed to take a picture every 5 seconds and used to record images of the test tubes for 27 hours. After recording, the footage was analyzed frame by frame to determine the exact time when the first visible crystal of CaSO<sub>4</sub> precipitated.

### **3.7 In-Column CaSO<sub>4</sub> Precipitation**

The potential for in-column precipitation of CaSO<sub>4</sub> was studied using a small scale column setup. An 11 mm glass column was filled with a 50/50 mixture, by mass, of polystyrene anion exchange resin and polyacrylic anion exchange resin. A dilute solution of NaCl was passed through the column to ensure the resin was in chloride

form. The column was then washed with DI water until the conductivity of the effluent matched that of the influent.

A synthetic influent solution was prepared that simulated the actual feedwater given in **Table 2.1**. The regenerant solution, synthetic RO concentrate, was a simulated RO concentrate had the synthetic influent solution already been subjected to ion exchange and RO at 80% recovery. **Table 3.5** gives the exact composition for each solution.

**Table 3.5** Composition of synthetic feedwater and regenerant solution

	Synthetic Feedwater	Synthetic Regenerant
Na <sup>+</sup>	50 meq/L	250 meq/L
Mg <sup>2+</sup>	5 meq/L	25 meq/L
Ca <sup>2+</sup>	25 meq/L	125 meq/L
Cl <sup>-</sup>	60 meq/L	400 meq/L
SO <sub>4</sub> <sup>2-</sup>	20 meq/L	-

During one cycle, 20 bed volumes of synthetic influent solution were passed down flow through the column and collected for analysis. Next, 4 bed volumes of synthetic RO concentrate solution was passed upflow through the column and collected using a fractional collector. The empty bed contact time for the column was purposely kept as low as possible to avoid any possible in-column precipitation. Immediately after passing regenerant, another 20 BV of influent solution was passed to ensure that there was never an extended period where the column could be in a supersaturated state.

The process of passing synthetic influent followed by passing synthetic RO concentrate constituted 1 cycle. For the first 3 cycles, after passing regenerant solution,

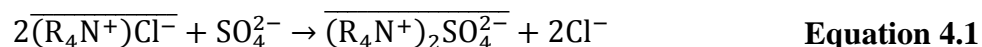


the collected samples were covered in Parafilm and left to precipitate. After at least 24 hours, samples were then taken and measured for calcium and sulfate to determine the post-precipitation concentration of calcium and sulfate. During the fourth regeneration cycle, samples from the column effluent of the column were taken and immediately diluted 1:100 and analyzed for calcium and sulfate to determine the pre-precipitation concentration of calcium and sulfate in solution.

## 4. Control of ion exchange selectivity through mixing

### 4.1 Background on ion exchange chemistry

The HIX-RO process is based on the selective removal of sulfate by a chloride-loaded strong base anion exchange resin as detailed in **Equation 4.1**.



The equilibrium constant,  $K$ , for an ion exchange reaction is known as the selectivity coefficient, and for the reaction between sulfate and chloride,  $K_{S/C}$  can be calculated by

$$K_{S/C} = \frac{\overline{[SO_4^{-2}]}[Cl^-]^2}{[SO_4^{-2}]\overline{[Cl^-]}^2} \quad \text{Equation 4.2}$$

If chloride and sulfate are the only anionic species present, then the fraction of sulfate in solution,  $x_S$ , and the total equivalent concentration,  $C_T$ , of anions in solution in eq/L is

$$x_S = \frac{2[SO_4^{-2}]}{[Cl^-] + 2[SO_4^{-2}]} = \frac{2[SO_4^{-2}]}{C_T} \quad \text{Equation 4.3}$$

Similar calculations can be performed to calculate the fraction of each species on the resin,  $y_S$

$$y_S = \frac{2\overline{[SO_4^{-2}]}}{Q} \quad \text{Equation 4.4}$$

In which  $Q$  is the total resin capacity in eq/g. For chloride,  $x_C$  and  $y_C$  are calculated in the same manner, and substituting **Equation 4.3** and **Equation 4.4** into **Equation 4.2** results in

$$K_{S/C} = \frac{y_S x_C^2 C_T}{x_S y_C^2 Q} \quad \text{Equation 4.5}$$

From a purely theoretical point of view,  $K_{S/C}$  is not a constant and may vary depending on experimental conditions. However, due to the small amount of variation over which  $K_{S/C}$  can change, it is a valid assumption that  $K_{S/C}$  remains constant.<sup>57,68,69</sup> The units of  $K_{S/C}$  are extremely important. While  $x$  and  $y$  are unitless,  $C_T$  and  $Q$  may be expressed in different units. Most commonly,  $C_T$  has units of [meq/L] and  $Q$  has units of [meq/g] making the overall units of  $K_{S/C}$  [g/L]. From these terms the separation factor, denoted by  $\alpha_{S/C}$ , may be calculated

$$\alpha_{S/C} = \frac{y_S x_C}{x_S y_C} \quad \text{Equation 4.6}$$

When  $\alpha_{S/C} > 1$ , sulfate is the preferred species and vice versa.  $\alpha_{S/C}$  is significantly different from  $K_{S/C}$  and is *not* a constant. The value of  $\alpha_{S/C}$  will vary depending on several factors most importantly solution concentration and composition. Changing the total solution concentration,  $C_T$ , has a more significant effect on  $\alpha_{S/C}$  than changing solution composition, i.e.  $x_S$  or  $x_C$ .

The term  $\alpha$  can also be found in chromatography ( $\alpha^{Chr}$ ) when comparing the relative retention of one species compared to another. The value of  $\alpha^{Chr}$  for species “A” and “B” is calculated using **Equation 4.7**

$$\alpha_{A/B}^{Chr} = \frac{t_A - t_m}{t_B - t_m} \quad \text{Equation 4.7}$$

in which  $t_A$ ,  $t_B$ , and  $t_m$  are the total retention times for “A”, “B”, and the mobile phase, respectively.<sup>70</sup> In general, the concept of  $\alpha$  for both cases is the same: how preferred is one species compared to the other? For chromatography, this is a comparison of how long after the mobile phase has exited does the species exit. For ion exchange, it is the ratio of what fraction of the species is on the resin compared to in solution. While the general idea is the same, numerically  $\alpha^{IX} \neq \alpha^{Chr}$ .

## 4.2 Determination of resin separation factor using a batch system

Following the procedure detailed in **Section 3.2.2**,  $\alpha_{S/C}$  may be determined for a given solution  $C_T$ . Knowing the total resin capacity and the initial concentration of sulfate,  $x_S$  and  $y_S$  may be calculated using **Equation 4.3** and **Equation 4.4**, respectively. Plotting  $x_S$  vs.  $y_S$  gives one of three curves shown in **Figure 4.1**.

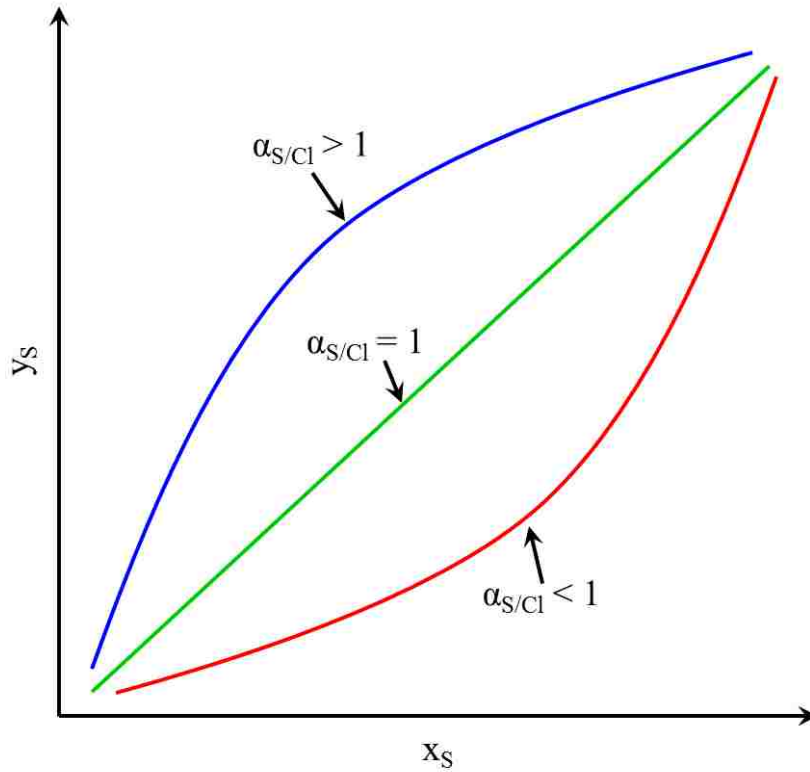


**Figure 4.1** Generalized isotherm curves for sulfate/chloride system

When the curve is above the diagonal then sulfate is preferentially removed by the resin and  $\alpha_{S/C}$  is greater than 1. Similarly, when the curve is below the diagonal  $\alpha_{S/C}$  is less than 1 and chloride is the preferred species. The diagonal line represents the case when  $\alpha_{S/C}$  is exactly equal to 1 and neither chloride nor sulfate is preferred. Calculation of  $\alpha_{S/C}$  may be performed in two different ways. First,  $\alpha_{S/C}$  may be calculated at each point gathered during the batch isotherm and the individual values can be averaged. However, a more precise method is to consider all the data points equally by determining the total area above and below the curve created. The area below the isotherm curve is calculated using the trapezoid method and the area above the curve is equal to one minus the area

below the isotherm. Finally, **Equation 4.8** may be solved for  $\alpha_{S/C}$  using a numerical solver as there is no explicit answer for  $\alpha_{S/C}$ .<sup>58</sup>

$$\frac{\text{Area below isotherm}}{\text{Area above isotherm}} = \frac{(\alpha^2 - \alpha - \alpha \ln \alpha)/(\alpha - 1)^2}{1 - (\alpha^2 - \alpha - \alpha \ln \alpha)/(\alpha - 1)^2} \quad \text{Equation 4.8}$$

### 4.3 Determination of resin separation factor using a column system

For a binary chloride/sulfate system, a glass column is packed with resin in chloride form. A solution containing both chloride and sulfate is passed through the column following the procedure in **Section 3.2.3**, and samples are collected until the influent and effluent concentrations are equal.

The total area below the curves is the total mass of sulfate or chloride that exited the column. The total mass that was actually passed through the column is determined from the volume of solution passed and the feedwater composition. The difference between these two values is the mass of sulfate or chloride that was sorbed by the column. **Equation 4.3** and **Equation 4.4** are used to determine  $x_S$  and  $y_C$ , respectively, and subsequently  $\alpha_{S/C}$  can be calculated by **Equation 4.6**.

### 4.4 Determination of resin separation factor from the selectivity coefficient

Previously described methods in **Sections 4.2** and **4.3** can only determine  $\alpha_{S/C}$  at one  $C_T$ . For the HIX-RO system,  $C_T$  is not constant and changes depending on the feedwater or RO concentrate composition. It becomes beneficial to determine  $\alpha_{S/C}$  at various concentrations without having to run batch or column studies. At least one isotherm

must be run to determine  $K_{S/C}$  for a given resin and  $\alpha_{S/C}$  may be theoretically determined at any  $C_T$ . For a binary where sulfate and chloride are the only anions present

$$x_S + x_C = 1 \quad \text{Equation 4.9}$$

and

$$y_S + y_C = 1 \quad \text{Equation 4.10}$$

**Equation 4.9** and **Equation 4.10** are rearranged and substituted into **Equation 4.5** and rearranged to **Equation 4.11**

$$\frac{y_S}{(1 - y_S)^2} = \frac{KQx_S}{(1 - x_S)^2 C_T} \quad \text{Equation 4.11}$$

and  $y_S$  can be determined using the quadratic equation

$$y_S = \frac{\frac{2A + 1}{A} - \sqrt{\left(\frac{2A + 1}{A}\right)^2 - 4}}{2} \quad \text{Equation 4.12}$$

in which

$$A = \frac{KQx_S}{(1 - x_S)^2 C_T} \quad \text{Equation 4.13}$$

Only the negative root of the solution is a valid solution as the positive root gives a value of  $y_S$  greater than 1. Simplifying **Equation 4.12** results in **Equation 4.14**

$$y_S = \frac{2A + 1 - \sqrt{4A + 1}}{2A} \quad \text{Equation 4.14}$$

And  $\alpha_{S/C}$  may be determined using **Equation 4.6**. This solution is valid assuming  $K_{S/C}$  is constant at a given  $x_S$  and  $C_T$ .

#### 4.5 Theoretical prediction of resin separation factor for two mixed resins

For a mixture of two resins the separation factor,  $\alpha_{S/C}$ , for each individual resin remains the same, but the bulk separation factor,  $\alpha_{S/C}^*$ , is different and describes the entire resin mixture. For a mixture of two different resins “A” and “B” with masses  $m_A$  and  $m_B$ , the ratio of resin A,  $\Phi_A$ , is

$$\Phi_A = \frac{m_A}{m_A + m_B} \quad \text{Equation 4.15}$$

Similarly for resin B

$$\Phi_B = \frac{m_B}{m_A + m_B} = 1 - \Phi_A \quad \text{Equation 4.16}$$

The total ion exchange capacity of the system is therefore

$$Q^* = Q_A \Phi_A + Q_B (1 - \Phi_A) \quad \text{Equation 4.17}$$

Calculation of  $\alpha_{S/C}^*$  is similar to **Equation 4.6**

$$\alpha_{S/C}^* = \frac{y_S^* x_C}{x_S y_C^*} \quad \text{Equation 4.18}$$



in which

$$y_S^* = \frac{y_S^A Q_A \Phi_A + y_S^B Q_B (1 - \Phi_A)}{Q^*} \quad \text{Equation 4.19}$$

and  $y_S$  for either resin may be calculated using **Equation 4.14**.

Using this method, it is possible to generate a range of mixing ratios over which the HIX-RO process will be favorable. Using the same selectivity data used to create **Figure 2.2** and **Figure 2.3**, **Figure 4.2** shows the change in  $\alpha_{S/Cl}^*$  with different mixing for the San Joaquin Valley water (composition given in **Table 2.1**).

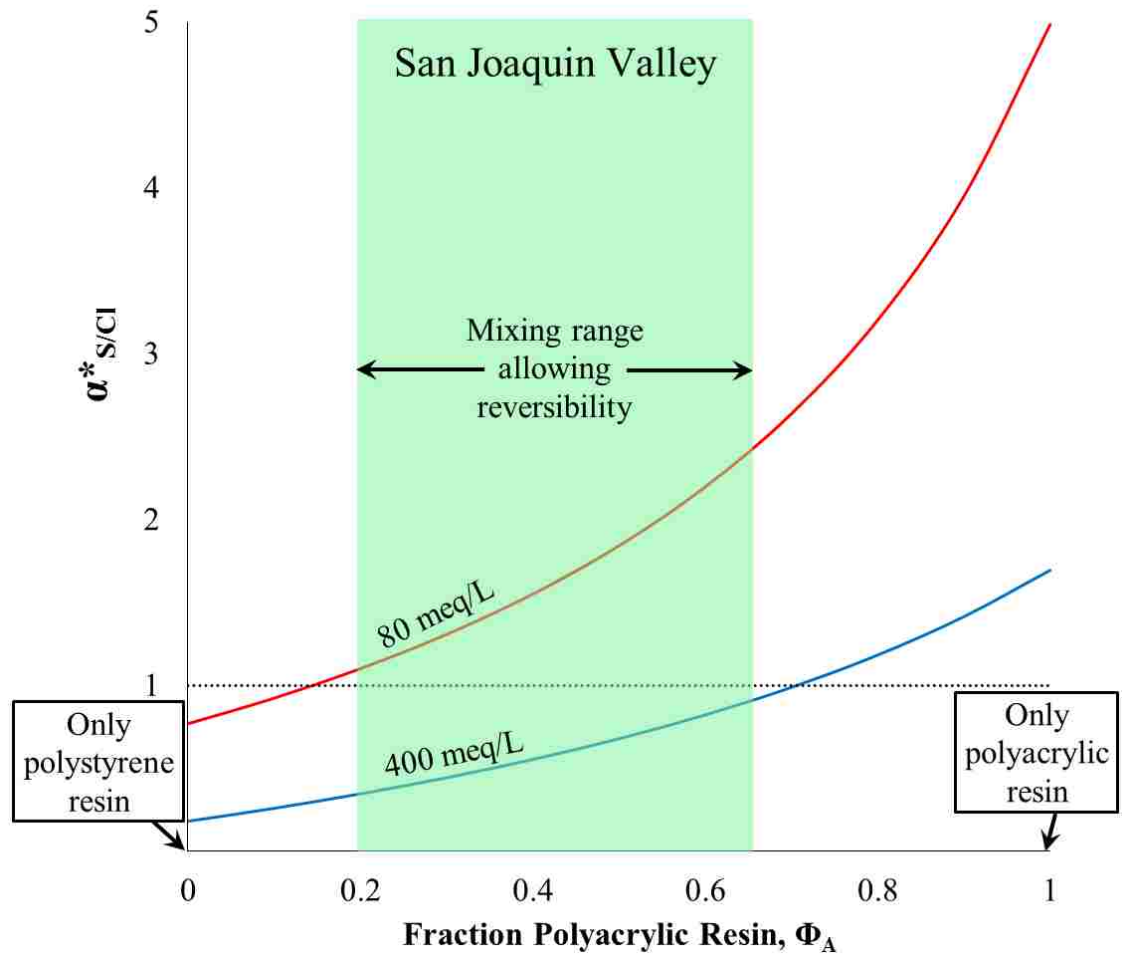


**Figure 4.2** Variation in theoretical  $\alpha^*_{S/Cl}$  with changing mixing ratio

Based on these theoretical calculations, the initial HIX-RO runs were chosen to use a 50/50 mixture of polystyrene and polyacrylic resins as it gives  $\alpha^*_{S/Cl} > 1$  at feedwater concentrations and  $\alpha^*_{S/Cl} < 1$  at RO reject concentrations.

#### **4.6 Classification of resin properties affecting sulfate selectivity**

There are several properties of the ion exchange resin which may affect the overall resin sulfate selectivity:

1. Composition of the polymer matrix
2. Size of the functional group
3. Basicity of the functional group

Matrix type refers to the base polymer that has been functionalized to give ion exchange capabilities. The two most commonly used polymers are polyacrylate and polystyrene. Variations in the basicity and size of the functional group also affect selectivity. Weak base resins selectivity remove divalent ions more than resins with strong base functional groups.<sup>59</sup> The size of the functional group also affects selectivity. Steric hindrance between an ion and the functional group will change the overall selectivity. Replacing a quaternary ammonium functional group ( $\text{R-N}^+(\text{CH}_3)_3$ ) with a triethylamine group ( $\text{R-N}^+(\text{CH}_2\text{CH}_3)_3$ ) hinders the ability of divalent ions like sulfate to interact with the functional group resulting in lowered sulfate selectivity.<sup>71</sup>

Comparing resin matrix effects only, the polyacrylic resin has higher affinity toward sulfate than the polystyrene resin with the same functional groups. This effect can be attributed to the fact that the polyacrylic resin has higher capacity than the polystyrene resin implying that for a given ion exchange bead, there are more active sites for sulfate to interact with making adsorption easier.

The effects of changing the basicity of the functional group is shown in **Figure 4.3**. The isotherms for the polyamine and tertiary amine resins are garnered from selectivity data in the open literature.<sup>58</sup>

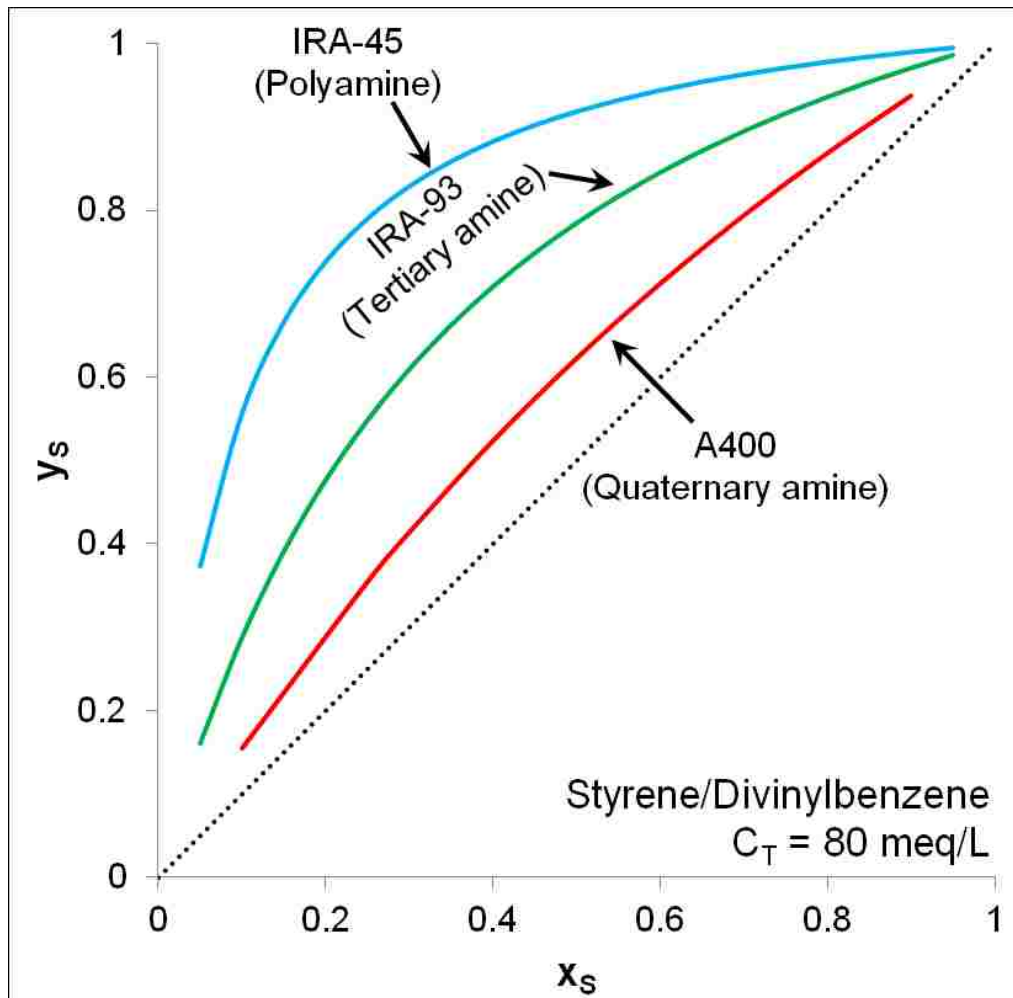


**Figure 4.3** Effect of changing basicity of functional group

Resins with weaker base functional groups exhibit higher affinity toward sulfate than those with strong base functional groups. In other words, the order of sulfate selectivity follows:

$$\text{polyamine} > \text{tertiary} > \text{quaternary}$$

In total, resins with a polyacrylic matrix or weak base functional groups have higher affinity toward sulfate than resins with a polystyrene matrix or strong base functional group.

#### 4.7 Experimental measurement of individual resin separation factor

Six batch studies were performed for all three resin types at 80 meq/L total ion concentration. The resulting isotherm curves generated from these batch tests are shown in **Figure 4.4**.

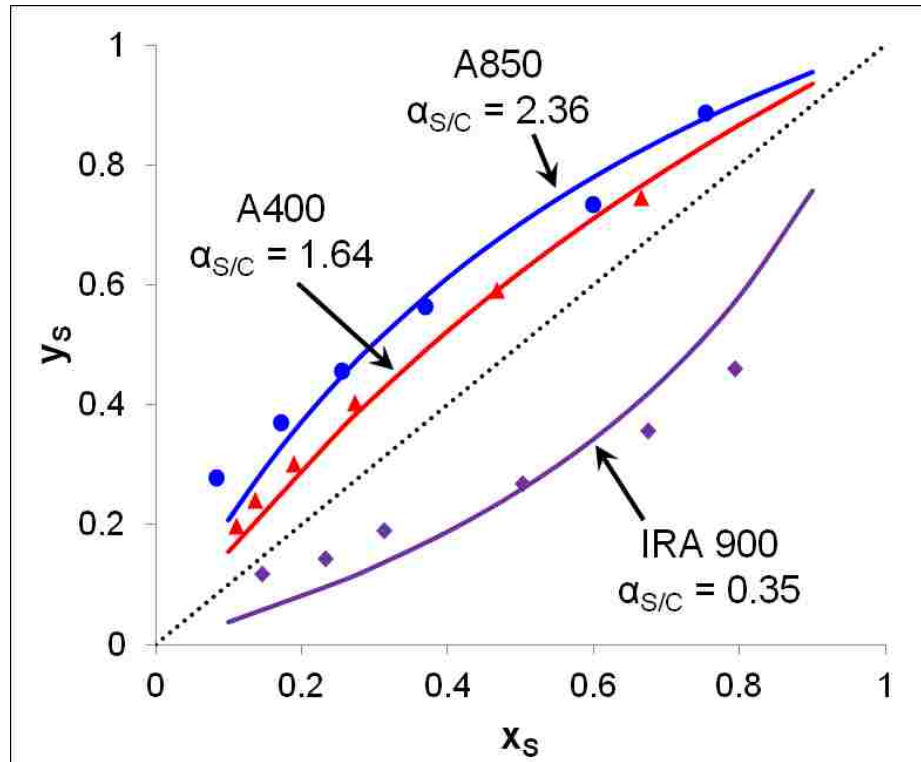


**Figure 4.4** Batch testing results for strong base polystyrene, strong base polyacrylic resin and polystyrene with triethylamine functional group at 80 meq/L

The separation factor,  $\alpha_{S/C}$ , was determined by **Equation 4.6** from the measured data and using **Equation 4.5**,  $K_{S/C}$  values were also determined. A list of the pure resin parameters is in **Table 4.1**.

**Table 4.1** Measured pure resin parameters

	Polystyrene (A400)	Polyacrylic (A850)	IRA 900
Q (meq/g dry resin)	1.8	2.2	3.6 <sup>72</sup>
$\alpha_{S/C}$ at 80 meq/L	1.68	2.36	0.35
$K_{S/C}$ (g/L)	85.1	114.9	6.47

#### 4.8 Experimental measurement of mixed resin separation factors

Both batch and column isotherms were performed to determine mixed resin selectivity using the methods described in **Sections 3.2.2** and **3.2.3**. From theoretical predictions, a 50/50 mixture of polystyrene and polyacrylic resins would result in the highest efficiency. Therefore, isotherms at both 80 meq/L and 400 meq/L were carried out for the 50/50 resin mixture and are shown in **Figure 4.5**.

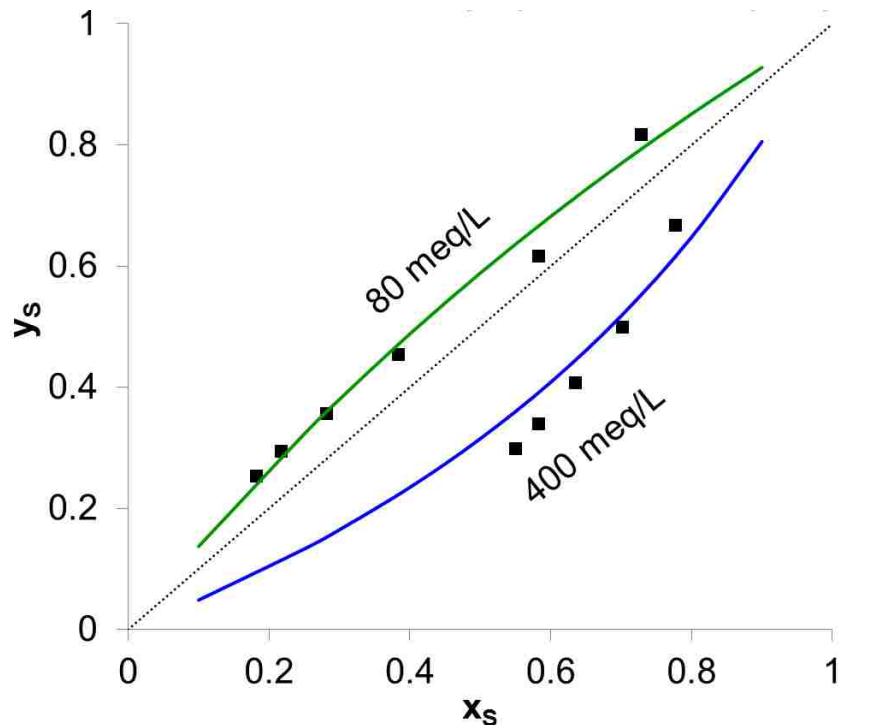


**Figure 4.5** Batch isotherms for 50/50 mixture of polystyrene and polyacrylic resins at 80 meq/L and 400 meq/L

In addition to the 50/50 mixture, isotherms were performed on two other mixing ratios at 80 meq/L: 25:75 and 75:25. Individual results from isotherms are shown in **Appendix II – Isotherm Data** and a summary of the results from pure and mixed isotherms is shown in **Figure 4.6** along with the theoretical  $\alpha_{S/Cl}$ .

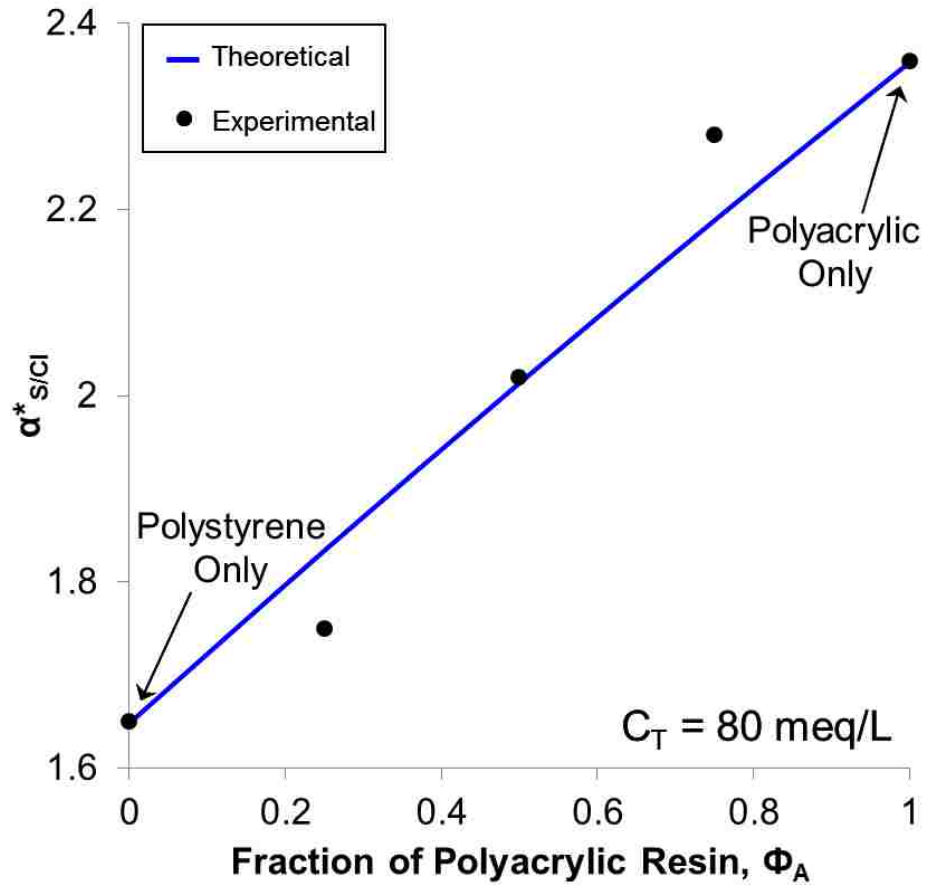


**Figure 4.6** Variation in  $\alpha_{S/Cl}$  with changing fraction of polyacrylic resin at 80 meq/L

It is clear from **Figure 4.6** that theoretical predictions of  $\alpha^*_{S/Cl}$  based on the pure resin isotherm data align well with experimental data.

#### **4.9 Individual resin selectivity compared to bulk resin selectivity**

For the mixed bed system, a unique paradox arises when two separate resins with different selectivities when placed in the same column together exhibit a completely different selectivity. When mixing two resins together, resin “A” and resin “B”, for the individual resin beads, the presence of B has no effect on the separation factor of resin A and the presence of A has no effect on the separation factor of resin B. Yet, when the bulk mixture of the two resins is considered the overall separation factor will be significantly different. In other words: what difference does mixing make?

The best way to answer this question is to compare the best-case scenario of using two separate columns with one mixed column. For an HIX-RO system with one column there is only one possible process configuration: influent and reject pass through the same column. But with 2 different ion exchange columns, one preferring sulfate and the other chloride, there are now 4 possible process configurations depending on the order as shown in **Figure 4.7**.

The order of the columns will significantly affect the overall sulfate removal efficiency. The best case scenario is a situation that produces an RO feed that has low sulfate and ensures good regeneration. The question of what order is best is more easily determined by solving a more general question: given two columns, one with an unfavorable isotherm and another with a favorable isotherm, what order will allow for the most removal of contaminant?



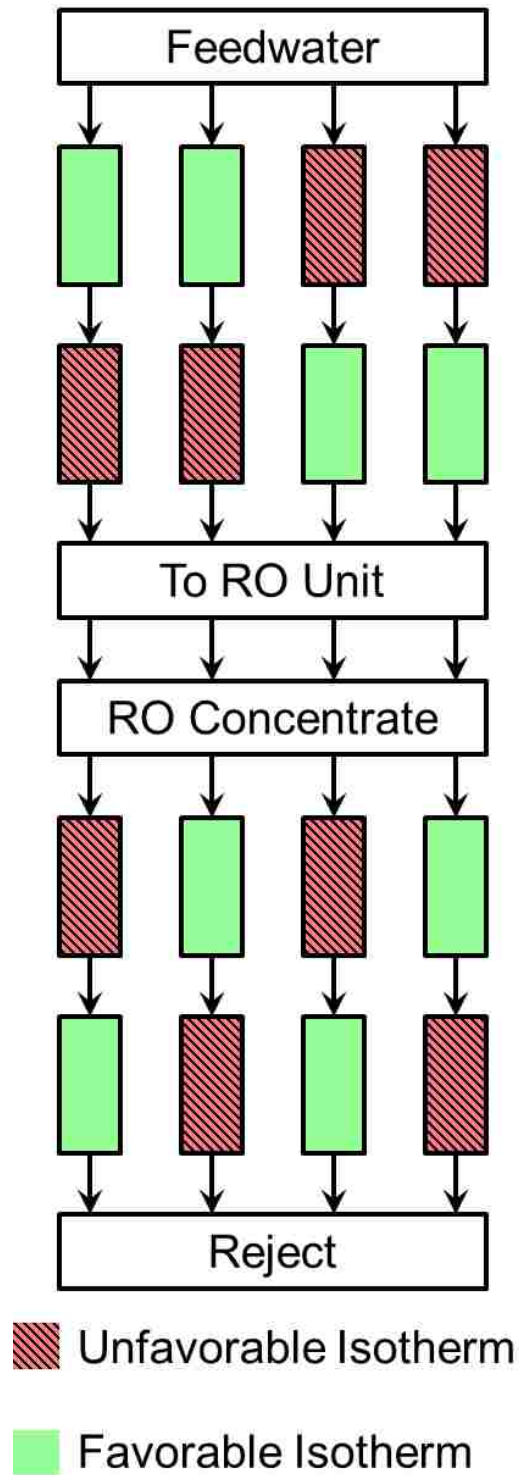


**Figure 4.7** Four possible configurations for a two column HIX-RO system

For an unfavorable isotherm, contaminant breakthrough is gradual and there will always be a measurable quantity of contaminant in the effluent. For the favorable isotherm, no contaminant is seen until the bed is completely exhausted. **Figure 4.8** shows generalized breakthrough curves for both situations.<sup>73</sup>

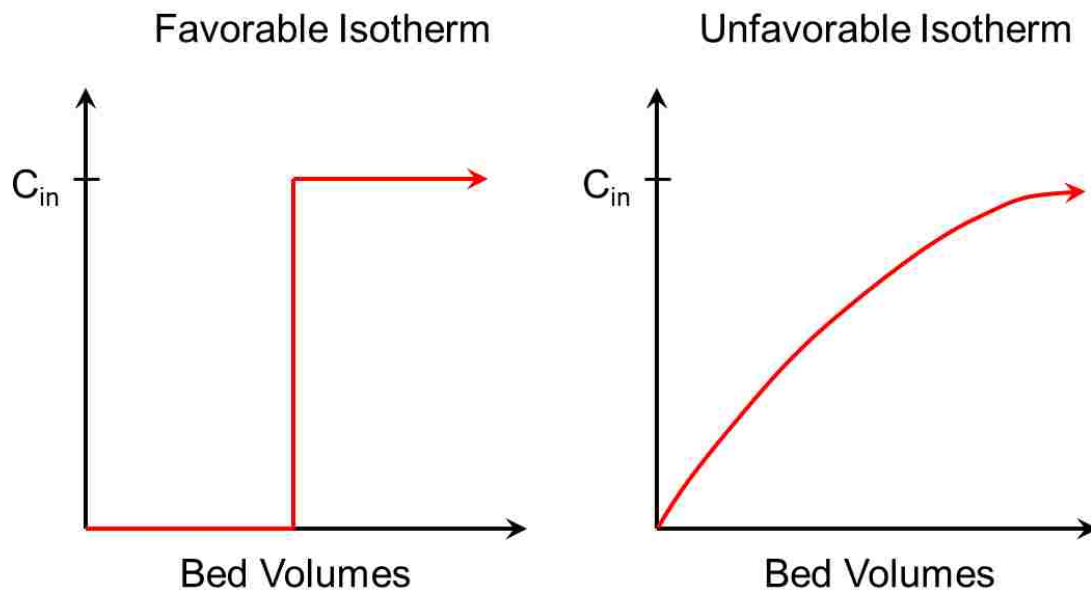


**Figure 4.8** Breakthrough curve for unfavorable and favorable isotherms

For the first step of the process, sulfate removal, the goal is to produce a stream that has as little sulfate as possible. There are two cases: favorable followed by unfavorable and vice versa. Between these two scenarios the best arrangement is the unfavorable column followed by the favorable column. The reasoning is that any sulfate that exits the first column is then favorably picked up by the second column resulting in a sharp breakthrough. **Figure 4.9** shows the theoretical breakthrough curves for both cases.

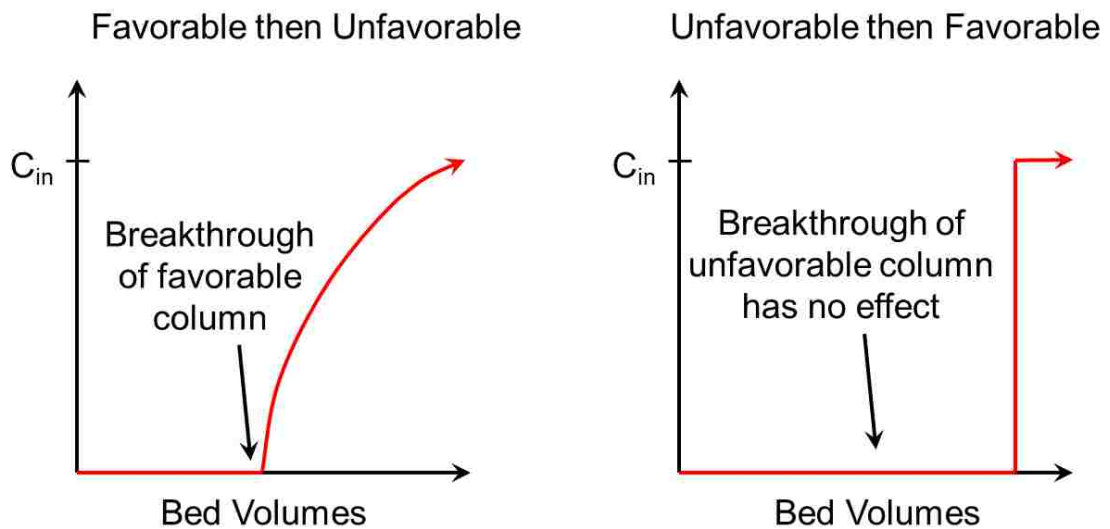


**Figure 4.9** Theoretical breakthrough curves for both scenarios

Based on this argument, the arrangement of an unfavorable column followed by a favorable column would result in the lowest amount of sulfate in RO feed. A mixed bed of ion exchange resin instead acts as an “average” of the 4 possible two-column configurations, and therefore, from a theoretical point of view, two separate columns should provide higher removal efficiency than a single mixed bed column. However, the gain in removal from using separate columns is minimal.

Using the methods described in **Chapter 5**, it is possible to calculate the differences between the four possible configurations and the mixed bed. Using a feedwater containing 20 meq/L  $\text{SO}_4^{2-}$  and 60 meq/L  $\text{Cl}^-$  and 2 different resins, the theoretical RO feed was calculated for 50 cycles of HIX-RO and is shown in **Figure 4.10**.

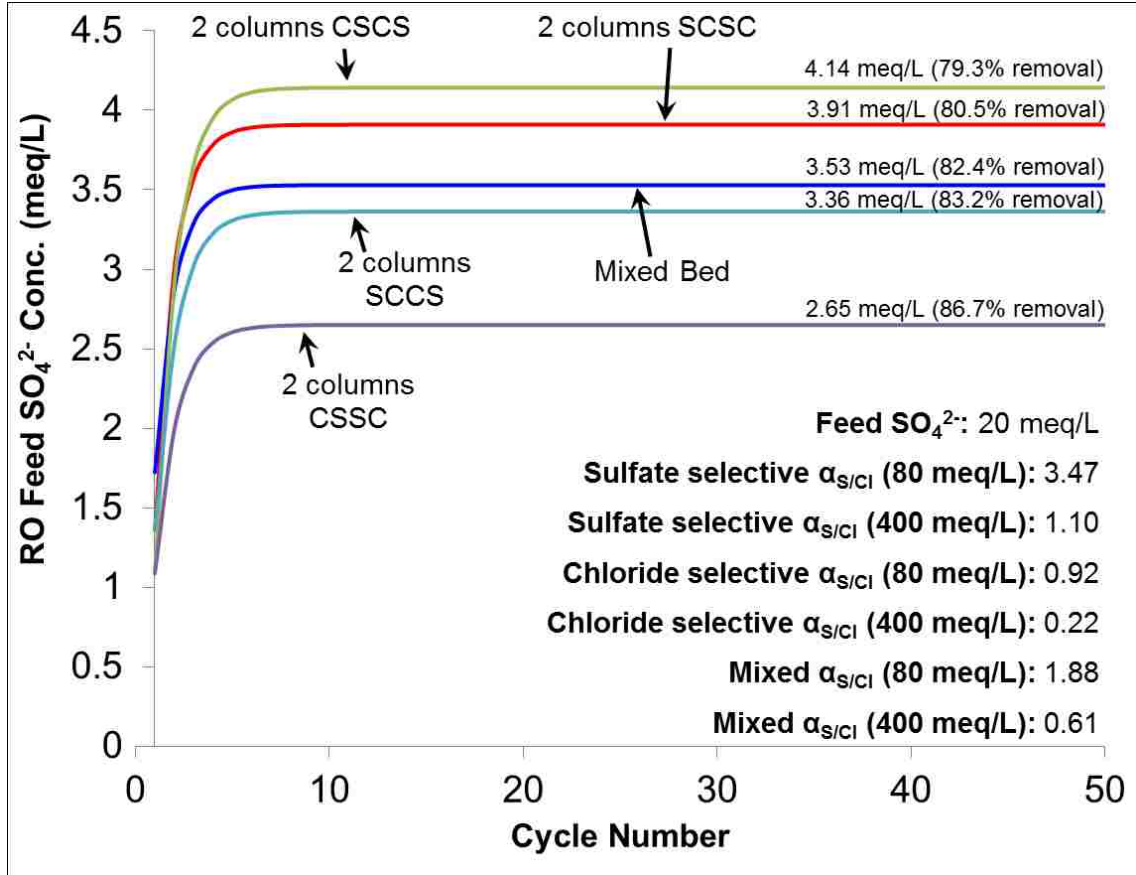


**Figure 4.10** Theoretical comparison between two columns in series with one mixed column

The theoretical RO feed for all 4 arrangements of a two column and a mixed bed HIX-RO system is plotted in **Figure 4.10**. Each two column system is labeled by an abbreviation. For example, “SCCS” means passing the feedwater through the sulfate selective column then the chloride selective column, performing RO, and taking the concentrate and passing it through the chloride selective column then the sulfate selective column. As predicted earlier, the CSSC arrangement does, in fact, provide the

highest amount of sulfate removal (86.7%) and, more interestingly, the concentration of the mixed column RO feed (3.53 meq/L  $\text{SO}_4^{2-}$ ) is almost an exact average of all four column effluents giving further proof that a mixed column acts like an average of the 4 arrangements. However, the advantage gained from using 2 columns is minimal. Even for the worst configuration (CSCS) almost 80% removal is achieved, and comparing the mixed bed (82.4% removal) to the best two column system (86.7%) there is only a slight gain. In total, theory predicts that two columns would result in higher removal but modeling predicts that the gain from doing so is not meaningful.

While the modeling results are consistent with the hypothesis that different breakthrough curves affect the overall sulfate concentration, other effects may also play a role in a mixed system compared to a two-column system. The overall selectivity coefficient of an ion exchange reaction is calculated by

$$K_{S/C} = \frac{y_S x_C^2 C_T}{x_S y_C^2 Q} \quad \text{Equation 4.20}$$

For a mixed bed system, both resins will be in contact with the same feedwater solution: i.e.  $x_S$  will be the same for both resins. However, for a two-column system, the first column will be exposed to one  $x_S$  while the second column will be exposed to the effluent  $x_S$  from the first column. Even though  $C_T$  is constant, changing  $x_S$  will also affect  $\alpha_{S/Cl}$ . For example, **Figure 4.11** below is a plot of how  $\alpha_{S/Cl}$  changes with different  $x_S$  values at two different  $C_T$  values.

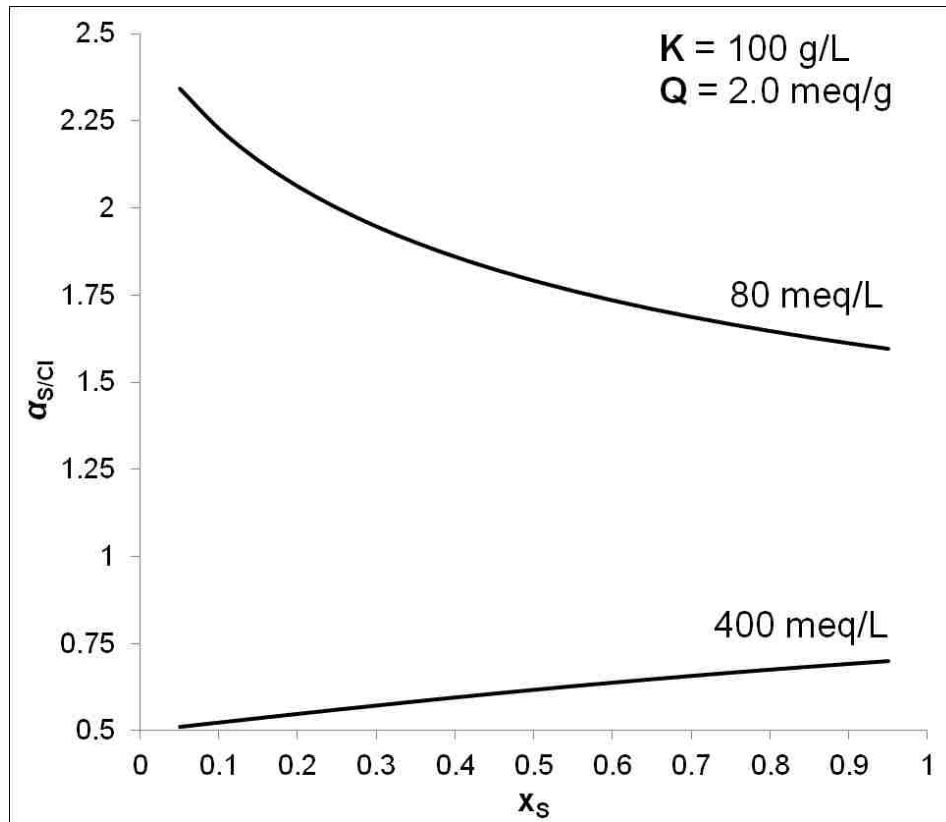


**Figure 4.11** Depression of  $\alpha_{S/Cl}$  with increasing  $x_S$

At 80 meq/L as  $x_S$  decreases, the calculated value of  $\alpha_{S/Cl}$  increases, and the opposite effect is seen at 400 meq/L. For a two-column system, each column will be exposed to a different  $x_S$  value and, therefore, there will be variations in  $\alpha_{S/Cl}$  for both resins.

Both the effects of small changes in  $\alpha_{S/Cl}$  due to varying  $x_S$  values and the order of the columns explains why two separate columns may provide different effluent sulfate concentrations. However, theoretical results predict that the difference between a two-column and a mixed bed system are minimal.

## 5. Modeling a Hybrid Ion Exchange-Reverse Osmosis System

### 5.1 Background

Since the efficiency of the HIX-RO process is inherently dependent upon proper selection of ion exchange resin, development of a model of the system would help reduce or eliminate lengthy lab scale studies. The goal of this model was to accurately predict what sulfate removal efficiency would be for a set of inputs (e.g. resin selectivity, process recovery, membrane rejection, etc.). The ion exchange and RO processes are completely distinct so each system was modeled in a different manner.

### 5.2 Modeling a Reverse Osmosis System

During reverse osmosis, the feedwater is fed under high pressure to the RO membrane separating it into two streams: permeate and concentrate. The recovery of the RO process,  $R_P$ , is given by the ratio between the permeate flow rate,  $Q_P$ , and feed flow rate,  $Q_F$ .

$$R_P = \frac{Q_P}{Q_F} \quad \text{Equation 5.1}$$

Reverse osmosis membranes are unable to reject all salt and there will be salt leakage through the membrane. The amount of salt rejection,  $R_S$ , for the membrane is

$$R_S = 1 - \frac{C_P}{C_F} \quad \text{Equation 5.2}$$

$C_P$  and  $C_F$  are the permeate and feed concentrations, respectively. Typical RO membranes have ~99% rejection.<sup>74</sup> For a given feedwater composition, a permeate recovery, and a salt rejection the concentration of the concentrate,  $C_C$ , may be calculated by a mass balance.<sup>75</sup>

$$C_C = \frac{C_F}{1 - R_P} [1 - R_P(1 - R_S)] \quad \text{Equation 5.3}$$

Therefore, for a given feedwater concentration, salt rejection, and recovery the theoretical concentration of the concentrate from the RO process can be determined.

### 5.3 Modeling an ion exchange column

Significant difficulties lie in modeling the effluent from an ion exchange column. The ion exchange column is an unsteady state plug flow reactor (PFR) with pore volume. The general solution to this system is given by **Equation 5.4**<sup>76</sup>

$$\left(\frac{1 - \varepsilon}{\varepsilon}\right) \frac{Q}{C_T} \rho \frac{\partial y_S}{\partial t} + \frac{\partial x_S}{\partial t} + u_0 \frac{\partial x_S}{\partial z} = 0 \quad \text{Equation 5.4}$$

In which  $\varepsilon$  is the void space,  $\rho$  is the resin density,  $u_0$  is the superficial liquid velocity, and  $z$  is the distance from the inlet. Solving this partial differential equation is possible for well-defined reaction rates, but the reaction rate of ion exchange sorption is ill-defined.<sup>77</sup> Instead, the system was modeled as a group of continuous stirred tank reactors (CSTRs) in series which greatly simplifies the system as the solutions to equilibrium ion exchange problems are easily calculated.<sup>78,79</sup> In addition, the influent



solution was split into four parts and fed through the system piece by piece. **Figure 5.1** is a representation of how the system was modeled.

Since the HIX-RO is designed not to waste any solution, after regeneration the first few bed volumes of influent solution will mix with any remaining regenerant solution still in the pore space of the column. If there is any sulfate present it will be present in the effluent solution which was taken into account in the model by assuming that 25% of volume of liquid present in the pore space will mix with 75% of the influent solution. The mass balance for each CSTR was calculated as follows:

$$\begin{array}{|l}
 \text{(Mass of species in solution)}_i \\
 + \\
 \text{(Mass of species in pore space)}_i \\
 + \\
 \text{(Mass of species on resin)}_i
 \end{array}
 =
 \begin{array}{|l}
 \text{(Mass of species in solution)}_f \\
 + \\
 \text{(Mass of species in pore space)}_f \\
 + \\
 \text{(Mass of species on resin)}_f
 \end{array}
 \quad \text{Equation 5.5}$$

The mass of an individual species in solution or pore space is calculated by

$$\text{Total mass in solution} = xC_TV \quad \text{Equation 5.6}$$

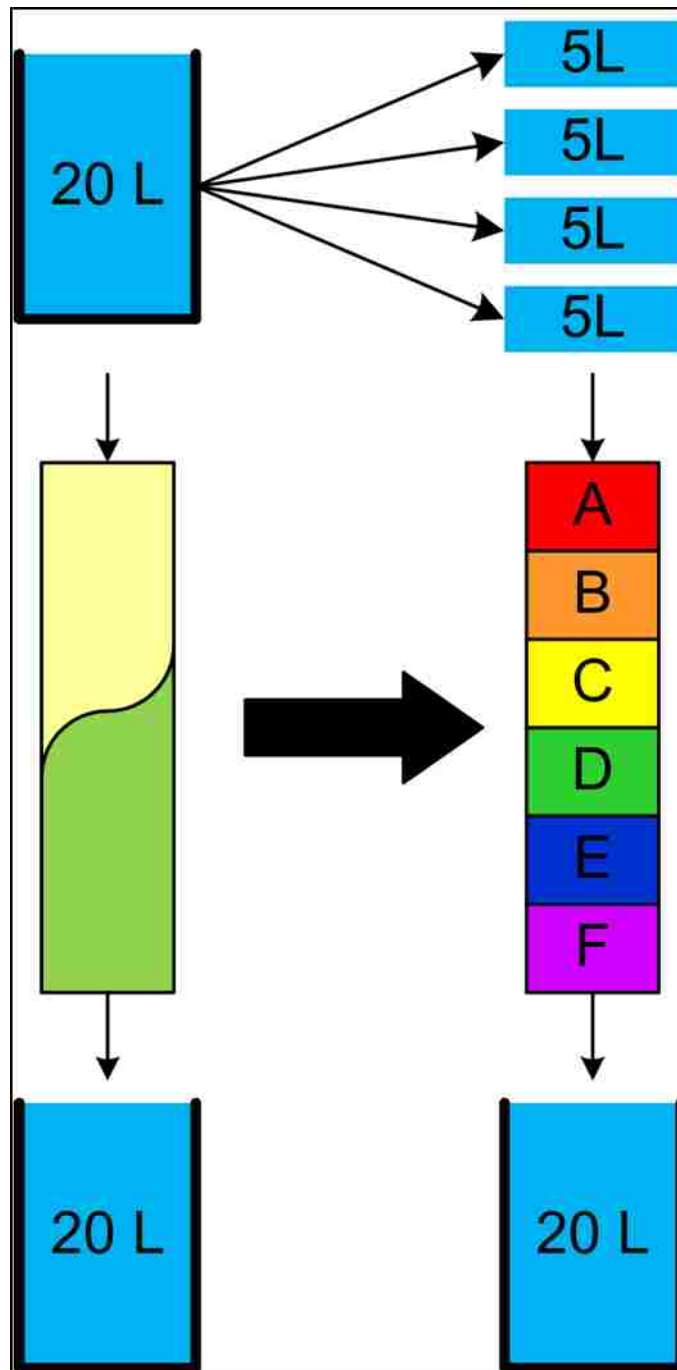


**Figure 5.1** Simplification of ion exchange column as a series of CSTRs

and the mass of an individual species on the resin is calculated by

$$\text{Total mass on resin} = yQm \quad \text{Equation 5.7}$$

Combining Equations 5.5-5.7 results in

$$\begin{aligned} (x_i C_T V)_{\text{influent}} + (x_i C_T V)_{\text{pore}} + y_i Qm \\ = (x_f C_T V)_{\text{influent}} + (x_f C_T V)_{\text{pore}} + y_f Qm \end{aligned} \quad \text{Equation 5.8}$$

Everything on the left hand side of the equation is known and the only unknowns on the right hand side are  $x_f$  and  $y_f$ , but  $y_f$  can be calculated from  $x_f$  using **Equation 4.14**. Now, the theoretical effluent from the ion exchange column can be calculated by solving **Equation 5.8** for  $x_f$  over a series of successive cycles.

#### 5.4 Importance of resin selectivity on process efficiency

In order to achieve high process efficiency during HIX-RO, resin selectivity must switch between sulfate selective and chloride selective depending on the water composition. In order to determine how important this requirement is, the model was run for two different situations: an unfavorable situation in which resin selectivity was always greater than 1, and a favorable case in which resin selectivity was greater than 1 during sulfate removal and less than 1 during regeneration.

In the unfavorable case, the model was run by fixing the resin separation factor,  $\alpha_{S/C}$ , at 1.5 during both normal operation and regeneration. The theoretical results of 50 cycles is shown in **Figure 5.2**.

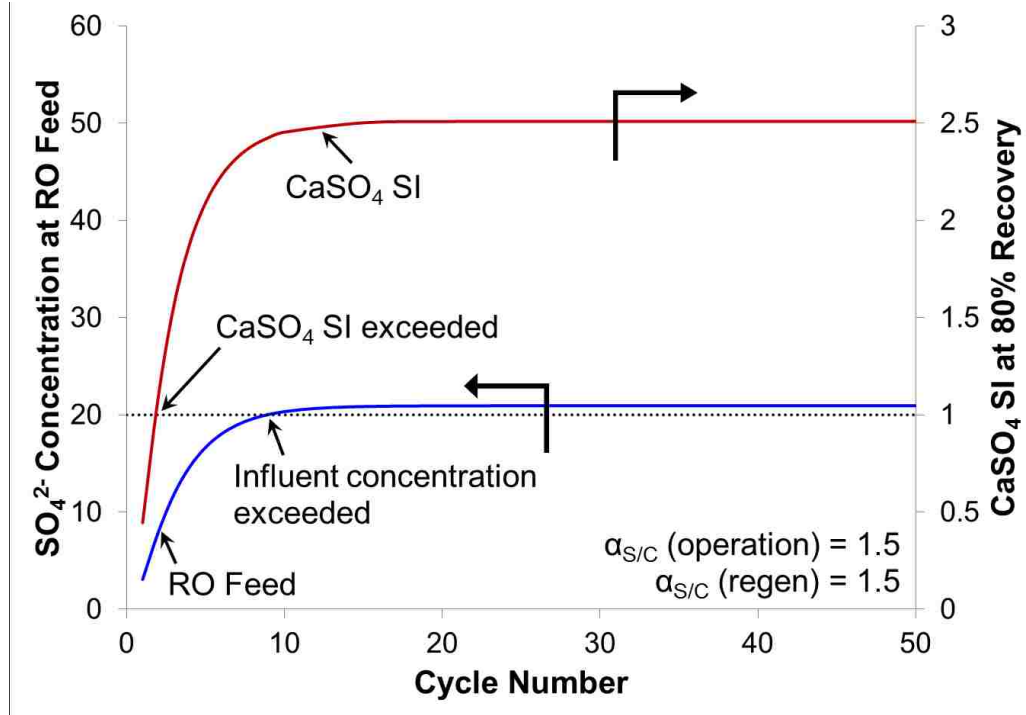


**Figure 5.2** Theoretical  $\text{SO}_4^{2-}$  concentration in RO feed with fixed  $\alpha_{S/C} = 1.5$

There are several important results to note. First, the concentration of sulfate at the RO feed started very low but then broke through to the influent sulfate concentration in less than 3 cycles. Due to selectivity coefficient being always greater than 1, regeneration of the resin is not occurring and the resin capacity is quickly exhausted. As a result, no sulfate is removed from solution. The concentration exiting the column is actually slightly higher than the influent concentration; this result is attributed to the fact that there will be a high concentration of sulfate left in the pore space of the column in between runs. Since no sulfate removal is occurring, the “regenerant” is just a concentrated brine of chloride and sulfate. When the influent solution passes through

the column, this extra solution then mixes with the lower concentration feedwater and results in even higher than influent concentrations of sulfate. The combination of no sulfate removal and a slight increase in concentration of sulfate going to RO, the SI values for calcium sulfate are almost immediately exceeded.

**Figure 5.3** shows the case in which the ion exchange column was properly designed and  $\alpha_{S/C} = 1.5$  at feedwater concentrations and  $\alpha_{S/C} = 0.5$  at RO concentrate concentrations. In this case, sulfate removal is almost 75%, reaches equilibrium, and remains below the influent concentration for 50 cycles.

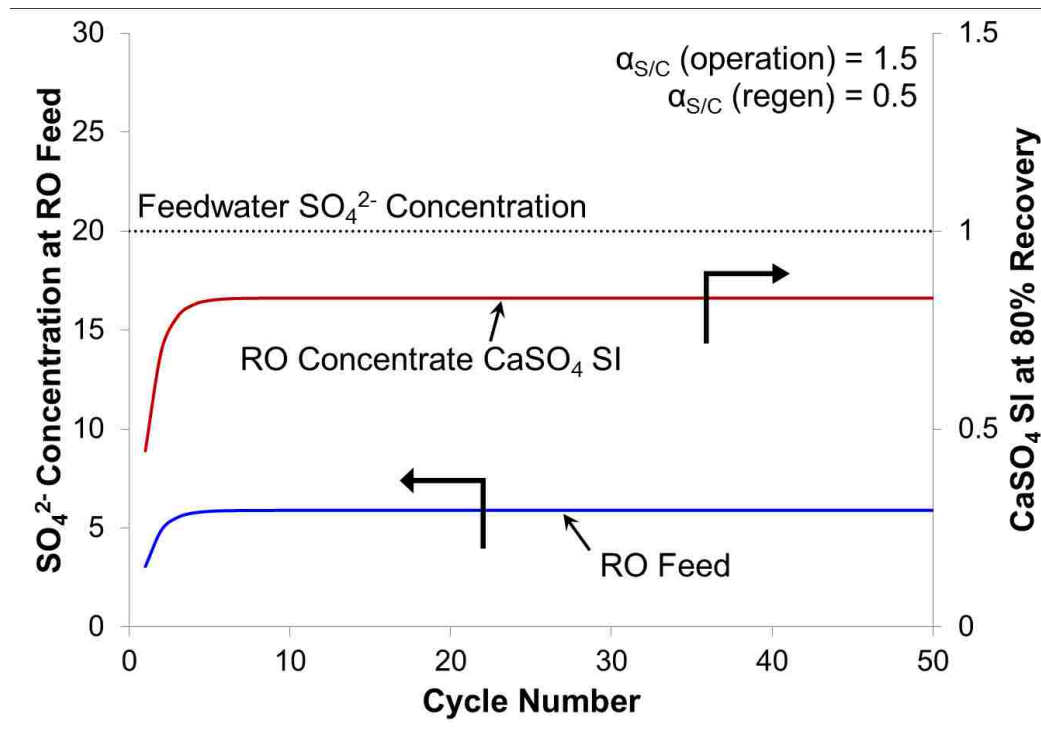


**Figure 5.3** Theoretical  $\text{SO}_4^{2-}$  concentration in RO feed with  $\alpha_{S/C} = 1.5$  and  $\alpha_{S/C} = 0.5$

Again, these results are in line with theoretical predictions: a properly designed ion exchange column is able to remove sulfate consistently without requiring any external regenerant, and as a result the SI values for  $\text{CaSO}_4$  never exceeds 1.

In total, in order for the HIX-RO process to be sustainable and not require additional regenerant,  $\alpha_{S/C}$  must be greater than 1 at influent concentrations but less than 1 at RO reject concentration.

## 6. Lab-scale study of a Hybrid Ion Exchange-Reverse

### Osmosis System

The data from experiments and modeling in **Chapter 4** and **Chapter 5** are evidence that selective removal of sulfate from brackish water sources is possible using a properly designed ion exchange column. Using the experimental setup described in **Section 3.3** six different HIX-RO runs were performed using different modifications to the resin mixture and feedwater composition as detailed in **Table 3.2**. The only differences between the 6 HIX-RO runs are the resin used and/or the water composition.

For all HIX-RO runs, at least ten cycles were performed. This minimum was chosen as it will exceed the total capacity of the ion exchange column. A typical 1L anion exchange column has 2000 meq total capacity. For a 20L of feedwater with 20 meq/L  $\text{SO}_4^{2-}$ , after ten cycles 4000 meq of sulfate would have been in contact with the column: at least two times the total capacity of the resin.

#### 6.1 Results from HIX-RO Runs

Since the concern is the prevention of calcium sulfate scaling, data regarding the quality of the RO permeate are not presented. However, the conductivity of the RO permeate for all cycles within all six runs the conductivity of the permeate never exceeded 1000  $\mu\text{S}$ . This indicates that the integrity of the RO membrane was not compromised during any HIX-RO runs, and that little to no ions were lost due to permeation through the membrane.

### 6.1.1 Run 1: Mixed bed polystyrene and polyacrylic resins with Feedwater “A”

For Run 1, the ion exchange bed was a 50/50 mixture of polystyrene and polyacrylic resins: a properly designed HIX-RO system. The concentration of sulfate at the exit of the ion exchange column (feed to RO) is shown in **Figure 6.1**.

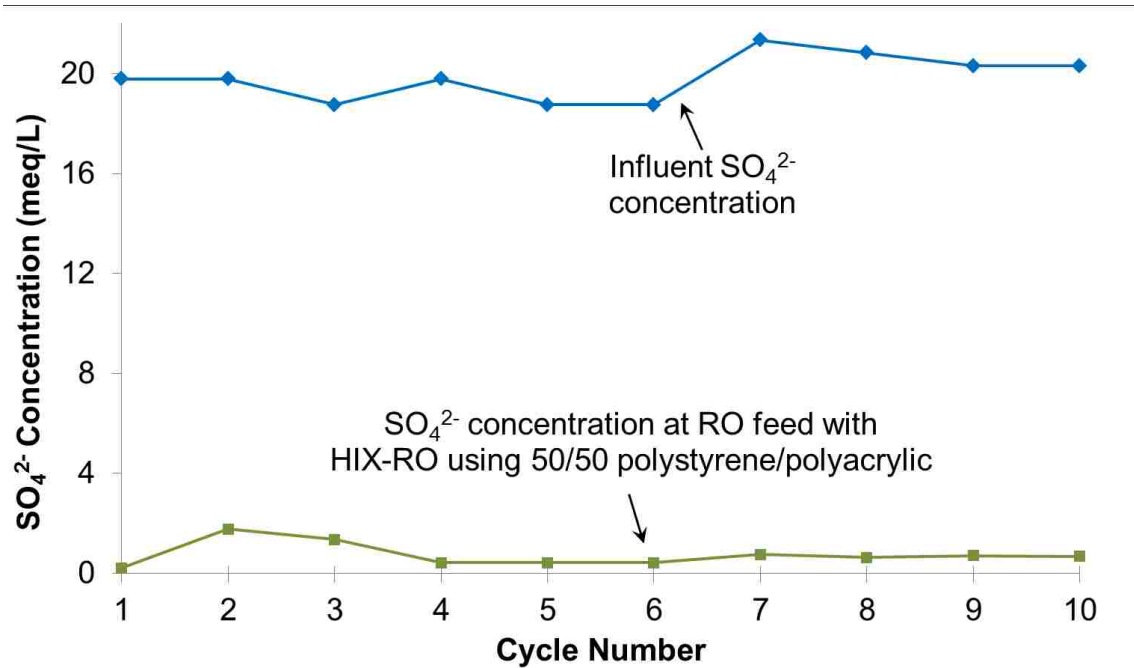


**Figure 6.1** Concentration of sulfate at feed to RO for Run 1

For 10 successive cycles, the sulfate concentration at the exit of the ion exchange column was reduced by 90% or greater: a significant reduction.

However, the issue is not the presence of sulfate but its potential for formation of  $\text{CaSO}_4$  during RO. Since no  $\text{Ca}^{2+}$  was present in the synthetic feedwater solution, theoretical calculations must be performed to determine the concentration of  $\text{Ca}^{2+}$  that would be present in the concentrate. Using the actual feedwater  $\text{Ca}^{2+}$  concentration, the



measured recovery for each cycle, and assuming no loss through the RO membrane, the theoretical concentration of  $\text{Ca}^{2+}$  can be calculated. By combining the theoretical  $\text{Ca}^{2+}$  concentration with the measured  $\text{SO}_4^{2-}$  values, the supersaturation index (SI) for  $\text{CaSO}_4$  was determined using OLI and is shown in **Figure 6.2**; note that the y-axis is plotted log-scale.<sup>61</sup>

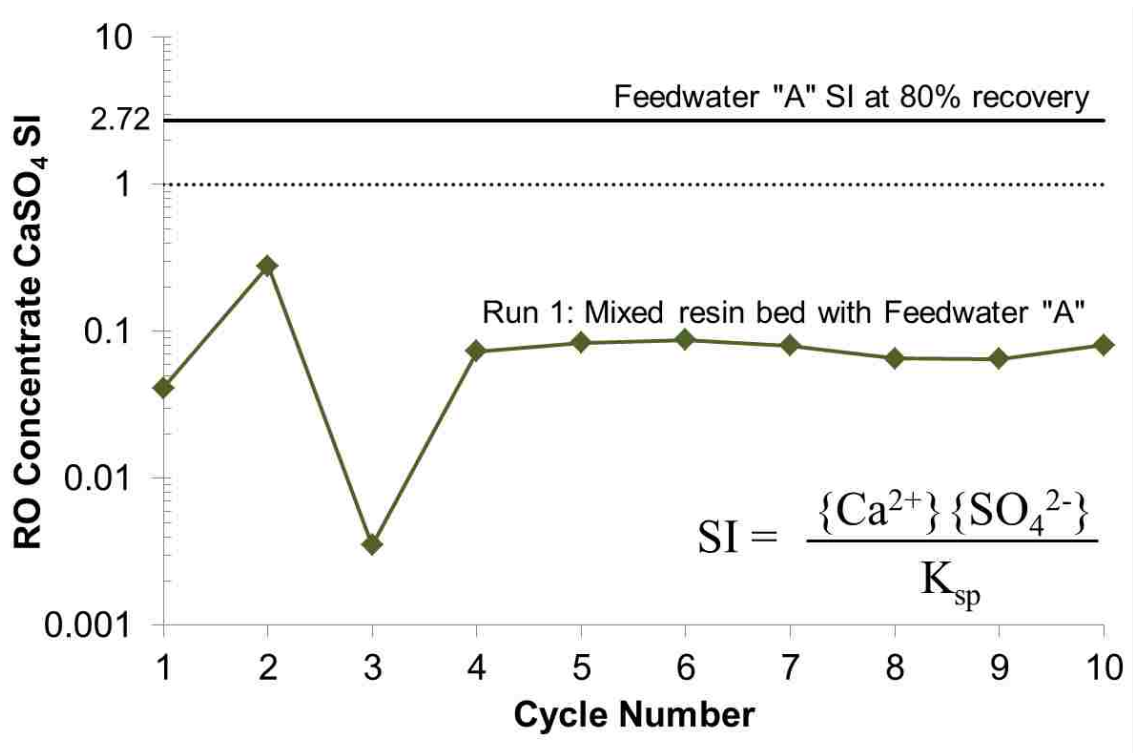


**Figure 6.2** Calculated SI values for  $\text{CaSO}_4$  in RO Concentrate for Run 1

This method of back-calculating the concentration of  $\text{Ca}^{2+}$  in order to determine  $\text{CaSO}_4$  SI values in the RO concentrate was performed for all 6 runs. For all 10 cycles of Run 1, SI never exceeded 1 and there was never a threat of  $\text{CaSO}_4$  scaling.

Sustainability of the HIX-RO process is demonstrated by performing a mass balance on sulfate for the entire HIX-RO system. For each cycle, the amount of sulfate entering (from the influent) and exiting the system (from the waste ion exchange regenerant solution) was determined and is shown in **Figure 6.3**.

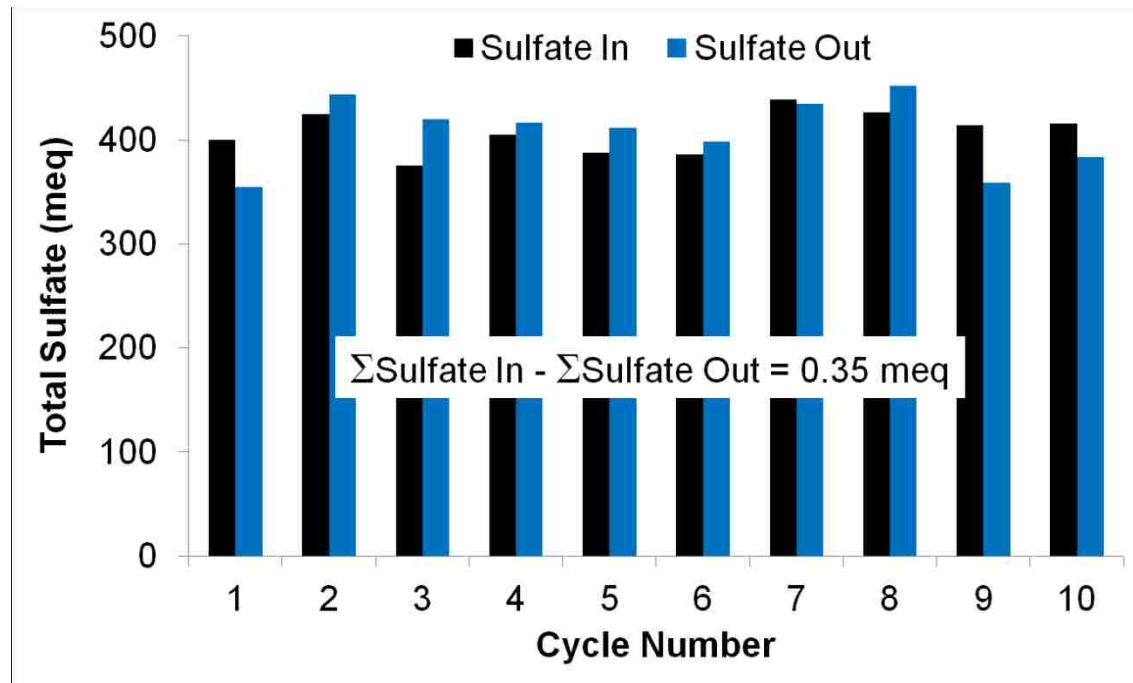


**Figure 6.3** Mass balance on sulfate entering/exiting system for Run 1

Results show that the mass of sulfate entering and exiting the system during each cycle was approximately equal. The mass balance over the entire 10 cycles was off by 0.35 meq sulfate which is negligible considering that the total mass of sulfate entering the system over the 10 cycles was approximately 4000 meq. For chloride, a mass balance on the ion exchange column was performed and is shown in **Figure 6.4**.

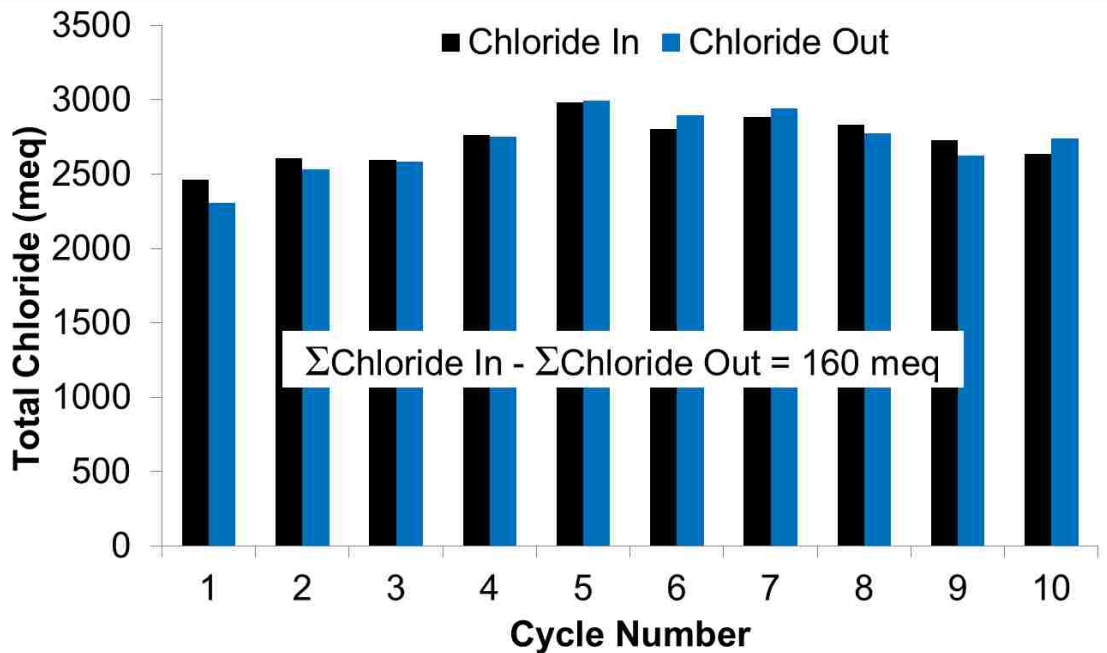


**Figure 6.4** Mass balance on chloride entering/exiting system for Run 1

For each cycle the mass of chloride entering and exiting the IX column was approximately equal, and over the entire 10 cycles the mass balance on chloride was off by 160 meq. Again, this difference is negligible considering that the total mass of  $\text{Cl}^-$  entering the system was about 12,000 meq.

While the use of a mixed bed anion exchange column to reduce sulfate was successful, it is equally important to demonstrate that not just any type of anion exchange resin can be chosen. An improperly designed ion exchange column would result in incomplete regeneration or lower sulfate removal. To this end, five other runs with different types/mixtures of ion exchange resins were performed.

### 6.1.2 Run 2: Pure strong base polyacrylic with feedwater “A”

According to the theoretical predictions from **Section 2.3**, performing HIX-RO using only a strong base polyacrylic resin should suffer from incomplete regeneration due to  $\alpha_{S/C}$  always being greater than 1. **Figure 6.5** is a plot of the effluent concentration of sulfate from the pure strong base polyacrylic resin run compared to the mixed bed run.

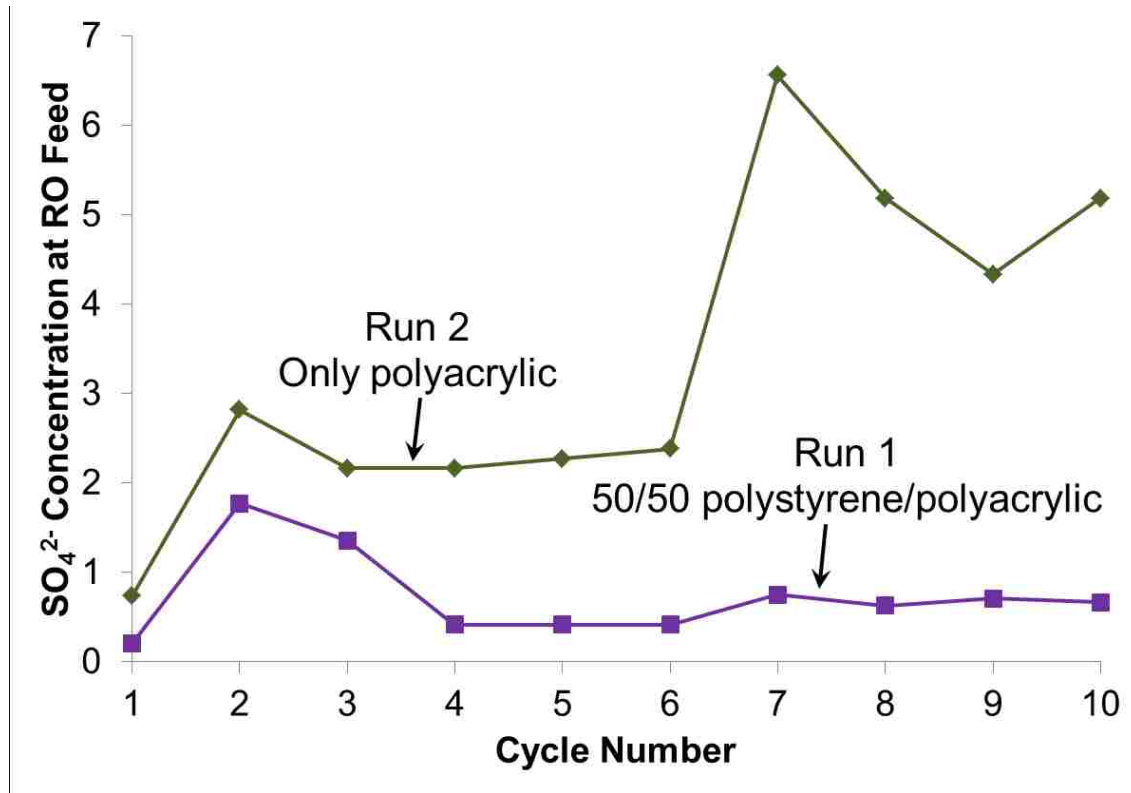


**Figure 6.5** Concentration of sulfate at feed to RO for Runs 1 and 2

Here, the results are not the same as the theoretical predictions made as the strong base polyacrylic resin was able to remove sulfate for 10 cycles. However, the removal rate of sulfate was less than that for the polystyrene/polyacrylic mixture.

The fact that the acrylic resin was able to reduce sulfate can be explained by looking at the isotherm data. Using the  $K_{S/C}$  value of the polyacrylic resin from **Table 4.1**,  $\alpha_{S/Cl}$  at 400 meq/L would be 0.69. The pure polyacrylic resin alone does not fall within the desired parameters of HIX-RO:  $\alpha_{S/Cl}$  is greater than 1 at influent concentrations and less than 1 at RO concentrate concentrations. However, the removal of sulfate was lower than for the mixed resin system. A possible explanation as to why the polyacrylic resin showed poorer results even though  $\alpha_{S/C}$  had the correct values was due to inefficient regeneration. A mass balance on the system, **Figure 6.6**, shows that there was some accumulation of sulfate on the resin: approximately 150 meq of sulfate.

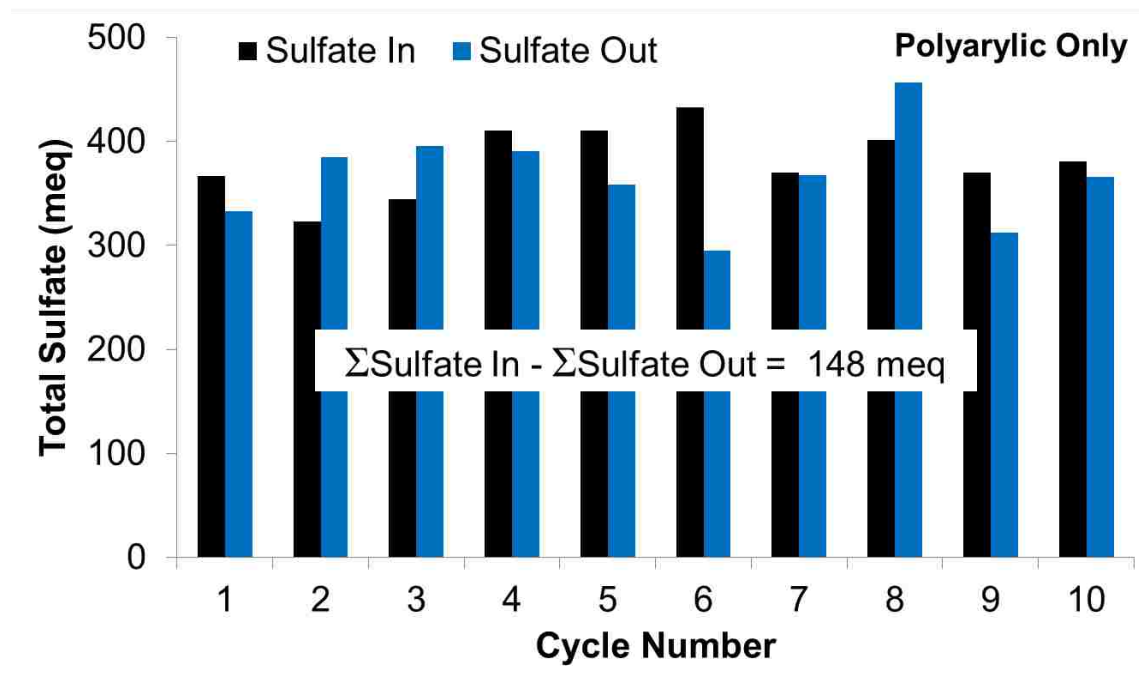


**Figure 6.6** Mass balance for polyacrylic HIX-RO Run

In addition, the system had not yet come to equilibrium. It is difficult to predict what the final sulfate concentration would be once the system reached steady state, but from

**Figure 6.6**, sulfate concentration in the last four cycles was tending to increase which can be interpreted that if the system had been run for more cycles, the sulfate concentration may have been higher.

Comparison of supersaturation indices, plotted log-scale in **Figure 6.7**, shows that while the polyacrylic resin was able to prevent sulfate scaling, the mixed resin system was able to more effectively reduce the CaSO<sub>4</sub> SI.

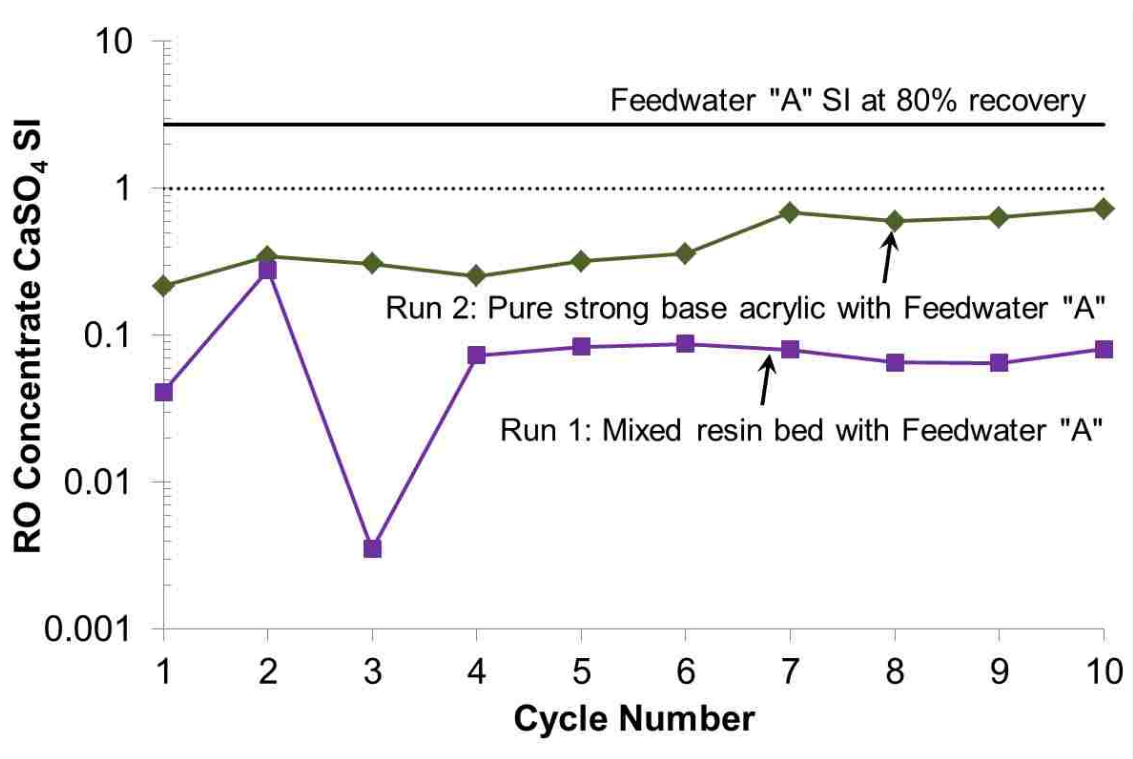


**Figure 6.7** Calculated SI Values for CaSO<sub>4</sub> in RO Concentrate for Runs 1 and 2

It is interesting to note that the reduction in SI for the polyacrylic resin alone was not as much as the mixed bed, but was still able to reduce SI below 1. These data further reinforce the hypothesis that as long as  $\alpha_{S/Cl} > 1$  at influent concentrations and  $\alpha_{S/Cl} < 1$

at reject concentrations, the HIX-RO process is capable of removing sulfate, but the level of sulfate removal is dictated by the range of  $\alpha_{S/Cl}$ .

### 6.1.3 Run 3: Pure weak base polyacrylic with feedwater “B”

The HIX-RO run with a pure weak base polyacrylic resin is significantly different from previous HIX-RO runs. From the theoretical selectivity data,  $\alpha_{S/Cl}$  is significantly greater than 1 at all concentrations: 10.0 and 3.83 at 80 meq/L and 400 meq/L, respectively.<sup>58</sup> Indeed, for the first 12 cycles sulfate was not detected in the IX effluent as shown in **Figure 6.8**. Only after cycle 12 did sulfate begin to appear in the IX effluent.

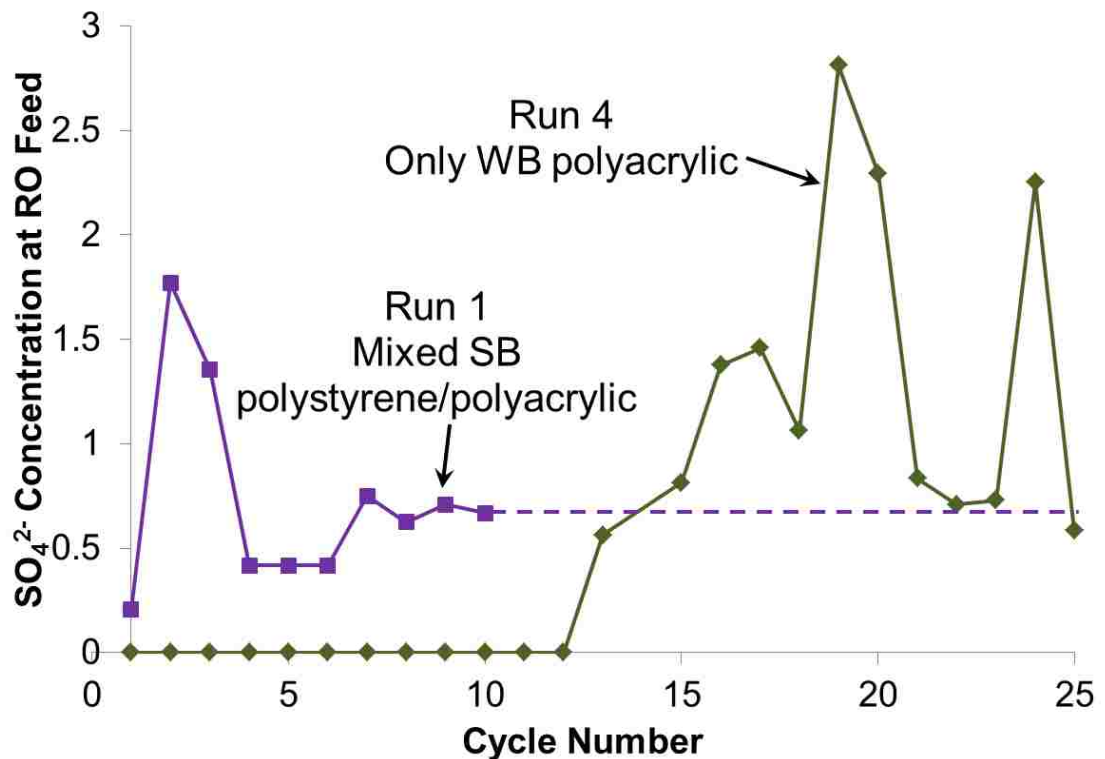


**Figure 6.8** Concentration of sulfate at feed to RO for Runs 1 and 3

More importantly, sulfate concentration in the reject stream from the HIX-RO process was also very low indicating that sulfate was accumulating on the resin. **Figure 6.9** gives the mass balance for the entire HIX-RO system. For the first twelve cycles, almost 100% of the influent sulfate was accumulating on the resin due to lack of regeneration. After the 12<sup>th</sup> cycle, the total mass on the resin begins to reach a steady state and by cycle 19 there is little variation. The steady-state mass of sulfate on the resin is approximately 1300 meq; compared to the total resin capacity, 2700 meq, 47% of the resin is in sulfate form.

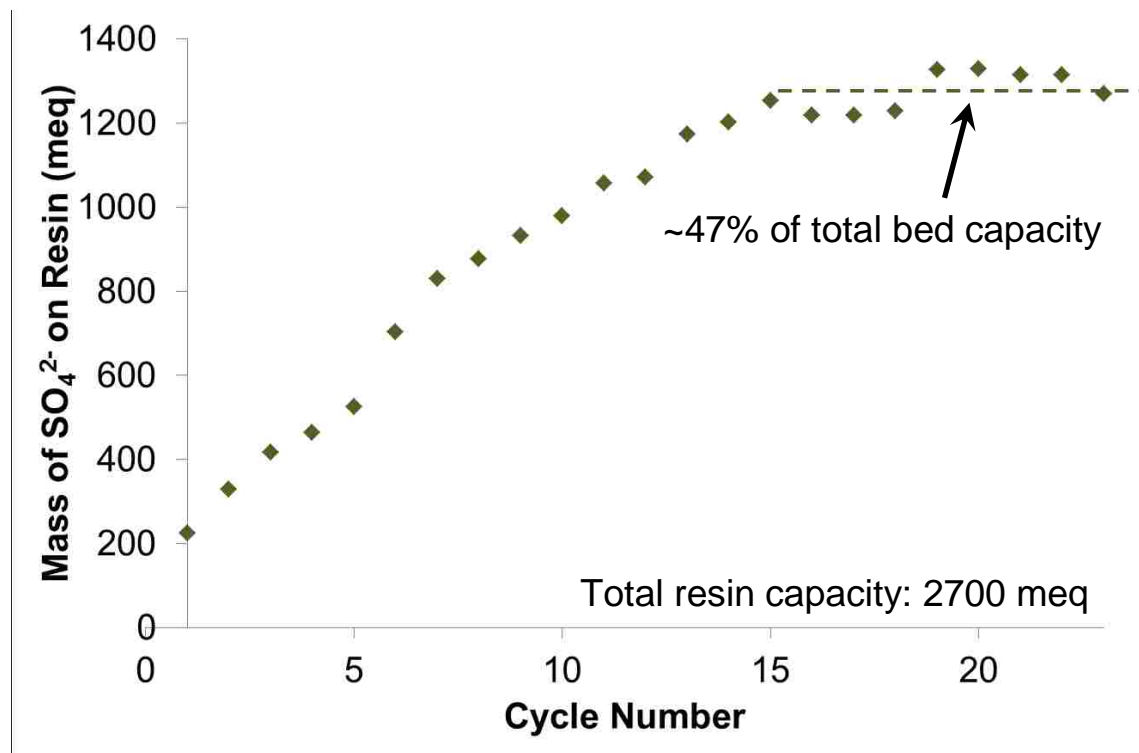


**Figure 6.9** Mass balance on sulfate entering/exiting system for Run 3



The SI values, plotted log-scale in **Figure 6.10**, for the first twelve cycles were 0, but continuously increased until the system came to equilibrium around cycle 15.

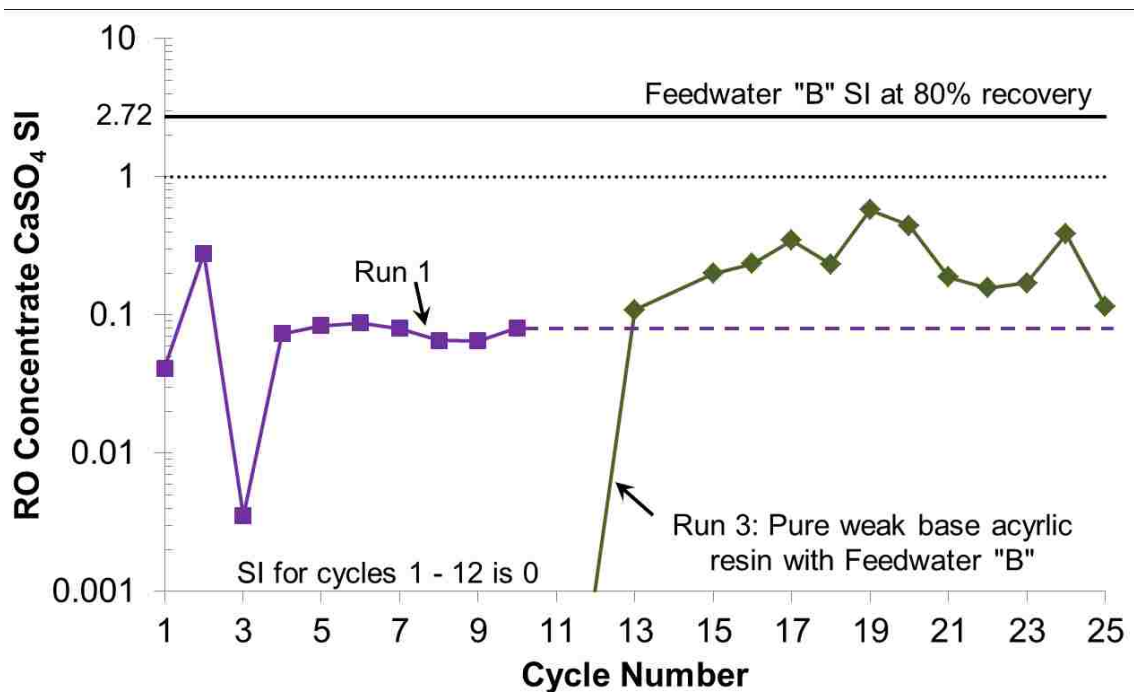


**Figure 6.10** Calculated SI values for CaSO<sub>4</sub> in RO Concentrate for Runs 1 and 3

Due to the fact that  $\alpha_{S/Cl}$  was greater than 1 during regeneration (further indicated by the accumulation of sulfate on the resin), the pure weak base polyacrylic resin was unable to remove as much sulfate as the mixed resin system. As such, the mixed bed system again had a lower SI value than the pure resin.

#### 6.1.4 Run 4: Pure strong base polystyrene with feedwater “C”

Ten cycles of HIX-RO with only strong base polystyrene resin were performed with a more concentrated version of the feedwater used in Runs 1 - 3. During Run 3, the improperly designed ion exchange column accumulated sulfate on the resin, but sulfate

scaling was still prevented. By increasing the feedwater concentration to 150 meq/L and using the polystyrene resin, the improperly designed HIX-RO system should be unable to remove enough  $\text{SO}_4^{2-}$  to prevent scaling.

**Figure 6.11** is a log-scale plot of the SI values; for all ten cycles SI was greater than 1.

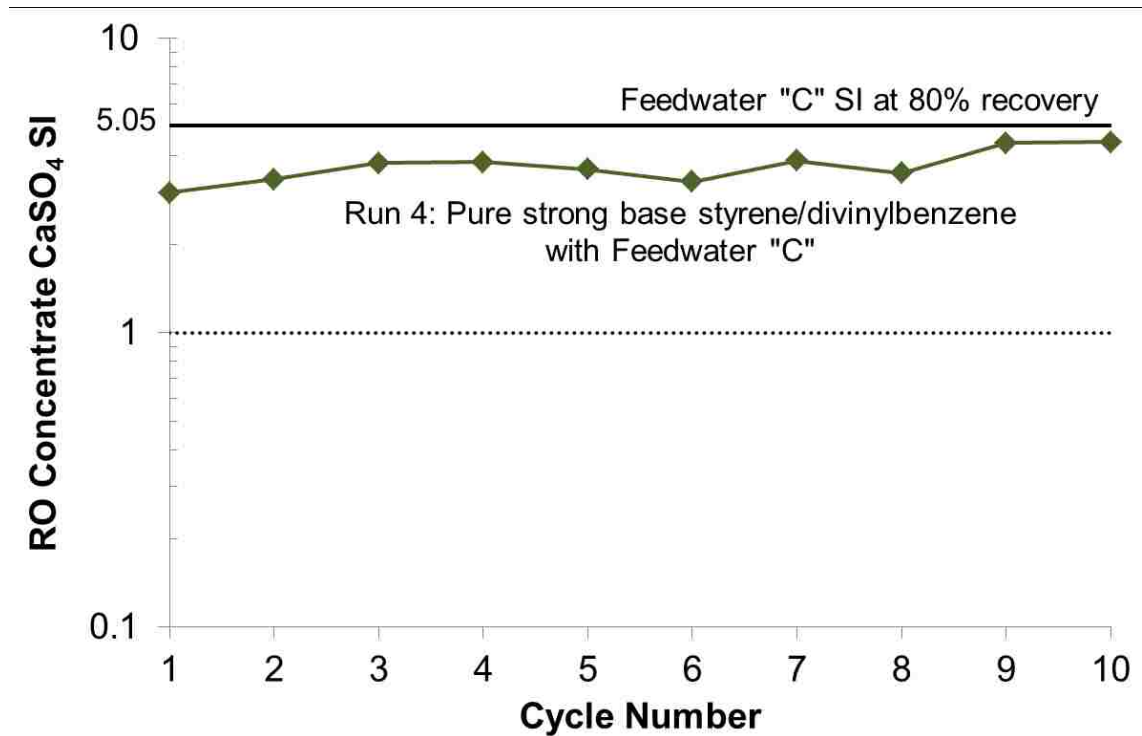


**Figure 6.11** Calculated SI values for  $\text{CaSO}_4$  in RO Concentrate for Run 4

These results provide strong evidence to the hypothesis that not any combination of a resin with a feedwater will result in high sulfate removal.

### **6.1.5 Run 5: Mixed bed polystyrene and polyacrylic with phosphate selective resin with feedwater “D”**

In addition to sulfate, phosphate is also a concern when treating water such as it may precipitate as calcium phosphate at typical pH values. Phosphate is commonly found in secondary wastewater effluent.<sup>75,80</sup> Since phosphate mainly exists as the divalent anion  $\text{HPO}_4^{2-}$  at typical pH values for feedwater, HIX-RO may be able to remove phosphate in addition to sulfate. Therefore, for Run 5 with a mixed resin bed, phosphate was added to the feedwater.

In the past, the ion exchange resin LayneRT was shown to have very high affinity for phosphate;<sup>81</sup> for the first 9 cycles of Run 5, 10% of the mixed resin bed was replaced by the phosphate selective resin LayneRT. For reasons which are explained later in this section, during cycles 10-13 LayneRT was removed and the influent phosphate concentration was doubled.

Calcium sulfate SI values for all 13 cycles were calculated and are shown in **Figure 6.12**.

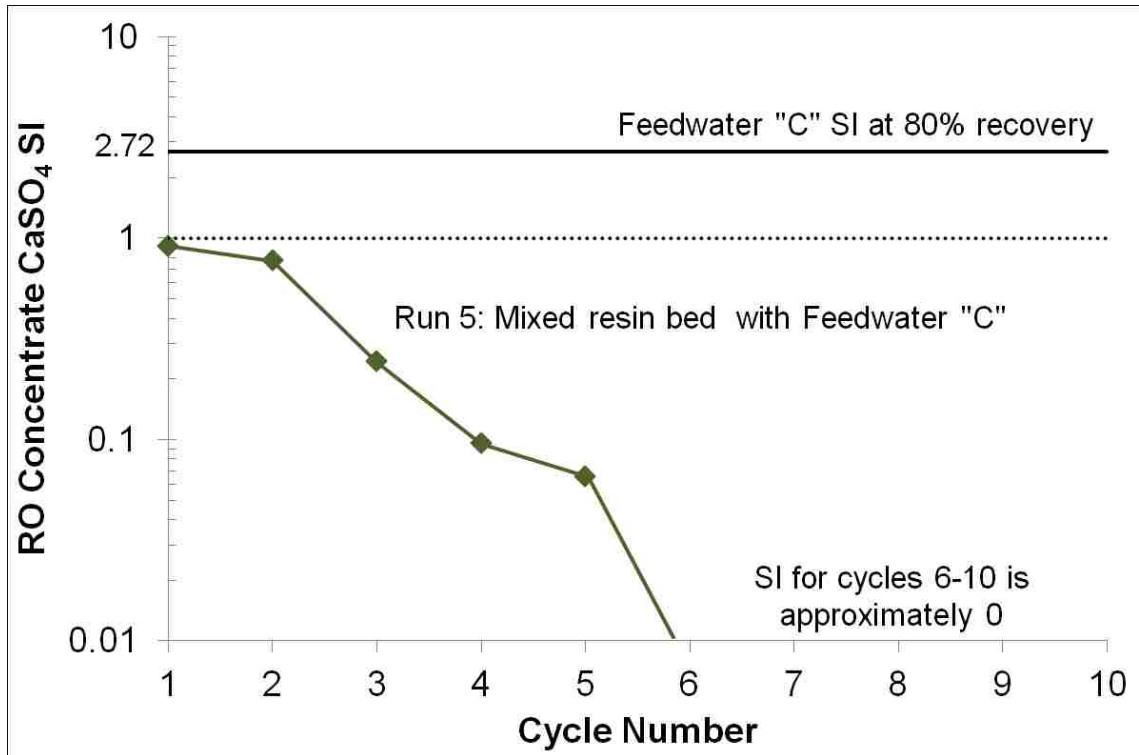


**Figure 6.12** Calculated SI values for CaSO<sub>4</sub> in RO Concentrate for Run 5

Similar to Run 1, no threat to sulfate scaling was seen for any cycle. Performing a mass balance on sulfate, shown in **Figure 6.13**, again, all sulfate adsorbed during the process was removed during regeneration.

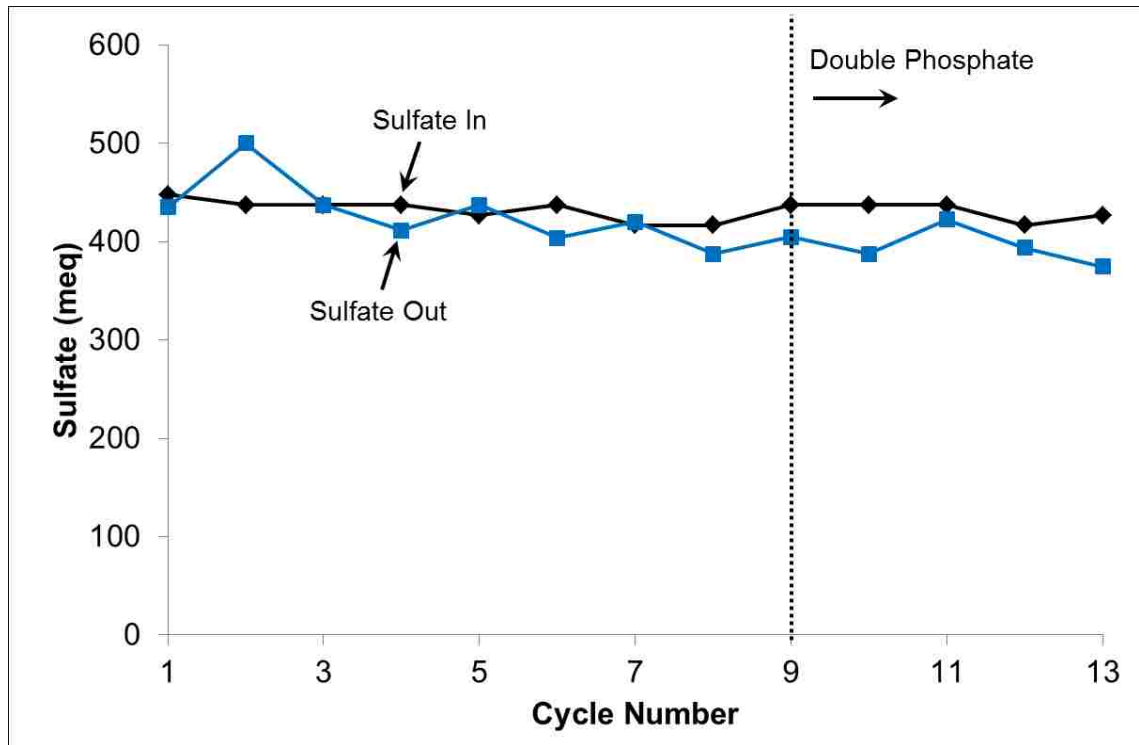


**Figure 6.13** Mass balance on sulfate for Run 5

These results are similar to the results obtained from Run 1: a properly designed HIX-RO system can remove a significant portion of sulfate with little accumulation of sulfate on the resin. The only difference between the two runs was the addition of phosphate, and from the results it is clear that presence of phosphate did not have any effect on the removal of sulfate. This result is expected since phosphate is a trace species and most ion exchange resins show higher affinity toward sulfate than phosphate.<sup>81</sup>

The concentration of phosphate in the influent and IX effluent/RO feed is shown in **Figure 6.14**.

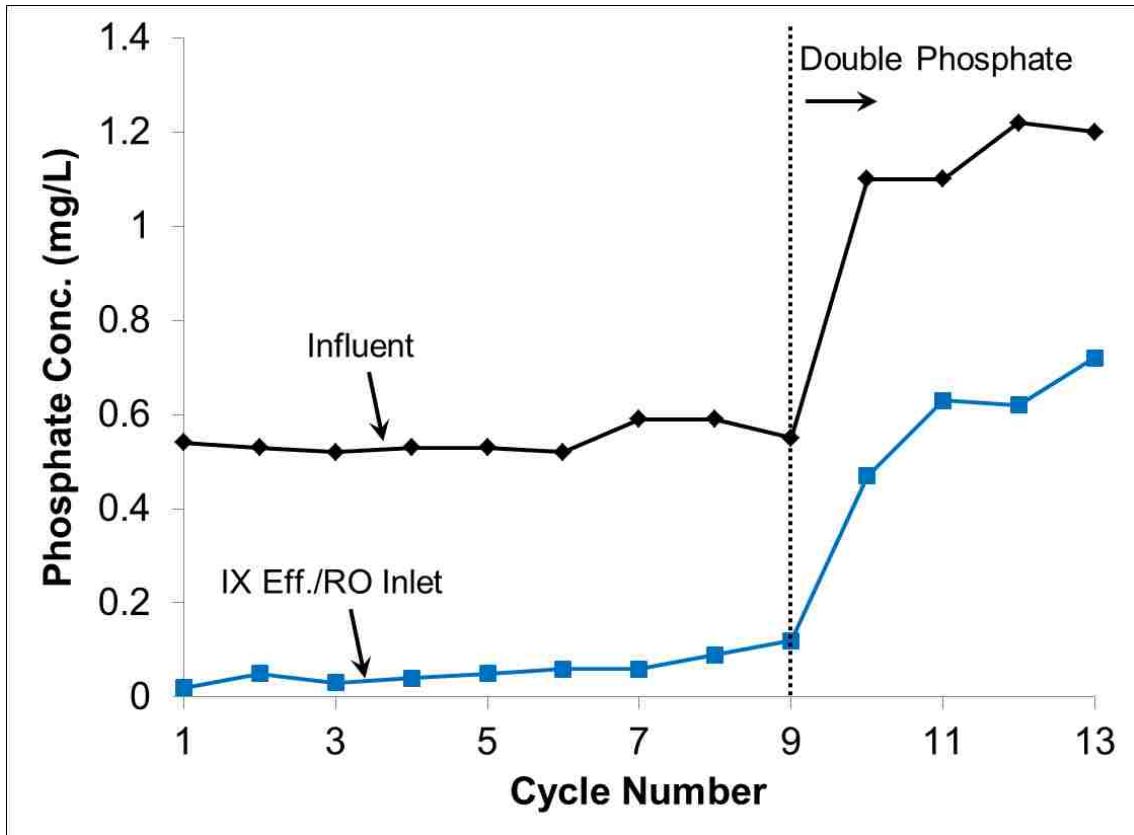


**Figure 6.14** Concentration of phosphate in influent and IX effluent/RO feed

For the first nine cycles, a 95% reduction in phosphate was observed. It was assumed that all phosphate removal was occurring due to the presence of LayneRT, but it was necessary to test this hypothesis. So for cycles 10-13, all LayneRT was removed from the column and the phosphate concentration was doubled. The doubling of phosphate was necessary since the phosphate concentration was very small and it would have taken a large number of cycles in order to see what the phosphate concentration would be at system equilibrium. By doubling the concentration, it was hoped phosphate equilibrium would be reached sooner.

Indeed, after LayneRT resin was removed the phosphate removal rate dropped to less than 50%. It can therefore be concluded that the LayneRT resin was the main cause of phosphate removal. Performing a mass balance on phosphate for the entire system, shown in **Figure 6.15**, shows that for the first nine cycles (with LayneRT) all phosphate was accumulating on the bed and little to no phosphate was being removed from the resin during regeneration.

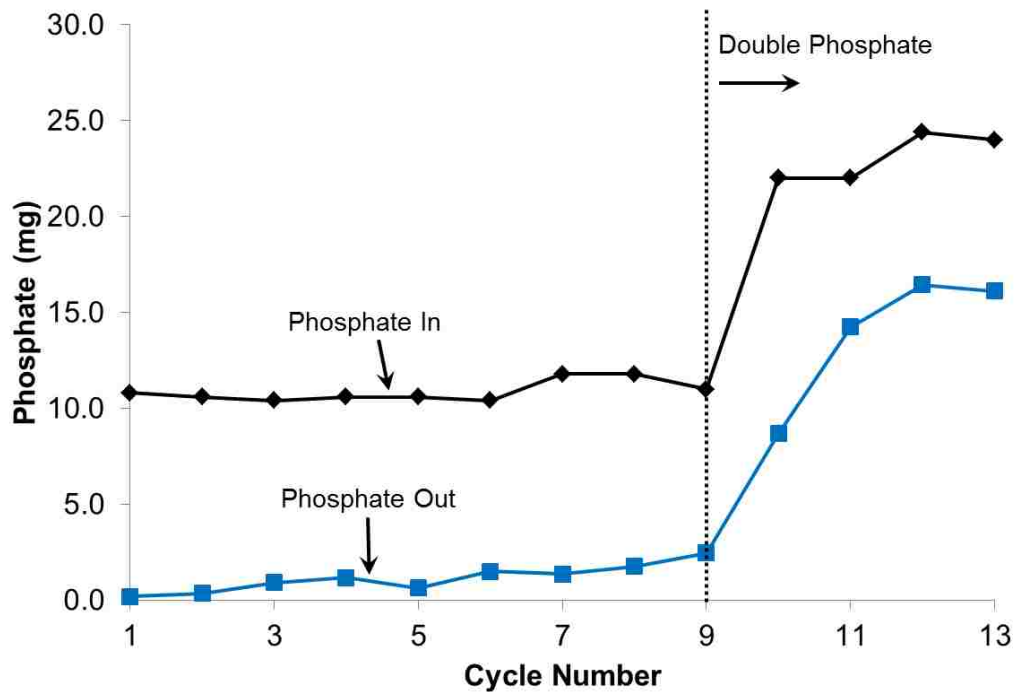


**Figure 6.15** Mass balance on phosphate for Run 5

After LayneRT is removed (cycles 10-13), 39% to 67% of the influent phosphate was recovered during regeneration giving further evidence that LayneRT was the main mechanism for phosphate removal and regeneration was not occurring. The inability of using waste brine to regenerate LayneRT is expected as LayneRT does not remove

phosphate through an ion exchange reaction but through the formation of inner sphere complexes with iron nanoparticles.<sup>81</sup>

### 6.1.6 Run 6: Pure polystyrene with triethylamine functional groups with feedwater “E”

The final HIX-RO run was performed with only a polystyrene resin with triethylamine functional groups. Using the isotherm data from **Section 4.7**, it is predicted that  $\alpha_{S/Cl}$  for IRA-900 is 0.35 at 80 meq/L, so very little removal was expected. Indeed, low sulfate removal was observed and as a result the SI, plotted log-scale in **Figure 6.16**, was not reduced enough to prevent  $\text{CaSO}_4$  precipitation.

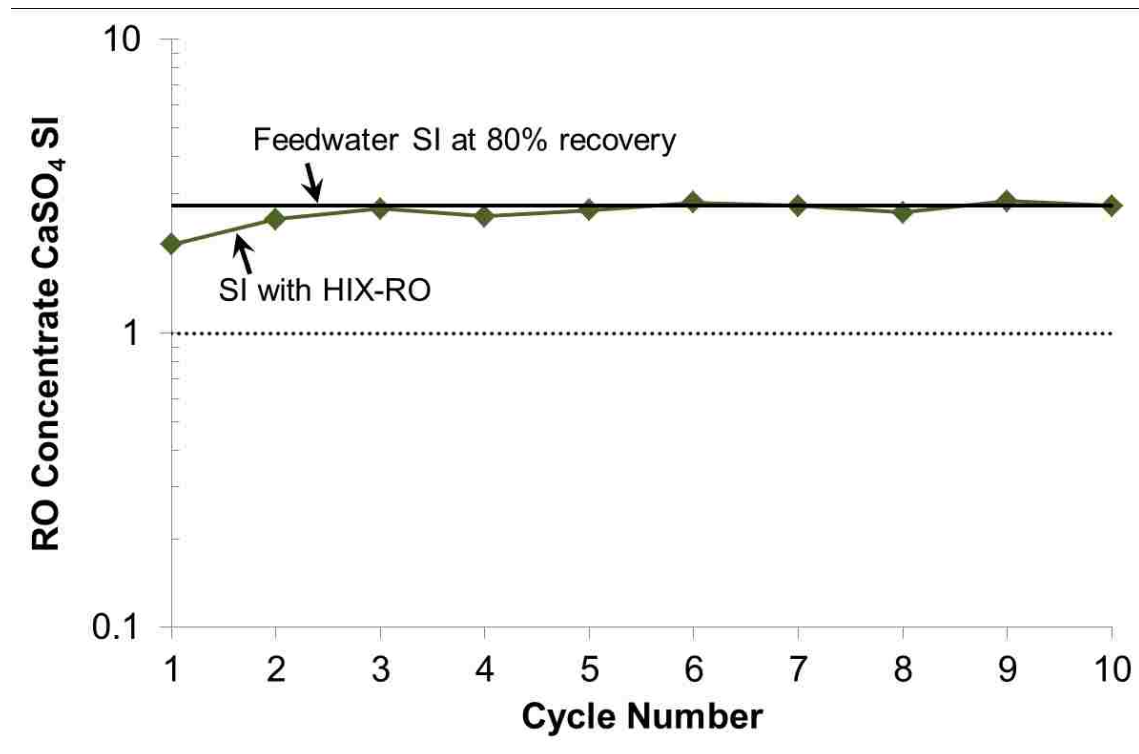


**Figure 6.16** Calculated SI values for  $\text{CaSO}_4$  in RO Concentrate for Run 6



Similarly, phosphate was also not removed as shown in **Figure 6.17**.

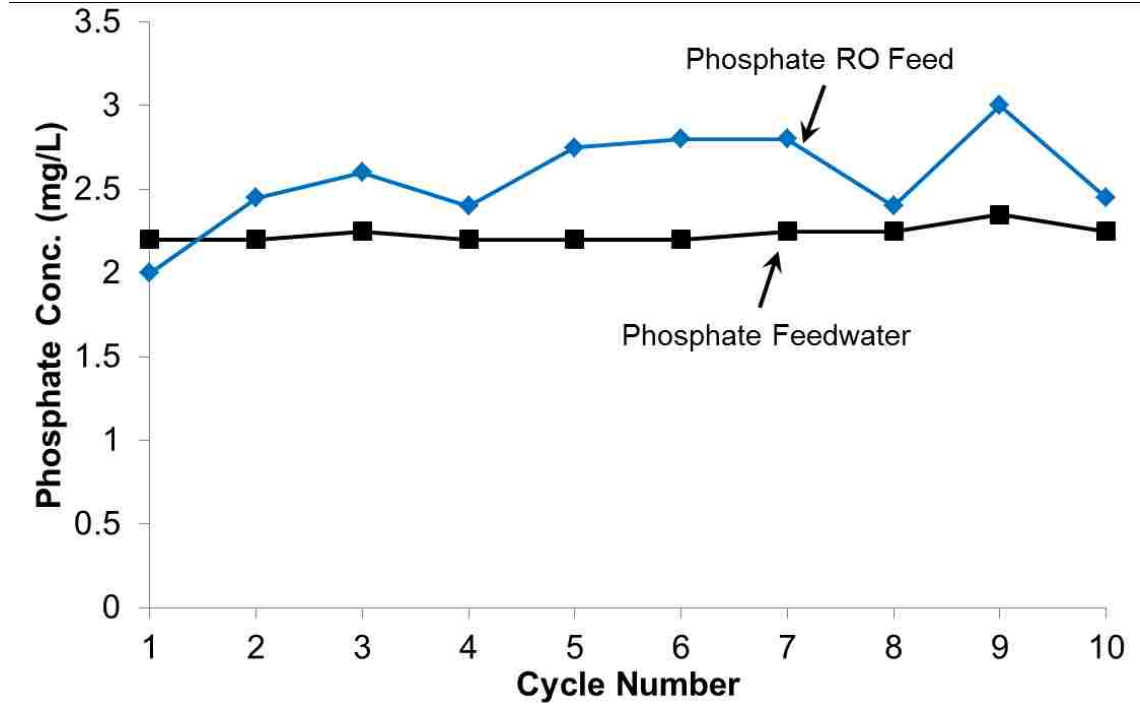


**Figure 6.17** Concentration of phosphate at feed to RO for Run 6

## 6.2 Summary of all HIX-RO Runs

From the results of all six HIX-RO, the following conclusions can be drawn:

1. A properly designed ion exchange column is effective at removing sulfate and preventing the precipitation of  $\text{CaSO}_4$

Results from Runs 1 and 5 provide evidence that high sulfate removal occurs when using a properly tuned ion exchange column. For both of these cases,  $\text{CaSO}_4$  SI values were significantly less than 1 and scaling was prevented.

2. An improperly designed column may remove sulfate but may not provide as high removal as a properly designed system

Results from Runs 2 and 3 provide evidence that even for systems in which  $\alpha_{S/Cl}$  has not been tuned, sulfate removal and prevention of scaling is still possible. However, the amount of removal compared to the tuned system was less.

3. Not every combination of feedwater and resin will result in sulfate removal

In situations when the value of  $\alpha_{S/Cl}$  is significantly different from the best case scenario, no reduction in scaling occurs which is similar to the results from Runs 4 and 6.

4. HIX-RO is not only applicable to sulfate

During Run 5 in cycles 10-13, a 50% reduction in phosphate was measured. While the main focus of this study was sulfate removal, phosphate is another divalent anion that easily precipitates with calcium. If phosphate removal is desired, similar experiments may be done for phosphate/chloride separation factors to ensure high phosphate removal.

### **6.3 Characterization of potential for in-column precipitation of CaSO<sub>4</sub>**

During regeneration of the ion exchange column, the effluent from the column is a highly concentrated brine of sulfate and the formation of CaSO<sub>4</sub> may be a problem. Precipitation of CaSO<sub>4</sub> inside the column could cause clogging of the ion exchange bed or, worse, inhibition of portions of the resin. This would not only result in higher head

losses through the column but reduced efficiency from the reduction in available ion exchange sites.

### **6.3.1 Measurement of CaSO<sub>4</sub> Precipitation Kinetics**

The precipitation of CaSO<sub>4</sub> is not instantaneous. The rate is dependent upon several factors including: induction time, presence of seed crystals, and how well-mixed the bulk solution is.<sup>38</sup> It is therefore necessary to determine how quickly CaSO<sub>4</sub> will precipitate relative to a typical bed contact time. The rate of CaSO<sub>4</sub> precipitation kinetics were measured using the procedure described in **Section 3.6**. Briefly, different volumes of stock solutions of CaCl<sub>2</sub> and Na<sub>2</sub>SO<sub>4</sub> were added to large test tubes and mixed creating supersaturated solutions of CaSO<sub>4</sub> with varying SI values. A video camera was set up to record when precipitation occurs for each SI value and the results are plotted in **Figure 6.18**. From the fitted line, the time for CaSO<sub>4</sub> to precipitate with an SI value of 2.72 (the SI value of the regenerant) is approximately 120 minutes.

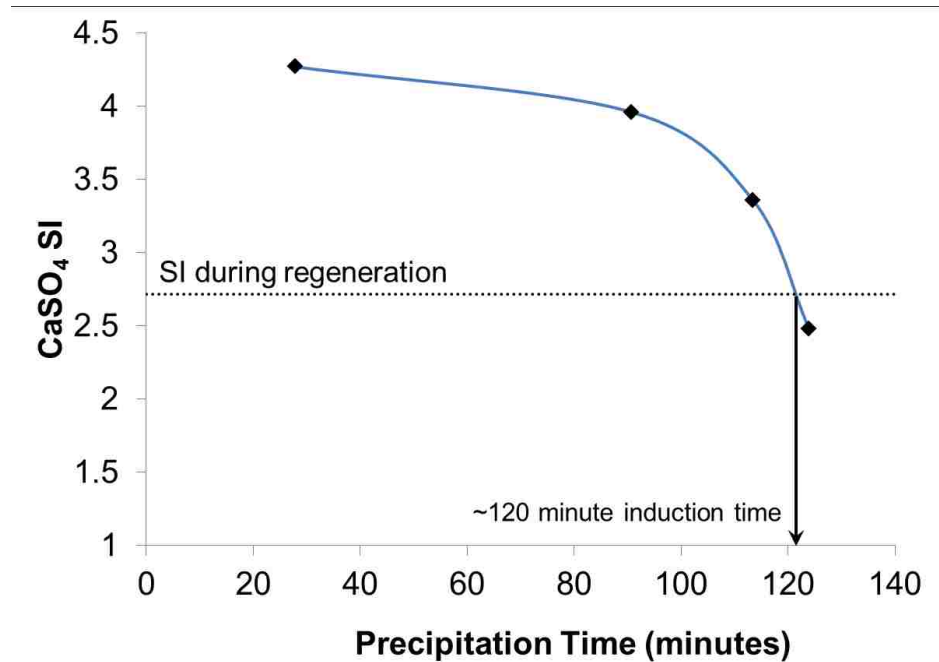


**Figure 6.18** Time for visible precipitation of CaSO<sub>4</sub> with varying SI values

### 6.3.2 Small scale in-column precipitation study

Following the procedure detailed in **Section 3.7**, a study on the potential for in-column precipitation of CaSO<sub>4</sub> was performed. Synthetic influent and regenerant solutions were passed through a 50/50 mixture of polystyrene and polyacrylic anion exchange resins.

During regeneration, the empty bed contact time was 10 minutes which is significantly less than the predicted time for CaSO<sub>4</sub> precipitation.

Three consecutive cycles were run and no precipitate was observed within the mixed-bed anion exchange column. However, after 120 minutes, visible precipitates were formed in the tubes of the sample collector, as shown in **Figure 6.19**.

For more quantitative information, samples were collected from the effluent during the third cycle. Samples were collected during regeneration and small aliquots of effluent regenerant were immediately diluted to prevent precipitation. Calcium and sulfate were analyzed in the diluted samples and after 24 hours and SI values were calculated using OLI.<sup>61</sup> The calculated SI values are plotted log-scale in **Figure 6.20** against bed volumes of reject regenerant passed for the two sets of samples. While the effluent solution was, in fact, supersaturated with  $\text{CaSO}_4$ , no visible precipitation occurred inside the column.

In addition to visible inspection, samples of ion exchange resin were extracted from the column and analyzed using SEM-EDX to determine if any calcium was present inside the bead. Before analysis, beads were washed with deionized water and left to air dry for 24 hours. Individual beads were then sliced using a razor blade dipped in liquid nitrogen and analyzed using the procedure outlined in **Section 3.2.4**.

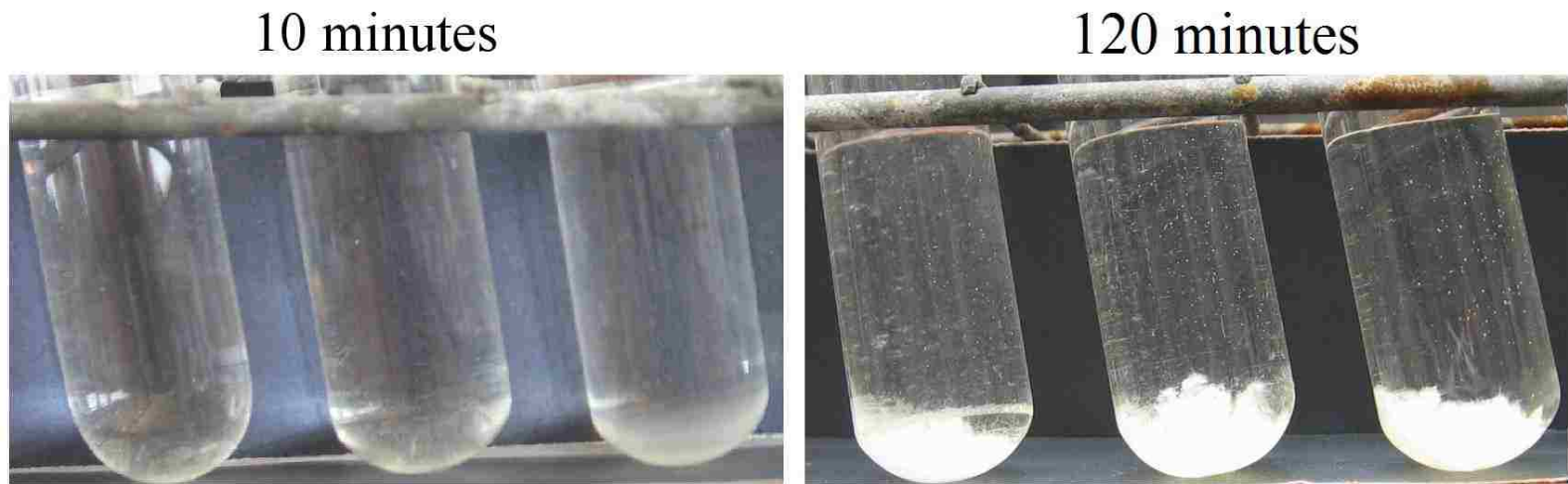


**Figure 6.19** Formation of  $\text{CaSO}_4$  precipitate after 120 minutes

Results from analysis of 7 different ion exchange resin halves showed that none of the resins analyzed had any trace of calcium. A representative EDX spectrum is shown in **Figure 6.21**.

The composition of the bead contained carbon, nitrogen, chlorine, oxygen, and sulfur but no calcium. These elements are expected for a strong base anion exchange resin. Carbon is present in the resin matrix, nitrogen in the quaternary ammonium functional group, and chloride, sulfur, and oxygen would be any chloride or sulfate ions occupying the exchange sites.

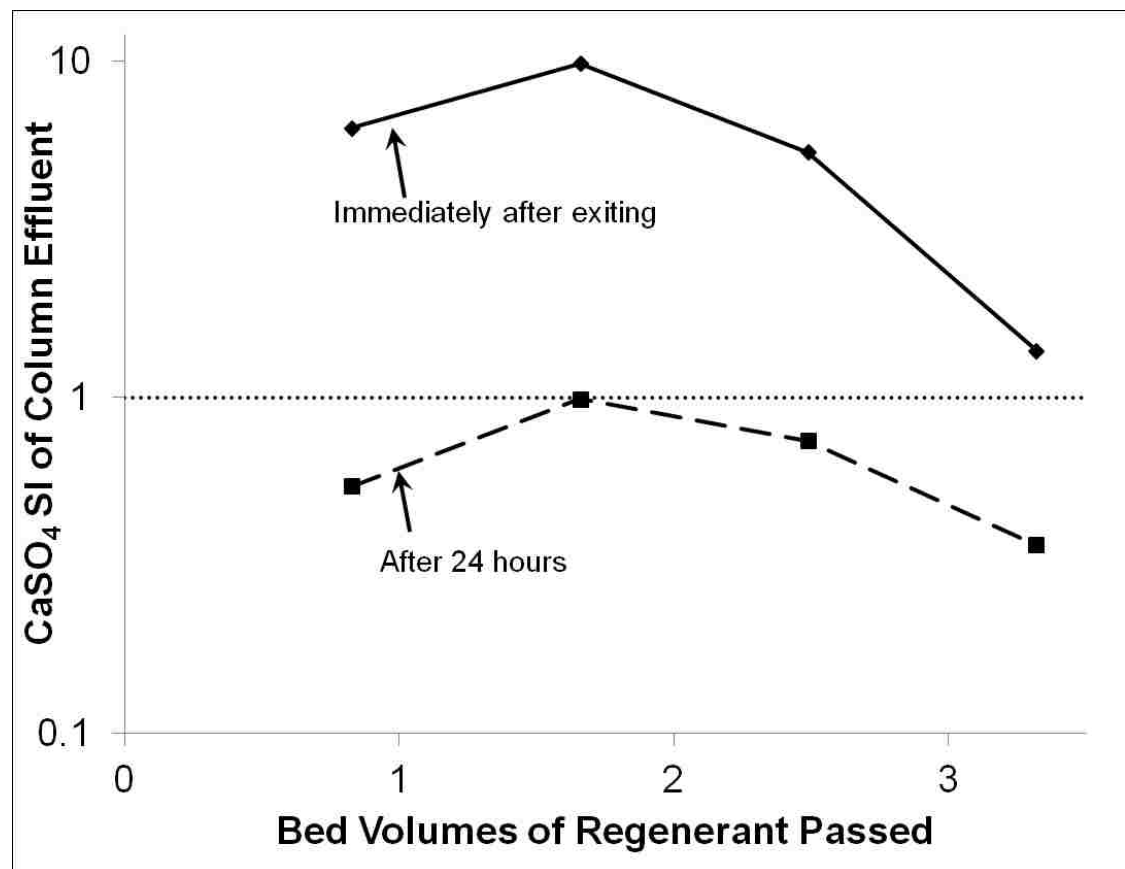


**Figure 6.20** CaSO<sub>4</sub> SI values immediately after exiting and after 24 hours

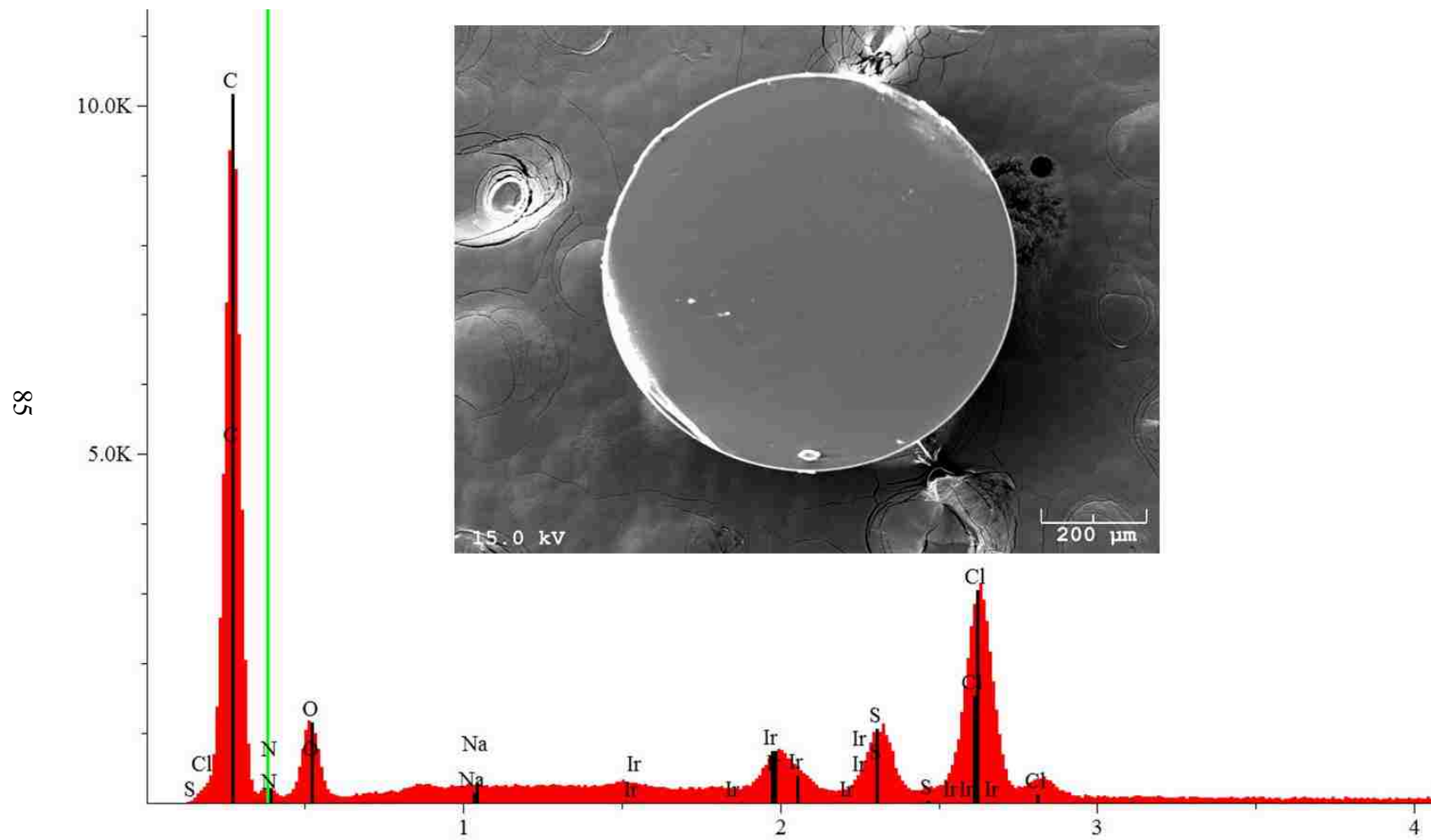


**Figure 6.21** Representative EDX spectrum of resin bead



### 6.3.3 Explanation for lack of in-column precipitation

There are two reasons why no  $\text{CaSO}_4$  precipitated inside of the ion exchange column. The first is that the bed contact time was kept at only 9.3 minutes which is significantly shorter than the kinetics of  $\text{CaSO}_4$  formation. Even though the supersaturation index was greater than 1 for the first 3 bed volumes, precipitation would take more than 120 minutes (from **Figure 6.18**), but the bed contact time was significantly less. Similar results from previous research have demonstrated that if an ion exchange reaction results in thermodynamically favorable precipitation, no precipitation may occur; this concept is known as ion exchange induced supersaturation or IXISS.<sup>82</sup>

The second reason for the lack of in-column  $\text{CaSO}_4$  formation is due to Donnan membrane effects. The large number of positively charged sites on the ion exchange resin makes transfer of  $\text{Ca}^{2+}$  to inside the bead highly unfavorable. For example, an anion exchange resin with 2 meq/g capacity can theoretically possess up to  $1.20 \times 10^{21}$  positive sites per gram of resin.

Estimation of the concentration of  $\text{Ca}^{2+}$  inside the resin can be performed by assuming that only  $\text{Ca}^{2+}$  and  $\text{Cl}^-$  are present in solution, and the resin is in chloride form. For these assumptions, **Equation 6.1** is valid

$$[\text{Ca}^{2+}]_i [\text{Cl}^-]_i^2 = [\text{Ca}^{2+}]_o [\text{Cl}^-]_o^2 \quad \text{Equation 6.1}$$

in which subscripts “i” and “o” are the concentration of the ion inside or outside of the resin, respectively. If the total capacity of the resin is 2.2 M and  $x$  mol/L of  $\text{Ca}^{2+}$  enter the resin, then the amount of  $\text{Cl}^-$  inside the resin is therefore  $2+2x$ . If the regenerant

concentration is 400 meq/L, then  $\text{Cl}^-$  will be 0.4M and  $\text{Ca}^{2+}$  will be 0.2M. Subbing these values into **Equation 6.1** results in

$$(x)(2.2 + 2x)^2 = (0.2M)(0.4M)^2 \qquad \text{Equation 6.2}$$

Solving for  $x$ , gives an inter-resin  $\text{Ca}^{2+}$  concentration of  $6.53 \times 10^{-3}$  M or 13.1 meq/L which is only ~3% of the total calcium in the regenerant.

Due to the inability of calcium to enter inside the resin combined with slow reaction kinetics, precipitation with sulfate inside is highly unfavorable.

## **7. Key Contributions and Future Work**

### **7.1 Key Findings**

This study focused on using ion exchange resin to selectively remove and replace sulfate by chloride from brackish waters in order to allow for increased recovery in desalination processes. The elimination of sulfate from the feedwater prevents the formation of calcium sulfate during desalination which allows higher recovery and a reduction in the volume of produced brine and a reduction in the amount of antiscalant required.

The proposed Hybrid Ion Exchange-Reverse Osmosis (HIX-RO) process uses the produced concentrate solution from the reverse osmosis process as a regenerant for the ion exchange column eliminating any requirement for purchasing or preparing regenerant solution. This is achieved by properly designing the ion exchange column to preferentially remove sulfate from the feedwater but selectively pick up chloride from the RO concentrate brine. Key findings from this study are:

- 1. Ion exchange resin selectivity can be controlled through mixing of characteristically different resins**

After characterization of resin properties, the separation factor can be determined for any combination of resins with any feedwater composition through a series of calculations. These calculations allow the HIX-RO process to be tuned to any brackish water and RO recovery combination. The only modification necessary is changing the type or ratio of mixing of different resins.

**2. The HIX-RO process is able to effectively prevent sulfate scaling for a well-designed system**

All HIX-RO runs with a 50/50 mixture of polyacrylic and polystyrene resins were able to significantly reduce or eliminate sulfate present in the feed to the RO unit. In addition to the high removal of sulfate, calculations show that there was no threat to precipitation of  $\text{CaSO}_4$  throughout the process.

**3. Improperly designed HIX-RO systems may or may not provide sulfate removal**

Other HIX-RO runs with varying resin mixtures and changes demonstrate that when the ion exchange column has not been tailored to the feedwater it is not possible to achieve the same amount of sulfate removal for a properly designed setup. Furthermore, sulfate removal may occur, but the amount of sulfate removed was always less than the properly designed system. For cases where the resin never preferred sulfate, very little removal was observed and the ion exchange column was unable to prevent scaling. In total, not every combination of resin and feedwater will result in prevention of scaling; only systems where the column has been properly designed will ensure high sulfate removal.

#### **4. CaSO<sub>4</sub> will not precipitate inside the ion exchange column during regeneration**

During regeneration, there is a high concentration of sulfate in the regenerant and a high potential for the precipitation of CaSO<sub>4</sub>. However, while it may be thermodynamically favorable, the timescale for the kinetics of CaSO<sub>4</sub> precipitation is much longer than the usual empty bed contact time for an ion exchange system. In addition, the Donnan Membrane Effect prevents Ca<sup>2+</sup> from entering inside the resin.

## **7.2 Future Work**

### **7.2.1 Field-scale testing**

During lab scale studies of HIX-RO, sulfate scaling was effectively controlled by using a proper mixture of ion exchange resins. However, the current system has only been operated in a semi-continuous method; the ion exchange column and RO system were completely separated from each other. In addition, there was little to no variation in the composition of the feedwater. The next important step in proving the efficacy of the HIX-RO process would be to set up a system at an actual desalination plant. Field testing of HIX-RO would help identify any unforeseen issues while demonstrating that the process can be operated in a continuous fashion.

### **7.2.2 Phosphate removal**

While the initial focus of HIX-RO is for the prevention of CaSO<sub>4</sub> scaling, calcium phosphate is another common precipitate in desalination systems. Since phosphate mainly exists as a divalent anion, there is no foreseeable reason why the HIX-RO

system cannot also be designed to remove phosphate in addition to sulfate. A similar plot to Figure 4.2 may be created for phosphate/chloride and superimposed on the sulfate/chloride plot and anywhere the two shaded areas line up, the system may provide both sulfate and phosphate removal.

### **7.2.3 Improved ion exchange modeling**

The model used to simulate the ion exchange column as a series of CSTRs was a simplification of the actual system. Solving the actual partial differential equation (**Equation 5.4**) is possible but was not meant to exactly predict the effluent concentration from the column. The goal was to determine how important resin selectivity was to the process efficiency; i.e. what values of  $\alpha_{S/Cl}$  result in high sulfate removal. When comparing the predicted effluent to the actual effluent concentration from experimental runs there is a significant difference. If the HIX-RO system is to be installed in a real-life situation it would necessitate improving the model to ensure the predicted concentration of sulfate closely match the experimentally measured sulfate concentration.

## References

- (1) United States Environmental Protection Agency. Fiscal Year 2011: Drinking and Ground Water Statistics. <http://water.epa.gov/scitech/datait/databases/drink/sdwisfed/upload/epa816r13003.pdf> (accessed September 20, 2014).
- (2) Averyt, K.; Meldrum, J.; Caldwell, P.; Sun, G.; McNulty, S.; Huber-Lee, a; Madden, N. Sectoral Contributions to Surface Water Stress in the Coterminous United States. *Environ. Res. Lett.* **2013**, *8*, 035046.
- (3) Scanlon, B. R.; Faunt, C. C.; Longuevergne, L.; Reedy, R. C.; Alley, W. M.; McGuire, V. L.; McMahon, P. B. Groundwater Depletion and Sustainability of Irrigation in the US High Plains and Central Valley. *Proc. Natl. Acad. Sci. U.S.A.* **2012**, *109* (24), 9320-9325.
- (4) Ye, L.; Grimm, N. B. Modelling Potential Impacts of Climate Change on Water and Nitrate Export from a Mid-Sized, Semiarid Watershed in the US Southwest. *Clim. Change* **2013**, *120*, 419–431.
- (5) MacDonald, G. M. Severe and Sustained Drought in Southern California and the West: Present Conditions and Insights from the Past on Causes and Impacts. *Quat. Int.* **2007**, *173-174*, 87–100.
- (6) MacDonald, G. M. Climate Change and Water in Southwestern North America Special Feature: Water, Climate Change, and Sustainability in the Southwest. *Proc. Natl. Acad. Sci. U.S.A.* **2010**, *107* (50), 21256–21262.

- (7) Sabo, J. L.; Sinha, T.; Bowling, L. C.; Schoups, G. H. W.; Wallender, W. W.; Campana, M. E.; Cherkauer, K. a; Fuller, P. L.; Graf, W. L.; Hopmans, J. W.; et al. Reclaiming Freshwater Sustainability in the Cadillac Desert. *Proc. Natl. Acad. Sci. U.S.A.* **2010**, *107* (50), 21263–21270.
- (8) Gober, P.; Kirkwood, C. W. Vulnerability Assessment of Climate-Induced Water Shortage in Phoenix. *Proc. Natl. Acad. Sci. U.S.A.* **2010**, *107* (50), 21295–21299.
- (9) Reynolds, T.D.; Richards, P.A. *Unit Operations and Processes in Environmental Engineering*, Second Edition; PWS Publishing Company: Boston, 1996.
- (10) National Research Council. *Desalination: A National Perspective*; The National Academies Press: Washington, DC, 2008.
- (11) Nicot, J.; Walden, S.; Greenlee, L.; Els, J. A Desalination Database For Texas. October 2005. [http://www.beg.utexas.edu/environqlty/desalination/Final%20Report\\_R1\\_1.pdf](http://www.beg.utexas.edu/environqlty/desalination/Final%20Report_R1_1.pdf). (accessed September 20, 2014).
- (12) Mickley, M.C. Membrane Concentrate Disposal: Practices and Regulations, Desalination and Water Purification Research and Development Program Report No. 69. *Membrane Concentrate Disposal: Practices and Regulation*; U.S. Department of the Interior, September 2001.
- (13) Abdul-Wahab, S. a.; Al-Weshahi, M. a. Brine Management: Substituting Chlorine with On-Site Produced Sodium Hypochlorite for Environmentally Improved Desalination Processes. *Water Resour. Manag.* **2009**, *23*, 2437–2454.
- (14) Mickley, M.C. Desalination and Water Purification Research and Development Program Report No. 155. *Treatment of Concentrate*; US Department of the Interior Bureau of Reclamation. May 2009.



- (15) Younos, T. Environmental Issues of Desalination. *J. Contemp. Wat. Res. & Educ.* **2005**, *132*, 11-18.
- (16) Hasson, D.; Drak, A.; Semiat, R. Inception of CaSO<sub>4</sub> scaling on RO membranes at various water recovery levels. *Desalination* **2001**, *139*, 73-81.
- (17) Le Gouellac, Y. A.; Elimelech, M. Calcium Sulfate (Gypsum) Scaling in Nanofiltration of Agricultural Drainage Water. *J. Membr. Sci.* **2002**, *205*, 279–291.
- (18) Shih, W.; Rahardianto, A.; Lee, R.; Cohen, Y. Morphometric characterization of calcium sulfate dehydrate (gypsum) scale on reverse osmosis membranes. *J. Membr. Sci.* **2005**, *252* (1-2), 253-263.
- (19) Al-Amoudi, A.; Lovitt, R. W. Fouling Strategies and the Cleaning System of NF Membranes and Factors Affecting Cleaning Efficiency. *J. Membr. Sci.* **2007**, *303*, 4–28.
- (20) Gabelich, C. J.; Williams, M. D.; Rahardianto, A.; Franklin, J. C.; Cohen, Y. High-recovery reverse osmosis desalination using intermediate chemical demineralization. *J. Membr. Sci.* **2007**, *301* (1-2), 131-141.
- (21) Tzotzi, C.; Pahiadaki, T.; Yiantios, S.G.; Karabelas, A.J.; Andritsos, N. A study of CaCO<sub>3</sub> scale formation and inhibition in RO and NF membrane processes. *J. Membr. Sci.* **2007**, *296*, 171-184.
- (22) Lyster, E.; Au, J.; Rallo, R.; Giralt, F.; Cohen, Y. Coupled 3-D Hydrodynamics and Mass Transfer Analysis of Mineral Scaling-Induced Flux Decline in a Laboratory Plate-and-Frame Reverse Osmosis Membrane Module. *J. Membr. Sci.* **2009**, *339*, 39–48.

- (23) Alhseinat, E. A.; Sheikholeslami, R. A Reliable approach for Barite, Celestite and Gypsum scaling propensity prediction during reverse osmosis treatment for produced water. In *International Proceedings of Chemical, Biological, and Environmental Engineering vol. 21*, 2011 International Conference on Environment and BioScience; IACIST Press: Signapore, 2011; 52-57.
- (24) Antony, A.; Low, J. H.; Gray, S.; Childress, A. E.; Le-Clech, P.; Leslie, G. Scale Formation and Control in High Pressure Membrane Water Treatment Systems: A Review. *J. Membr. Sci.* **2011**, 383, 1–16.
- (25) Van Driessche, a E. S.; Benning, L. G.; Rodriguez-Blanco, J. D.; Ossorio, M.; Bots, P.; García-Ruiz, J. M. The Role and Implications of Bassanite as a Stable Precursor Phase to Gypsum Precipitation. *Science* **2012**, 336, 69–72.
- (26) Waly, T. Kennedy, M.D.; Witkamp, G.; Amy, G.; Schippers, J.C. The role of inorganic ions in the calcium carbonate scaling of seawater reverse osmosis systems. *Desalination* **2012**, 284, 279-287.
- (27) Rahardianto, A. Diagnostic characterization of gypsum scale formation and control in RO membrane desalination of brackish water. *J. Membr. Sci.* **2006**, 279, 655-668.
- (28) Florida Department of Environmental Protection. Desalination in Florida: Technology, Implementation, and Environmental Issues. April 2010 <http://www.dep.state.fl.us/water/docs/desalination-in-florida-report.pdf> (Accessed October 10, 2014).
- (29) Tang, W.; Ng, H.Y. Concentration of brine by forward osmosis: performance and influence of membrane structure. *Desalination* **2008**, 224, 143–153.

- (30) Martinetti, C. R.; Childress, A. E.; Cath, T. Y. High Recovery of Concentrated RO Brines Using Forward Osmosis and Membrane Distillation. *J. Membr. Sci.* **2009**, *331*, 31–39.
- (31) Cath, T. Y. Osmotically and Thermally Driven Membrane Processes for Enhancement of Water Recovery in Desalination Processes. *Desalin. Water Treat.* **2010**, *15*, 279–286.
- (32) Zhao, S.; Zou, L.; Tang, C. Y.; Mulcahy, D. Recent Developments in Forward Osmosis: Opportunities and Challenges. *J. Membr. Sci.* **2012**, *396*, 1–21.
- (33) Greenlee, L. F.; Testa, F.; Lawler, D. F.; Freeman, B. D.; Moulin, P.; Ce, P. The Effect of Antiscalant Addition on Calcium Carbonate Precipitation for a Simplified Synthetic Brackish Water Reverse Osmosis Concentrate. *Water Res.* **2010**, *44*, 2957–2969.
- (34) Greenlee, L. F.; Testa, F.; Lawler, D. F.; Freeman, B. D.; Moulin, P. Effect of Antiscalant Degradation on Salt Precipitation and Solid/liquid Separation of RO Concentrate. *J. Membr. Sci.* **2011**, *366*, 48–61.
- (35) Antony, A.; Low, J. H.; Gray, S.; Childress, A. E.; Le-Clech, P.; Leslie, G. Scale Formation and Control in High Pressure Membrane Water Treatment Systems: A Review. *J. Membr. Sci.* **2011**, *383*, 1–16.
- (36) McCool, B. C.; Rahardianto, A.; Cohen, Y. Antiscalant Removal in Accelerated Desupersaturation of RO Concentrate via Chemically-Enhanced Seeded Precipitation (CESP). *Water Res.* **2012**, *46*, 4261–4271.

- (37) Pérez-González, a; Urtiaga, a M.; Ibáñez, R.; Ortiz, I. State of the Art and Review on the Treatment Technologies of Water Reverse Osmosis Concentrates. *Water Res.* **2012**, *46*, 267–283.
- (38) Halevy, S.; Korin, E.; Gilron, J.; Box, P. O. Kinetics of Gypsum Precipitation for Designing Interstage Crystallizers for Concentrate in High Recovery Reverse Osmosis. *Ind. Eng. Chem. Res.* **2013**, *52*, 14647-14657.
- (39) Subramani, A.; Jacangelo, J. G. Treatment Technologies for Reverse Osmosis Concentrate Volume Minimization: A Review. *Sep. Purif. Technol.* **2014**, *122*, 472–489.
- (40) Hann, F. French Patent No. 846,628, Nov 15, 1938.
- (41) Kaufman, C.E. Treatment of Water for Boiler Feed. U.S. Patent 2,395,331, Feb 19, 1946.
- (42) Klein, G.; Villena-Blanco, M.; Vermeulen, T. Ion-exchange equilibrium data in the design of a cyclic sea water softening process. *I&EC Process Des. Dev.* **1964**, *3* (3), 280-287.
- (43) Klein, G.; Cherney, S. Ruddicks, E.L. Vermeulen, T. Calcium removal from sea water by fixed-bed ion exchange. *Desalination.* **1968**, *4* (2), 158-166.
- (44) United States Department of the Interior Office of Saline Water Research and Development. Seawater softening by ion exchange as a saline water conversion pretreatment. Progress Report 62. 1962. <http://digital.library.unt.edu/ark:/67531/metadc11622/m1/12/>
- (45) van Hoek, C.; Kaakinen, J.W.; Haugseth, L.A. Ion exchange pretreatment using desalting plant concentrate for regeneration. *Desalination.* **1976**, *19* (1-3), 471-479.

- (46) Kaakinen, J.W.; Eisenhauer, R.J. van Hoek, C. High recovery in the Yuma desalting plant. *Desalination*. **1977**, *23* (1-3), 357-366.
- (47) Wilf, M. Konstantin, M. Chencinsky, A. Evaluation of an ion exchange system regenerated with seawater for the increase of product recovery of reverse osmosis brackish water plant. *Desalination*. **1980**, *34*, 189-197.
- (48) Vermeulen, T. Tleimat, B. W.; Klein, G. Ion-exchange pretreatment for scale prevention in desalting systems. *Desalination*. **1983**, *47*(1-3), 149-159.
- (49) Barba, D.; Brandani, V.; Foscolo, P.U. A method based on equilibrium theory for a correct choice of a cationic resin in sea water softening. *Desalination*. **1983**, *48* (2), 133-146.
- (50) Shain, P.; Klein, G.; Vermeulen, T. A Mathematical Model of the Cyclic Operation of Desalination-Feedwater Softening by Ion-Exchange with Fluidized-Bed Regeneration. *Desalination*. **1988**, *69* (3), 135-146.
- (51) Muraviev, D.; Khamizov, R.Kh.; Tikhonov, N.A.; Morales, J.G. Clean (“Green”) Ion-Exchange Technologies. 4. High-Ca-Selectivity Ion-Exchange Material for Self-Sustaining Decalcification of Mineralized Waters Process. *Ind. Eng. Chem. Res.* **2004**, *43*, 1869-1874.
- (52) Tokmachev, M. G.; Tikhonov, N. a.; Khamizov, R. K. Investigation of Cyclic Self-Sustaining Ion Exchange Process for Softening Water Solutions on the Basis of Mathematical Modeling. *React. Funct. Polym.* **2008**, *68*, 1245–1252.
- (53) Mukhopadhyay, D. Method and Apparatus for High Efficiency Reverse Osmosis Operation. U.S. Patent 6,537,456, March 25, 2003.

- (54) Sarkar, S.; SenGupta, A.K. A new hybrid ion exchange-nanofiltration (HIX-NF) separation process for energy-efficient desalination: Process concept and laboratory evaluation. *J. Membr. Sci.* **2008**, *324*, 76-84.
- (55) Venkatesan, A. Wankat, P.C. Desalination of the Colorado River water: A hybrid approach. *Desalination* **2012**, *286*, 176-186.
- (56) Abdulgader, H. Al; Kochkodan, V.; Hilal, N. Hybrid Ion Exchange – Pressure Driven Membrane Processes in Water Treatment: A Review. *Sep. Purif. Technol.* **2013**, *116*, 253–264.
- (57) Helfferich, F. *Ion Exchange*; Dover Publications, Inc.: New York, 1995
- (58) Clifford, D.; Weber Jr., W.J. The determinants of divalent/monovalent selectivity in anion exchangers. *React. Polym.* **1983**, *1*, 77-89.
- (59) G. Boari, L. Liberti, C, Merli and R. Passino, Exchange equilibria on anion resins, *Desalination* **1974**, *15*(2), 145-166.
- (60) Aveni, A.; Boari, G.; Liberti, L.; Santori, M.; Monopoli, B. Sulfate removal and dealkalization on weak resins of the feed water for evaporation desalting plants. *Desalination* **1975**, *16*(2), 135-149.
- (61) *OLI Stream Analyzer*, Version 9.0; OLI Systems, Inc.: Cedar Knolls, NJ, 2013.
- (62) *Standard Methods for the Examination of Water and Wastewater*, 18<sup>th</sup> Edition; American Public Health Association: Washington, DC, 1992.
- (63) *USEPA SulfaVer 4 Method 8051*; Hach Company. DOC316.53.01135
- (64) *Product Manual for IonPac AG10 and AS10 Columns*; Thermo Scientific. Document No. 034519; 14 November 2008.

- (65) *Analytical Methods for Atomic Absorption Spectrometry*. The Perkin-Elmer Corporation, 1994.
- (66) Padungthon, S.; Li, J.; German, M.; SenGupta, A. K. Hybrid Anion Exchanger with Dispersed Zirconium Oxide Nanoparticles: A Durable and Reusable Fluoride-Selective Sorbent. *Environ. Eng. Sci.* **2014**, *31*, 360–372.
- (67) Snoeyink, V.L.; Jenkins, D. *Water Chemistry*; John Wiley & Sons: New York, 1980.
- (68) Gregor, H.P. Gibbs-Donnan Equilibrium in Ion Exchange Resin Systems. *J. Am. Chem. Soc.* **1951**, *73*(2), 642-650.
- (69) Gregor, H.P.; Abolafia, O.R.; Gottlieb, M.H. Ion-exchange resins. X. Magnesium-Potassium exchange with a polystyrenesulfonic acid cation-exchange resin. *J. Phys. Chem.* **1954**, *58*(11), 984-986.
- (70) Harris, C.D. *Quantitative Chemical Analysis*, 8<sup>th</sup> Edition; W. H. Freeman and Company: New York, 2010.
- (71) Clifford, D. A. Ion Exchange and Inorganic Adsorption. In *Water Quality and Treatment: A Handbook of Community Water Supplies*, 5th ed. Mays, L.W., Ed. American Water Works Association; McGraw-Hill: 1999; pp 9.1-9.91.
- (72) SenGupta, A. K.; Greenleaf, J. E. Arsenic in Subsurface Water: Its Chemistry and Removal by Engineered Processes. In *Environmental Separation of Heavy Metals: Engineering Processes*; SenGupta, A. K., Ed.; CRC Press LLC: Boca Raton, FL, 2002; pp 265-306.
- (73) Cussler, E.L. *Diffusion: Mass Transfer in Fluid Systems*; Cambridge University Press: Cambridge, 2009.

- (74) Uemura, T.; Henmi, M. Thin-Film Composite Membranes for Reverse Osmosis. In *Advanced Membrane Technology and Applications*; Li, N.N., Fane, A.G., Ho, W.S.W., Matsuura, T., Eds.; John Wiley & Sons, Inc.: New Jersey, 2008; pp 3-20.
- (75) Greenlee, L. F.; Lawler, D. F.; Freeman, B. D.; Marrot, B.; Moulin, P. Reverse Osmosis Desalination: Water Sources, Technology, and Today's Challenges. *Water Res.* **2009**, *43*, 2317–2348.
- (76) Lee, I.-H.; Kuan, Y.-C.; Chern, J.-M. Prediction of Ion-Exchange Column Breakthrough Curves by Constant-Pattern Wave Approach. *J. Hazard. Mater.* **2008**, *152*, 241–249.
- (77) Helfferich, F. Ion Exchange Kinetics. *J. Phys. Chem.* **1965**, *69*(4), 1178-1187.
- (78) Guter, G.A. Nitrate Removal from Contaminated Groundwater by Anion Exchange. In *Ion Exchange Technology: Advances in Pollution Control*; SenGupta, A.K., Ed.; Technomic Publishing Co. Inc.: Lancaster, PA, 1995; pp 61-148.
- (79) Wanakt, P.C. *Rate-Controlled Separations*; Blackie Academic & Professional: London, 1994.
- (80) Greenberg, G.; Hasson, D.; Semiat, R. Limits of RO Recovery Imposed by Calcium Phosphate Precipitation. *Desalination* **2005**, *183*, 273–288.
- (81) Blaney, L.; Cinar, S.; Sengupta, a. Hybrid Anion Exchanger for Trace Phosphate Removal from Water and Wastewater. *Water Res.* **2007**, *41*, 1603–1613.
- (82) Muraviev, D.N.; Khamizov, R. Ion-Exchange Isothermal Supersaturation: Concept, Problems, and Applications. In *Ion Exchange and Solvent Extraction*; SenGupta, A.K.; Marcus, Y., Eds.; Marcel Dekker, Inc.: New York, 2004; Vol. 16, pp 119-210.



- (83) Keyes, C.G.; Fahy, M.P.; Tansel, B, Eds.; *Concentrate Management in Desalination*; American Society of Civil Engineers: Reston, Virginia, 2012.
- (84) Hutchison, W.R. Deep-Well Injection of Desalination Concentrate in El Paso, Texas. *Southwest Hydrology*, March/April 2008, 28-30.
- (85) Swamee, P.K.; Jain, A.K. Explicit Equations for Pipe-Flow Problems. *ASCE J. Hydraul. Div.* **1976**, *102*(5), 657-664.

## **8. Appendix I – Cost Analysis**

The ultimate goal of HIX-RO is to install an ion exchange column at a preexisting desalination facility and operate the plant at increased recovery. No additional modifications to process are required apart from installation of the ion exchange column. It is necessary to determine what savings could be gained from the installation of an HIX-RO system.

### **8.1 Assumptions**

Several assumptions must be made before analysis can be performed:

1. Reductions in operational costs can only occur in two ways: elimination of antiscalant dosing and reducing concentrate pumping costs
2. Revenue from the extra drinking water produced is calculated from the current amount charged: \$6.827 per thousand gallons (value obtained from local water bill)
3. Only polyacrylic acid will be assumed to be dosed
4. Only the ion exchange resin will be calculated into the installation costs
5. Cost analysis will be performed on the largest inland desalination plant in the world, the Kay Bailey Hutchison Desalination Plant in El Paso, TX, which treats 18.5 MGD of water to produce 15.5 MGD of permeate and 3 MGD of reject brine<sup>83</sup>
6. A 50% decrease in volume of concentrate is achieved (i.e. 1.5 MGD)

## **8.2 Resin Costs**

For a 15.5 MGD flow rate and a 10 minute empty bed contact time, each ion exchange column would have to be at least 407.5 m<sup>3</sup>. For a properly operating HIX-RO system at least 2 columns would be required, but in case of maintenance, a third column would be required for backup. Therefore a minimum of 1222.4 m<sup>3</sup> of resin is needed.

Assuming the cost of resin is \$250 per ft<sup>3</sup>, the total cost of ion exchange resin for the system would be \$10.8 million.

## **8.3 Dosing Costs**

Assuming that all 15 MGD of influent feedwater is dosed with 6 mg/L of polyacrylic acid (from **Table 1.1**), 340.7 kg of polyacrylic acid are required each day. Assuming the cost of polyacrylic acid is \$10 per kg, the daily amount spent on antiscalant is about \$3500.

## **8.4 Revenue from increased recovery**

An extra 1.5 MGD of water would be produced. If the current cost of water is \$6.827 per 1000 gallons, the extra revenue from selling 1.5 MGD of water would be \$10,240.50 per day.

## **8.5 Pumping Requirements**

Calculation of pumping costs is achieved by determining the total amount of head needed to transport the concentrate down the pipeline considering both elevation differences and head loss from pipe friction.

The actual concentrate pipeline is 22 miles long and is made from HDPE<sup>84</sup>. There is no available data on the actual size of the pipeline apart from pictures. Using available pictures of the pipeline it is estimated that the diameter of the pipe is 16 inches (0.41 m) and the deep well injection site is approximately 50m higher in elevation than the desalination plant.

Assuming that the pressure at both ends of the pipe are equal, the energy equation for this system can be written as:

$$z_1 + h_L = z_2 + h_P \quad \text{Equation A1.1}$$

in which  $z_1$  and  $z_2$  represent the elevation at the plant and discharge point, respectively,  $h_L$  is the head loss from pipe friction, and  $h_P$  is the pumping head added to the system from the pumps. Pipe friction head loss is calculated from the Darcy-Weisbach Equation

$$h_L = f \frac{L V^2}{D 2g} \quad \text{Equation A1.2}$$

in which  $f$  is the friction factor,  $L$  is the length of the pipe,  $D$  is the pipe diameter,  $V$  is velocity through the pipe, and  $g$  is the gravitational constant. The friction factor  $f$  is calculated from **Equation A1.3**<sup>85</sup>

$$f = \frac{0.25}{\left[ \log \left( \frac{k_s}{3.7D} + \frac{5.74}{\text{Re}^{0.9}} \right) \right]^2} \quad \text{Equation A1.3}$$

in which  $k_s$  is the equivalent sand grain roughness of the pipe and  $Re$  is the Reynold's number calculated by

$$Re = \frac{VD}{\nu} \quad \text{Equation A1.4}$$

in which  $\nu$  is the kinematic viscosity of the fluid. After solving equation **Equation A1.1** for  $h_P$ , the amount of pumping power required ( $P$ ) is calculated by

$$P = \frac{\gamma Q h_P}{\eta} \quad \text{Equation A1.5}$$

in which  $\gamma$  is the specific weight of the fluid,  $Q$  is the flow rate, and  $\eta$  is the pump efficiency.

Due to the fact that the composition of water will change when calculation of the pumping power required is achieved by using the inputs listed in **Table A1.1**

**Table A1.1** Assumptions made when calculating head loss

Cost of electricity	8.35	¢/kWh
Distance to pump	35,405	meters
Pipe diameter	0.4064	m
Elevation at plant	1,205	m
Elevation at injection well	1,257	m
Pipe roughness ( $k_s$ )	0	
Kinematic Viscosity ( $\nu$ )	$1.00 \times 10^{-6}$	$\text{m}^2/\text{s}$
Specific Weight ( $\gamma$ )	9810	$\text{N}/\text{m}^3$
Pump efficiency ( $\eta$ )	80%	

**Table A1.2** gives the calculations for when reject flow rate is 3MGD and 1.5 MGD.

**Table A1.2** Calculation of pumping costs per day

Pumping rate	3	1.5	MGD
Pumping rate	0.131	0.066	m <sup>3</sup> /s
$V$	1.013	0.507	m/s
$Re$	$4.12 \times 10^5$	$2.06 \times 10^5$	
$f$	0.0136	0.0154	
Total head loss ( $h_L$ )	61.8	17.6	m
Total pumping head required ( $h_P$ )	113.8	69.6	m
Total Pumping Power Required	183.4	56.1	kW
<b>Total pumping cost per day</b>	<b>\$367.58</b>	<b>\$112.41</b>	<b>per day</b>

In total, before any changes to the system are made, the plant is estimated to spend \$3888.02 every day on antiscalant and pumping. After installation of the HIX-RO system, the plant would only spend \$112.41 per day and gain \$10,204.50 per day from increased water revenue resulting in a savings of \$14,016.11 per day. For a \$10.8 million installation fee, the system would be repaid within 2.1 years.

## 9. Appendix II – Isotherm Data

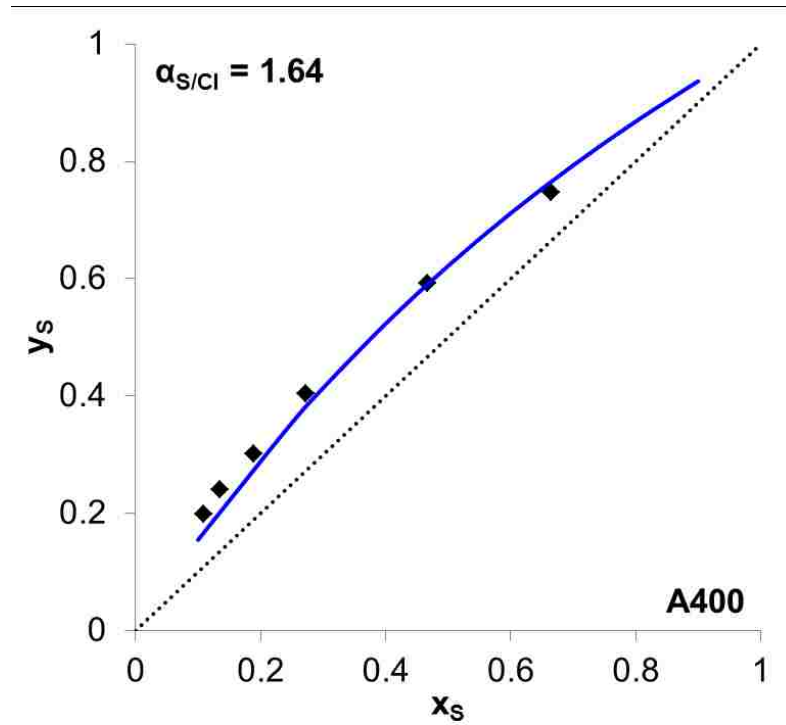


Figure A2.1 Pure A400 isotherm at 80 meq/L

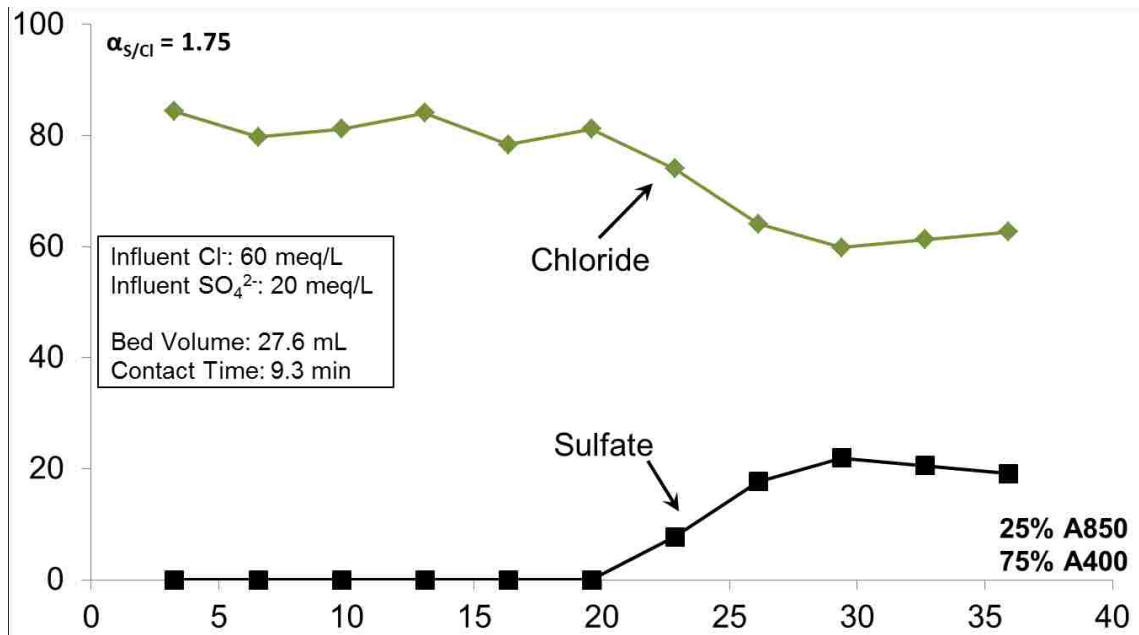
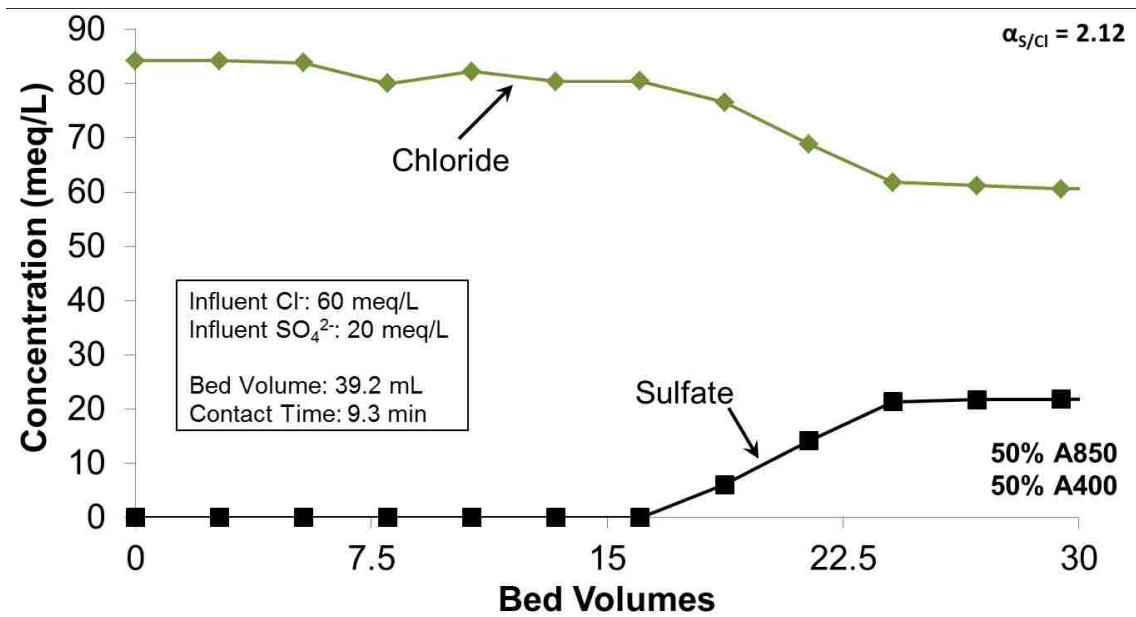
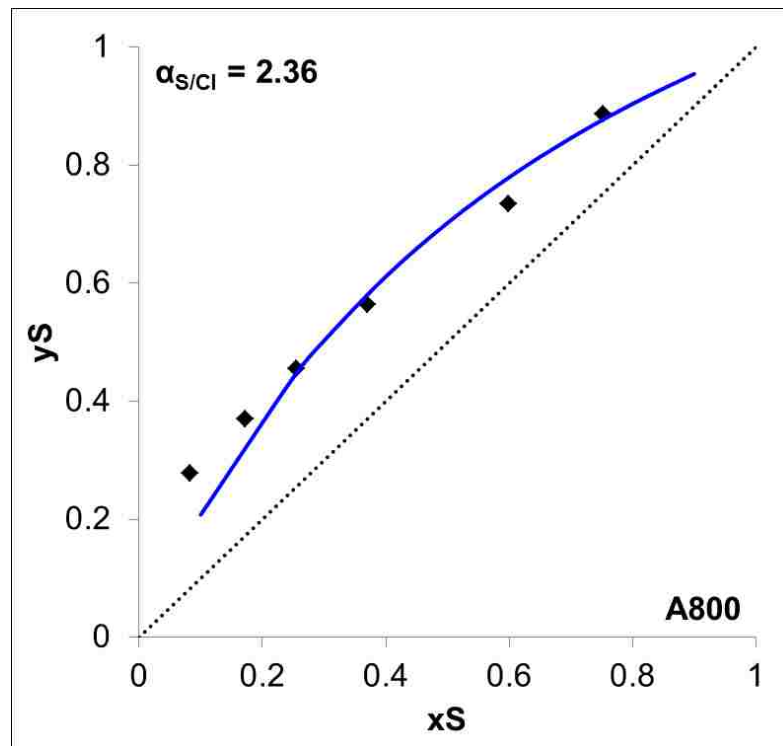


Figure A2.2 25% A400/75% A850 column run at 80 meq/L



**Figure A2.3** 50% A400/50% A850 column run at 80 meq/L



**Figure A2.4** Pure A850 Isotherm at 80 meq/L



## Vita

Ryan Casey Smith was born on August 17, 1986 to Joseph and Gale Smith in Flemington, NJ. In 2007 he passed the Fundamentals of Engineering Exam earning him the title of Engineer in Training. He graduated from Rowan University in 2008 *magna cum laude* with a Bachelor's Degree in Civil & Environmental Engineering and immediately went to Lehigh University to pursue a Master's Degree under Dr. Kristen Jellison. Upon completing Master's degree requirements in January 2010, he joined Dr. SenGupta's lab to begin Ph.D. research.

During his time at Lehigh he was the Teaching Assistant for Fluid Mechanics (3 times), Introduction to Environmental Engineering, Environmental Water Chemistry, Environmental Separation and Control, and Environmental Case Studies. In Spring 2014 he was the adjunct course instructor for CEE 170 Introduction to Environmental Engineering at Lehigh University.

In May 2014, he along with Dr. SenGupta, jointly submitted a patent application for the HIX-RO process: "Brackish Water Desalination Using Tunable Anion Exchange Bed" Application No.: 14/289,134.